Norwegian University
of Life Sciences

Master's Thesis 2024   60 ECTS
Faculty of Chemistry, Biotechnology and Food science (KBM)

Investigating the potential for nitrous oxide (N$_2$O) production from sediment microbiota, and its potential effect on growth of cobalamin-dependent microalgae

Kathrine Presthus Fylkesnes

MSc Biotechnology

Acknowledgements

Abstract

Microalgae are important primary producers of marine ecosystems. Many species require cobalamin (Vitamin B12), which is primarily related to the synthesis of methionine, where cobalamin is cofactor for the enzyme methionine synthase (METH). A gap of knowledge is the required amount of cobalamin needed for growth of cobalamin-dependent organisms and the potential environmental factors that can inactivate cobalamin. Nitrous oxide (N_2O) has shown to be a potent inactivator of cobalamin in clinical studies. The greenhouse gas is biologically produced by marine microorganisms, and it is not known whether the concentrations of N_2O usually found in marine environments can inhibit growth of cobalamin-dependent microalgae. The aim of this thesis was to investigate the effect of cobalamin depletion and N_2O exposure on growth of cobalamin-dependent microalgae.

The effect of different concentrations of N_2O on growth of cobalamin-dependent *E.coli* was established in an *E.coli* model system. Further, the potential for N_2O production from microbiota of enriched sediments was investigated in air-tight vials. Growth of cobalamin-dependent *I.galbana* and *T.lutea* upon cobalamin depletion was investigated by growing the microalgae in medium without cobalamin. Lastly, N_2O effect on algal cultures were tested through injecting growing cultures into air-tight vials containing N_2O, followed by measurements of oxygen levels.

It was found inactivation of growth of cobalamin-dependent *E.coli* when presence of saturated concentrations of N_2O. This concentration was substantially above the N_2O concentrations associated with marine environments and the observed accumulation from enriched sediments. The growth of the cobalamin-dependent microalgae was surprisingly not affected by the absence of cobalamin in medium. Through 16S rRNA analysis, the presence of bacteria was detected in the cultures of these microalgae. Lastly, it was not succeeded to evaluate the effect of N_2O on oxygen production from microalgae with the current experimental set-up.

In conclusion, saturated concentrations of N_2O was shown to inactivate growing cobalamin-dependent *E.coli*, but the exact inactivation concentration remains undetermined and requires further investigation. As the observed inactivation level was far above the N_2O concentrations associated with marine environments, the results suggests that the N_2O concentrations usually found in such environments are insufficient to impact the growth of resident cobalamin-dependent organisms. Further, if the non-observed effect of cobalamin depletion on growth of cobalamin-dependent microalgae is caused by the presence of cobalamin-producers or other factors could be investigated further. Lastly, as it was not possible to evaluate the effect of N_2O on microalgal growth, this should be investigated further.

Sammendrag

Mikroalger er viktige primærprodusenter i marine økosystemer. Mange arter krever kobalamin (Vitamin B12), primært for syntesen av metionin, hvor kobalamin er kofaktor for enzymet metionin syntase (METH). Det er ikke kjent hvor mye kobalamin som støtter vekst av kobalamin-avhengige organismer, eller mulige miljøfaktorer som kan inaktivere kobalamin. Gjennom kliniske studier har det blitt vist at lystgass (N_2O) kan inaktivere. Drivhusgassen blir blant annet produsert av marine mikroorganismer, og det er ikke kjent om de konsentrasjonene av N_2O som normalt opptrer i marine miljøer kan inaktivere vekst av kobalamin-avhengige mikroalger. Målet med denne oppgaven var å undersøke effekten av kobalamin og N_2O på vekst av kobalamin-avhengige mikroalger.

Effekten av forskjellige konsentrasjoner av N_2O på vekst av kobalamin-avhengig *E.coli* ble etablert ved bruk av et *E.coli* modell system. Videre ble potensialet for N_2O produksjon fra mikrobiota i anrikede sedimenter undersøkt i lufttette serumflasker. Effekten av kobalamin på vekst av de kobalamin-avhengige *I.galbana* og *T.lutea* ble etablert gjennom å dyrke mikroalgene i medium med og uten kobalamin. Til slutt ble effekten av N_2O på kobalamin-avhengige mikroalger testet ved å injisere voksende kulturer inn i lufttette serumflasker fylt med N_2O, etterfulgt av målinger av oksygennivå.

Det ble funnet inaktivering av vekst av kobalamin-avhengig *E.coli* ved metning av N_2O. Denne konsentrasjonen var mye høyere enn konsentrasjonene av N_2O som vanligvis finnes i naturlige marine miljø samt den observerte akkumuleringen i anrikede sedimenter. Et overraskende funn var at veksten av kobalamin-avhengig *I.galbana* og *T.lutea* ikke var påvirket av fravær av kobalamin i mediet. Det ble funnet tilstedeværelse av bakterier i stammekulturene av disse algene gjennom 16S rRNA sekvensering. Videre lyktes det ikke med å evaluere effekten av N_2O på oksygenproduksjon fra mikroalger med det gitte eksperiment-oppsettet.

For å konkludere, kan metning av N_2O inaktivere vekst av kobalamin-avhengig *E.coli*, men eksakt inaktiveringsonsentrasjon er fortsatt ikke kjent og krever videre undersøkelse. Likevel var den observerte inaktiverinskonsentrasjonen mye høyere enn de konsentrasjonene som vanligvis er i marine miljøer, hvilket peker mot at de konsentrasjonene av N_2O som normalt finnes i slike miljøer ikke påvirker veksten av kobalamin-avhengige organismer som lever der. Om den manglende effekten av kobalamin-fravær på veksten av kobalamin-avhengige mikroalger skyldes tilstedeværelse av kobalamin produsenter eller andre faktorer kan undersøkes nærmere. Til slutt, siden det ikke var mulig å si noe om effekten av N_2O på vekst av mikroalger, bør dette også undersøkes nærmere.

Abbreviations

DOM	Dissolved organic matter
DMSP	Dimethylsulfoniopropionate
DMS	Dimethyl sulfide
Cbl	Cobalamin
DMBI	5,6-dimethylbenzimidazole
UroIII	Uroporphyrinogen III
Cbi	Cobinamide
METH	Cobalamin-dependent methionine synthase
METE	Cobalamin-independent methionine synthase
DNRA	Dissimilatory nitrate reduction to ammonium
AOA	Ammonia-oxidizing archaea
AOB	Ammonia-oxidizing bacteria
SSU	Small ribosomal subunit
rRNA	Ribosomal ribonucleic acid
ELISA	Enzyme-linked Immunosorbent Assay
ATCC	American Type Culture Collection
CCAP	Culture Collection of Algae and Protozoa
OD	Optical density
OTU	Operational Taxonomic Unit
PCR	Polymerase chain reaction

Table of contents

1. Introduction

1.1 Marine ecosystems

More than 70% of the worlds surface is covered with water, with marine environments containing most of the total global water (Gleick et al., 1993, p. 13). Such environments cover a large variety of habitats of great importance for both eukaryotic and procaryotic organisms (Griffiths et al., 2017). The water column of marine environments, comprising planktonic habitats, is referred to as the pelagic zone. The benthic zone is located beneath the pelagic zone and comprises the sediments at the seafloor. Microbial communities in these environments serve important functions in the biogeochemical cycling of biologically relevant elements. There is a rapid exchange of energy, nutrients, and mass within and between the habitats of the pelagic and benthic zones, making marine ecosystems some of the most productive on Earth.

1.1.1 Anthropogenic impact on marine ecosystems

Marine ecosystems are favourable for the global human population, serving important ecosystem services such as sequestration of nutrients and supplying food and raw materials (Barbier, 2017). In present day, such ecosystems are among the most vulnerable in the world. Coastal development, pollution and other human activities have laid substantial pressure on the ecosystems, thus threatening their stability. Human activity has resulted in drastic changes of the marine environments, including loss and degradation of large areas such as seagrasses and coral reefs, loss of biodiversity and migration of species. Moreover, the increased population size has led to increased use of nitrogen as fertilizers in agricultural soil management (Kraft et al., 2011). Nitrogen is often limited in marine environments and partly controls the rate of primary production by phytoplankton (Doney, 2010). Runoff from agriculture and nitrogen disposal from fossil fuel and industry have led to increased supply of reactive nitrogen to marine ecosystems. Eutrophication can result in harmful algal blooms and increased load of organic matter, of which the decomposition requires substantial amounts of oxygen. This results in temporary or permanent anoxic conditions in certain areas, unliveable for fish and other animals. The changes in nutrient load, oxygen concentration, acidity, and temperature of the ocean as a result of human activity can have large effects on the microbial community composition and the biogeochemical cycling in marine environments (Breider et al., 2019; Doney, 2010).

1.1.2 The significance of micronutrients and vitamins in marine ecosystems

While macronutrients like carbon, nitrogen, sulphur and phosphorous, are required in large quantities by living organisms, micronutrients are only needed in trace amounts (Madsen, 2016, p. 360). They comprise a small percentage of the microbial cell dry weight, with iron comprising 0.2% and all other elements comprising less than 0.01%. Iron, cobalt, copper, manganese, and nickel are essential in the metabolism of many marine organisms. For instance, iron serves important functions in proteins while cobalt is an essential part of the cofactor cobalamin (Cbl).

Like micronutrients, vitamins are needed in trace amounts by living organisms. Auxotrophy for one or multiple vitamins is a common phenotype among many marine microorganisms (Balabanova et al., 2021; Sañudo-Wilhelmy et al., 2014). These vitamins are necessary for certain metabolic processes, but the organism is incapable of synthesizing them. Many marine microorganisms require one or more of the B-vitamins thiamine (B_1), biotin (B_7), and cobalamin (B_{12}), which needs to be provided by other biosynthesizing microorganisms (Croft et al., 2005; Sañudo-Wilhelmy et al., 2014). Thiamine acts as cofactor for a number of enzymes, including pyruvate decarboxylase, pyruvate oxidase and pyruvate dehydrogenase (Wang et al., 2024). Derivates of the vitamin, most notably thiamine pyrophosphate (TPP), are cofactors in many cellular processes. Biotin is involved in the metabolism of proteins, carbohydrates, and lipids, where it facilitates the transfer of CO_2 as cofactor for carboxylases, decarboxylases, and transcarboxylases (Waldrop et al., 2012). The most widespread cobalamin-dependency of prokaryotes and eukaryotes is related to the synthesis of methionine and succinyl-CoA, where it acts as cofactor for the enzymes methionine synthase (METH) and methylmalonyl-CoA mutase (Balabanova et al., 2021). Additionally, cobalamin is involved in anaerobic fermentation, amino acid conversion, and DNA synthesis in prokaryotes, serving as cofactor for glycerol dehydratase, ethanol ammonia lyase, aminomutases, and ribonucleoside diphosphate reductases.

1.1.2.1 The effect of environmental factors on vitamins

Both abiotic and biotic factors can influence the structure and function of vitamins. Thiamin can be degraded by specific enzymes, known as thiaminases, produced by bacteria and archaea (Sannino et al., 2018). The enzymes are grouped into thiaminase I and II, of which thiaminase II are most widely distributed amongst bacteria and archaea. Enzymes of group I and II degrade thiamine into pyrimidine and thiazole, using an organic substrate and water, respectively (Richter et al., 2023). Thiaminase activity has been reported in both plants and animal tissue

and has been linked to deficiencies and death (Sannino et al., 2018). For example, the demise of both trout and salmon has been linked to thiamine deficiency, resulting from the consumption of organisms containing high levels of thiaminase (Richter et al., 2023).

Cobalamin can react with various compounds, leaving it biologically inactive and unavailable for METH (Wood et al., 1968). Halogenated compounds, including methylene, chloride, chloroform, bromoform and iodoform, can react with cobalamin, resulting in the formation of halomethylcobalamin derivates. Biologically active cobalamin can also react with nitrous oxide (N_2O) (Alston, 1991). N_2O, a potent greenhouse gas with long lifetime, contributes substantially to global warming and is a source of ozone-depleting radicals in the atmosphere (Schneider et al., 2014).

1.2 Microalgae in marine environments

Microalgae are photosynthetic microscopic algae which together with cyanobacteria comprises phytoplankton (Glibert & Mitra, 2022). The biodiversity of algae is comprehensive, and more than 40 000 species are already identified (Hu et al., 2008). Major groups include green algae, diatoms, yellow-green algae, golden algae, red algae, brown algae, haptophytes, and dinoflagellates. Phytoplankton are important primary producers of marine ecosystems, and perform photosynthesis, using light to convert CO_2 into organic matter with the release of oxygen (Doney, 2010). The process of carbon fixation performed by phytoplankton in the upper layers of the ocean and following transportation to deeper parts, is referred to as the biological carbon pump (Glibert & Mitra, 2022). Given the substantial primary production rates of phytoplankton, they are central players in the complex metabolic networks of marine environments (Azam & Malfatti, 2007). As foundation of the food chain, they are consumed by zooplankton, which is further consumed by other larger organisms. A large fraction of the produced organic matter becomes dissolved organic matter (DOM), which includes smaller compounds like amino acids and carbohydrates. These compounds are made available for uptake by other microorganisms through excretion or cell lysis of phytoplankton. The majority of DOM is converted to CO_2 through respiration; however, some is assimilated at higher trophic levels in the food chain. Interactions are often mutualistic, and phytoplankton can assimilate compounds synthesized by other microbes, for instance vitamins (Kazamia et al., 2012).

1.2.1 Cobalamin dependency of microalgae

Cobalamin dependency is common amongst microalgae, and it is estimated that about half of all microalgal species are cobalamin auxotrophs (Croft et al., 2005). No relationship between algal phylogeny and cobalamin auxotrophy has yet been found, and all phyla shows representatives of both auxotrophs and non-auxotrophs. The requirement for cobalamin as cofactor amongst algae is primarily related to the synthesis of methionine, due to the presence of the cobalamin-dependent METH, encoded by the *metH* gene. Many microalgal species do not require cobalamin but have alternative cobalamin-independent metabolic pathways (Ellis et al., 2017; Helliwell et al., 2011). An alternative cobalamin-independent methionine synthase isoform called METE exists, encoded by the *metE* gene (Ellis et al., 2017). A correlation between the absence of a functional *metE* gene and cobalamin auxotrophy in microalgae has been found (Helliwell et al., 2011). The exact pathway for METE catalysation is less known than for METH. Despite a functional similarity between the two enzymes, they differ from each other in both sequence and protein folding (Pejchal & Ludwig, 2005).

Microalgal species that possess both isoforms of the enzyme has been observed, e.g. in *Chlamydomonas reinhardtii* (Croft et al., 2005)*.* The cobalamin dependent METH has a higher rate of catalysis than METE and is energetically favourable in conditions where cobalamin is available (Gonzalez et al., 1992). Co-cultivation of microalgae and bacteria has shown suppression of *metE* expression in microalgae, due to metabolic interactions between the bacteria and algae (Kazamia et al., 2012). Furthermore, suppression of *metE* expression has been observed upon addition of exogenous cobalamin to growing algae cultures (Ellis et al., 2017; Kazamia et al., 2012).

As no relationship between cobalamin auxotrophy and phylogeny has been observed, such auxotrophy is suggested to be a result of independent events of gene losses that have occurred during evolution (Croft et al., 2005). It is proposed that in cases where microalgae have been provided with an unlimited source of cobalamin, for instance through metabolic interactions with bacteria, selective pressure has resulted in keeping the energy-efficient, and cobalamin-dependent METH (Nef et al., 2019). This idea has been supported by laboratory experiments conducted on *C.reinhardtii* (Helliwell et al., 2014).

1.2.2 *Chlorella vulgaris* as a model for cobalamin independent microalgae

Chlorella vulgaris is a green algae species within the *Chlorophyta* taxon (Pepper & Gentry, 2014). The cells have a diameter of 2-10μm and shares many structural similarities with plant cells (Ahmad et al., 2020; Safi et al., 2014). It is a fresh-water species with rapid growth rate and high resistance towards harsh conditions and invaders (Safi et al., 2014). The protein content of *C.vulgaris* comprises over 55% of the dry weight of cells, and the microalgae is thus often used as a food supplement. Other applications include use within pharmaceuticals, cosmetics, animal feed and in aquaculture. *C.vulgaris* is one of the most commonly used microalgae in commercial aquaculture, where it can be used as food supplement or whole feed for fish, larvae and zooplankton (Ahmad et al., 2020).

No surveyed species within the *Chlorella* genus have yet been stated as cobalamin auxotrophs (Croft et al., 2005). Despite this, some surveyed *Chlorella* species have shown the ability to take up and store exogenous cobalamin (Maruyama et al., 1989). The physiological role of cobalamin in these species are not known, however, a relationship between the uptake of cobalamin and the production of secondary carotenoids was observed. Secondary carotenoids are involved in the structure and stability of the cell wall.

1.2.3 *Tisochrysis lutea* and *Isochrysis galbana* as models for cobalamin dependent microalgae

Tisochrysis lutea and *Isochrysis galbana* are two microalgal species found within the group of haptophytes and family *Isochrysidaceae* (Nef et al., 2019). They share a lot of morphological and structural similarities, and *T.lutea* was formerly classified as *I.galbana* (Bendif et al., 2013). The species are motile, due to the presence of flagella. The plastid colour is orange for *T.lutea* and brown for *I.galbana,* and the difference is most visible on cultures during stationary phase. *T.lutea* and *I.galbana* also differ genetically in the small ribosomal subunit (SSU). The microalgae are marine species that serves important roles in marine biogeochemistry. In addition to contributing to the marine primary production, they are central in the cycling of sulphur as significant producers of dimethylsulfoniopropionate (DSMP) (Malin & Steinke, 2004; Nef et al., 2019). DSMP is precursor of dimethyl sulfide (DMS), which is climatically relevant for the formation of cloud condensation nuclei. *I.galbana* and *T.lutea* has carotenoids as main pigment, and is of particular interest commercially for the presence of fucotaxin, due to a range of biological properties (Gao et al., 2020). The microalgae are also a potential for commercial use due to a high content of long chained polyunsaturated fatty acids (LC-PUFAs),

which are precursors of important biological compounds (Khozin-Goldberg et al., 2011). In the present day, the species are commonly used in commercial aquaculture, mainly as feed for zooplankton and juvenile fish.

Both *I.galbana* and *T.lutea* have shown to require cobalamin for growth (Croft et al., 2005; Nef et al., 2019). Genomic and transcriptomic data of *I.galbana* and *T.lutea* have revealed presence of the *metH* gene and corresponding cobalamin-dependent METH, and absence of the alternative *metE* gene (Nef et al., 2019). Growth assays conducted on *T.lutea* have shown biological dependency of cobalamin, with significant difference in growth rate between medium with and without cobalamin. Furthermore, *T.lutea* has been shown to take up and assimilate exogenous methionine, resulting in higher growth rate than when grown in the absence of cobalamin. This emphasizes that cobalamin dependency of such microalgae is primarily related to the methionine synthesis.

1.3. Cobalamin

Cobalamin has a large and complex structure, and is the most common cobalt-containing compound in living organisms (Balabanova et al., 2021). The molecule was first discovered in 1926 in liver homogenate and later purified from liver and kidney in 1948 (Minot & Murphy, 1926; Rickes et al., 1948; Smith, 1948). Given its biological relevance in both prokaryotes and eukaryotes, the molecule has been extensively studied and reviewed (Dereven'kov et al., 2016). However, the focus varies, and the literature is not always consistent. Consequently, the following sections aims to represent the consensus in literature, aligning with the majority of viewpoints within the current body of knowledge.

1.3.1 Structure of cobalamin

Cobalamin comprises a central corrin ring, with a cobalt atom located in the middle of the ring (Banerjee, 1997). The cobalt is coordinated equatorially by four surrounding pyrrole nitrogen atoms. Due to the properties of the cobalt atom, cobalamin can have three oxidation states: cob(III)alamin, cob(II)alamin, and cob(I)alamin (Dereven'kov et al., 2016). All forms are known under physiological conditions. Cob(III)alamin is mainly hexacoordinated, with the four pyrrole nitrogen coordinating the cobalt atom together with an upper and lower axial ligand.

These are placed in the β- and α-position of the cobalt atom. Placed in α-position is commonly 5,6-dimethylbenzimidazole (DMBI), which is bound to one of the pyrrole nitrogens. Various groups can place in β-position, thus forming different forms of cobalamins (Balabanova et al., 2021). A cyano, methyl, 5'-deoxyadenosyl or hydroxy group in β-position, gives cyanocobalamin, methylcobalamin, adenosylcobalamin, and hydroxycobalamin, respectively. Cob(II)alamin is mainly pentacoordinated, and the cobalt is coordinated by the four nitrogen and DMBI (Dereven'kov et al., 2016). Cob(I)alamin is mainly tetracoordinated, with the cobalt being coordinated by the four pyrrole nitrogen alone. The lack of additional groups in α- and β-position, is due to the electron density of the additional electrons (Matthews et al., 2008).

1.3.2 Biosynthesis of cobalamin

Methylcobalamin, adenosylcobalamin and hydroxycobalamin are the naturally occuring forms of cobalamin, while cyanocobalamin is the manufactured form and does not occur naturally (Balabanova et al., 2021). Methylcobalamin and adenosylcobalamin are unstable in light and are easily converted to hydroxycobalamin in aqueous solutions at room temperature. The *de novo* biosynthesis of adenosylcobalamin and methylcobalamin is complex with 30 enzymatic reactions, thus requiring a substantial genetic repertoire, only present in a few bacteria and archaea (Raux et al., 2000; Roth et al., 1993). The cobalamin producers are normally found in soil, oceans and digestive tracts of humans and animals (Balabanova et al., 2021). Metagenomic analysis performed on marine and soil environments have revealed that the majority of microorganisms with cobalamin production potential belongs to the phyla Proteobacteria, Actinobacteria, Firmicutes, Nitrospirae and Thaumarcheota (Doxey et al., 2015; Lu et al., 2020). Research suggests that the members of Thaumarcheota are of the most significant contributors to the cobalamin synthesis of oceans, also in the deeper parts and artic areas (Doxey et al., 2015). The largest contributors for cobalamin production potential has however been shown to vary with season (Beauvais et al., 2023). For instance, metagenomic analysis of the north-western Mediterranean Sea showed that Thaumarcheota was the largest contributor at winter, and α-proteobacteria were the largest during spring and summer.

The biosynthesis of cobalamin is genetically diverse and can differ between the biosynthesizing microbes (Balabanova et al., 2021). One anaerobic, one aerobic pathway, in addition to a salvage pathway exists. The anaerobic and aerobic pathway involves three main parts, starting with the synthesis of Uroporphyrinogen III (UroIII). This is followed by transformation to

cobinamide (Cbi), which involves the formation of the corrin ring and adenylation. Lastly, the lower axial ligand is synthesized and attached to the ring. The anaerobic genetic machinery is referred to as *cbi*, whilst the aerobic is called *cob*. Many enzymes and steps involved are similar for both pathways; however, some are pathway specific. The main difference is the use of oxygen to contract the corrin ring in the aerobic pathway and the timing of insertion of the cobalt atom. In the aerobic pathway, the insertion happens at a later stage than in the anaerobic pathway. The additional salvage pathway involves the uptake of exogenous Cbi, which through a series of enzymatic reactions forms adenosylcobalamin.

1.3.2.1 The significance of cobalamin producers in marine ecosystems

Despite a low abundance of bacteria with cobalamin production potential relative to non-producers, these species are still believed to have a significant effect on the entire marine community (Lu et al., 2020). The cobalamin concentration in seawater is estimated to be relatively low, with levels less than 4 pM (Sañudo-Wilhelmy et al., 2014). Hence, many cobalamin auxotrophs rely on the supply of cobalamin from producers, and the producers are therefore mediating the growth of many community members (Lu et al., 2020). Synergistic interactions and metabolic interdependencies between cobalamin producers and cobalamin auxotrophs are thus partly shaping the communities of such ecosystems (Gómez-Consarnau et al., 2018).

1.3.3 METH - Cobalamin-dependent methionine synthase

METH catalyses the formation of methionine from homocysteine, a process involving the transfer of a methyl group from tetrahydrofolate (CH_3-H_3-folate) to homocysteine through two half-reactions (Chanarin, 1980; Croft et al., 2005; Ellis et al., 2017). This leads to the formation of H_4-folate and methionine (Matthews et al., 2008). All reactions catalysed by METH is shown in Figure 1.1. The enzyme is composed of four modules, with different binding sites for CH_3-H_4-folate, homocysteine, CH_3-cob(III)alamin (methylcobalamin), and adenosylmethionine (Goulding et al., 1997). The CH_3-H_4-folate-binding and homocysteine-binding domain catalyse the transfer of a methyl group to and from cobalamin, respectively (Matthews et al., 2008). In the process, a methyl group is transferred from CH_3-cob(III)alamin to homocysteine, thus forming cob(I)alamin and methionine. Another methyl group is transferred to cob(I)alamin from CH_3-H_4-folate, resulting in the formation of CH_3-cob(III)alamin and H_4-folate.
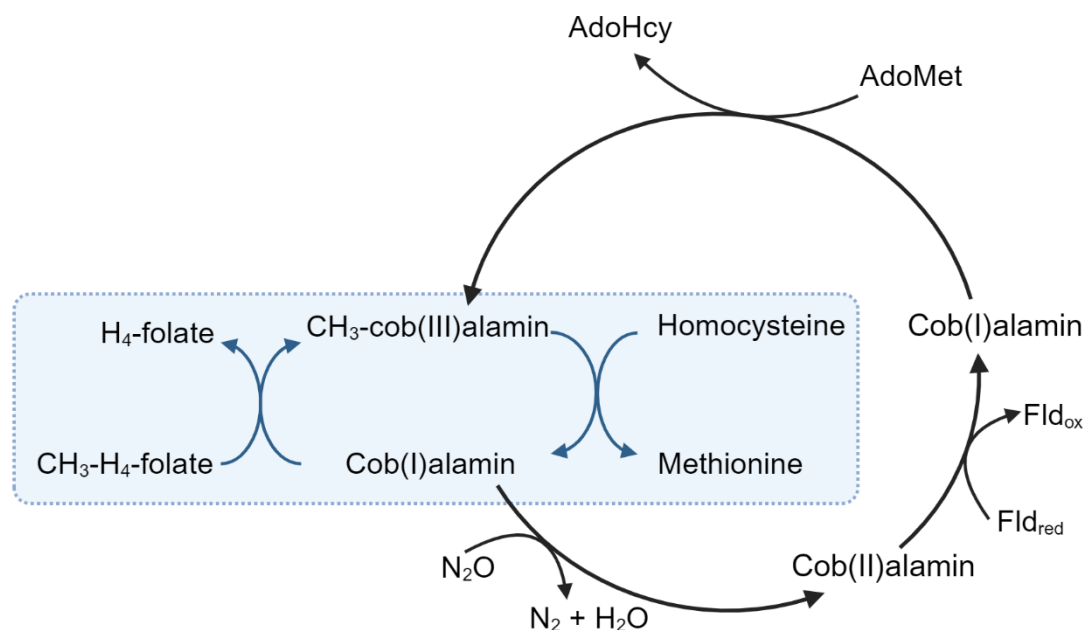
Figure 1.1 The reactions catalysed by methionine synthase. The reactions marked in blue is involved in the transfer of a methyl from CH_3-folate via cobalamin to homocysteine, forming methionine. The reactions marked in black show the oxidation of cob(I)alamin to cob(II)alamin by N_2O. Reactivation of cob(II)alamin involves the transfer of a methyl group to AdoMet. This figure is adapted from (Matthews et al., 2008).

1.3.4 Inactivation of cobalamin by N_2O

The reduced cob(I)alamin form is sensitive to oxidants, e.g. N_2O, and can be oxidized to the catalytically inactive state cob(II)alamin, resulting in an inactive METH enzyme (Alston, 1991; Drummond & Matthews, 1994). The oxidation of cob(I)alamin to cob(II)alamin by N_2O, results in the formation of N_2 and H_2O (Chanarin, 1980), as shown in Figure 1.1. Toxicity of N_2O was first reported in clinical studies of humans, where the treatment involved 50/50 N_2O/O_2 (Lassen et al., 1956). Later studies of rats showed that the enzyme activity of METH stopped upon exposure to 50/50 N_2O/O_2 (Deacon et al., 1980). In the same study, the enzyme activity was recovered after the exposure to N_2O ended. The last adenosylmethionine-binding domain of METH is important to restore the catalytic competency of the enzyme (Mendoza et al., 2023). It catalyses the reduction of cob(II)alamin to cob(I)alamin with flavodoxin as electron donor. Subsequently, cob(I)alamin is methylated with adenosylmethionine serving as the methyl donor, resulting in regenerated CH_3-cob(III)alamin.

1.4 N₂O – Nitrous oxide

1.4.1 Sources of N₂O in marine ecosystems

N_2O can be formed through both abiotic and biotic processes (Otte et al., 2019). Microbial communities of marine environments are central in the atmospheric N_2O budget and are important sources, primarily through the processes of denitrification and nitrification (Breider et al., 2019; Otte et al., 2019). Other processes with N_2O production potential includes dissimilatory nitrate reduction to ammonium (DNRA) and chemodenitrification, involving abiotic reduction of nitrite by Fe(II) (Otte et al., 2019). The net production of N_2O from marine microbial communities depends on environmental factors, such as substrate availability, oxygen concentration and pH. The increase in nitrogen load, in the forms ammonia (NH_4^+), and nitrate (NO_3^-), and oxygen depletion of marine environments due to anthropogenic activities makes the conditions suitable for production of N_2O (Kraft et al., 2011; Menon et al., 2007). Acidification of seawater, as a result of increased CO_2 emissions, has also been shown to have ability to increase the net production rate of N_2O (Breider et al., 2019).

1.4.1.1 Denitrification

Denitrification is the most energy efficient alternative to oxygen respiration (Schneider et al., 2014). Many microorganisms can perform denitrification, including both prokaryotes and eukaryotes. So far, most of the isolated and studied denitrifiers are found within phylum proteobacteria, common in soil and ocean sediments. The presence of nitrate and low or no oxygen are detected by specific nitrate sensors and oxygen-sensing regulators, which leads to expression of the denitrification machinery (Kraft et al., 2011). Denitrification starts with the reduction of nitrate to nitrite (NO_2^-), catalysed by nitrate reductase. Nitrate is further reduced to nitric oxide (NO), catalysed by nitrite reductase. Nitric oxide reductase catalyses the reduction of NO to N_2O. The last step involves reduction of N_2O to N_2, catalysed by nitrous oxide reductase.

Some microbes have the genetic potential of complete denitrification and can perform the entire process (Gao et al., 2019). Denitrification is modular and all enzymes of the machinery are not expressed simultaneously, and their expression can to a certain degree be regulated independently. In addition, truncated pathways are common, and many microbes possesses only one or a few enzymes (Lycus et al., 2017). It is therefore a potential for accumulation of intermediates during denitrification, depending on the environmental conditions. For instance, nitrous oxide reductase is sensitive to oxygen, and can lead to uncompleted denitrification and

accumulation of N_2O if the oxygen levels are too high (Schneider et al., 2014). The presence of sulphides, for instance, caused by sulphate reduction in lower sediments, can inhibit the reduction of NO and N_2O during denitrification (Sørensen et al., 1980).

1.4.1.2 Nitrification

N_2O production from marine communities can also occur as a by-product from nitrification (Freing et al., 2012). Nitrification is an aerobic process and occurs in oxygen-rich layers of the oceans. The pathway involves the oxidation of ammonia (NH_3) to nitrite with hydroxylamine (NH_2OH) as intermediate (Pajares & Ramos, 2019). This is catalyzed by the enzyme ammonia monooxygenase (AMO) and performed by ammonia-oxidizing bacteria (AOB), e.g *Nitrosomonas*, or ammonia-oxidizing archaea (AOA), e.g. *Nitrosopumilus*. Nitrite is further oxidized to nitrate, performed by nitrite oxidizers. Commamox, e.g. *Nitrospira*, are complete ammonia-oxidizers, capable of performing the entire nitrification pathway. AOB can produce N_2O through the process of nitrifier denitrification or through transformation of NH_2OH. Nitrifier denitrification involves the reduction of nitrite to N_2O via NO. AOA can also produce N_2O, however the exact pathways are less known.

1.4.2 Concentration of N_2O in marine environments

The concentration of N_2O in the seawater varies and is affected by different factors, including temperature, depth, latitude, and longitude. An exponential decay relationship between N_2O concentration and surface seawater temperature has been documented (Zhan & Chen, 2009). Low temperatures were seen to associate with high concentrations of N_2O. Furthermore, studies of surface seawater have shown concentrations of around 6.0 nM in tropical regions, while the concentrations in polar regions were around 18-19 nM (Zhan et al., 2017). Investigations of water columns in the Artic ocean, found the highest N_2O concentrations in waters furthest north (Hirota et al., 2009). Additionally, the concentrations tended to increase with depth, and ranged from 9.6 - 25.1 nM. The increasing trend in concentration with depth was also observed in the Subtropical Western North Pacific Ocean (Heo et al., 2022). The concentration of N_2O ranged from 5.6 - 8.9 nM in surface layers (0-200m), 13 - 35 nM in intermediate layers (200-1500m), and 20.6 - 24 nM in deep layers (>1500m). Comparisons of N_2O concentrations in the deep layers of the Atlantic, Indian and North Pacific ocean, showed differences in concentrations with the highest mean at 22.7 nM for the North Pacific and lowest at 13.6 nM for the North Atlantic (Bange & Andreae, 1999). It has also been proposed that the mean age of deep waters

can affect the N_2O concentrations, as multiple studies have shown a positive correlation between age and concentration (Bange & Andreae, 1999; Toyoda et al., 2019).

Supersaturation of N_2O has been found, with concentrations between 58.8 - 86.6 µM, in the permanently ice-covered, saline Lake Vida in Antarctica (Murray et al., 2012). The measured temperature and pH were -13.6^{o}C and 6.2 respectively, and the production and accumulation of N_2O was hypothesized to originate from denitrification or abiotic chemodenitrification. Moreover, supersaturation was also found in the permanently ice-covered Lake Bonney (Antarctica), with a maximum concentration of 41.6 µM (Prisu et al., 1996). The measured pH was 6.25 and the average temperature were below 0°C.

1.5 Metagenomic analysis of microbial community composition

Microorganisms are an essential part of various environmental habitats, including air, soil, water, and ocean sediments (Bharti & Grimm, 2021). Their significant role in the cycling of elements, production of metabolites, and in interactions with other organisms make microorganisms a subject of interest. The development of high-throughput sequencing approaches has advanced the area of metagenomics. The two main sequencing approaches for metagenomic analysis is shotgun sequencing and gene amplicon sequencing. Shotgun sequencing is based on the extraction of all DNA present in a complex sample, which is divided into shorter fragments that are sequenced independently. Gene amplicon sequencing is based on the amplification and sequencing of functionally conserved marker genes. The use of marker genes is favourable due to their ability to be amplified through polymerase chain reaction (PCR).

1.5.1 16S rRNA marker gene

The use of the 16S rRNA marker gene is a common benchmark for identifying the taxonomic composition of bacterial communities in complex samples (Winand et al., 2019). It is present in all bacteria and encodes the smallest ribosomal subunit (Mignard & Flandrois, 2006). The marker gene is around 1500bp in size and comprises of nine variable regions, referred to as V1-V9, which makes it possible to discriminate between bacteria at genus, species and sometimes strain level (Winand et al., 2019). The variable regions are flanked by ten conserved regions,

which allow the gene to be targeted with universal primers. Despite their universal application, these primers have limitations. There can be some variability even in the conserved regions, and as a result, they might not cover all taxa present and may not be fully representative of the entire prokaryotic diversity (Baker et al., 2003). Another limitation with the use of 16S rRNA in metagenome analysis is that variations in the gene copy number can lead to nondetection of species with low copy number (Winand et al., 2019).

1.6 Quantification of cobalamin in marine environments

The detection and quantification of cobalamin in marine environments are challenging, due to the picomolar concentrations present in seawater (Sañudo-Wilhelmy et al., 2014). It has been difficult to accurately estimate the concentration due to lack of sensitive analytical techniques. Cobalamin was long measured indirectly through microbial assay methods, using strains of bacteria or algae to detect cobalamin presence (Okbamichael & Sañudo-Wilhelmy, 2004). In recent years, methods involving direct measurement through high-performance liquid chromatography (HPLC) have been mostly utilized (Heal et al., 2014; Okbamichael & Sañudo-Wilhelmy, 2004). The Enzyme-linked Immunosorbent Assay (ELISA) is another alternative that has been widely used in quantification of cobalamin in food (Selva Kumar & Thakur, 2011). In addition to being rapid and give high accuracy, it is a more cost-effective alternative to chromatography methods.

1.6.2 Microbial assays

Microbial assays, such as the disc-diffusion method, are commonly used for testing the sensitivity of a culturable organism to an antibiotic (Balouiri et al., 2016). These assays can also be used for measuring the concentration of vitamins in samples (Baker & Sobotka, 1962). The principle of the disc-diffusion method starts with inoculating a test microorganism onto agar plates (Balouiri et al., 2016). Filter paper discs is impregnated with the test compound and are subsequently placed onto the agar surface. The test compound diffuses into the agar, and if a cobalamin-dependent test organism is used, the presence of cobalamin on discs will support growth (Diding, 1951).

1.6.3 ELISA

In addition to quantifying vitamins in a sample, ELISA is commonly used to quantify the concentration of proteins, hormones and drugs (Aydin, 2015). It exists four types of ELISA, referred to as direct, indirect, sandwich and competitive. Competitive ELISA can be used to quantify the concentration of an antigen in a sample through detecting interference in a signal. Firstly, the surface of wells is coated with antibodies specific to the antigen of interest. The samples are added to wells together with an enzyme-tagged antigen. The untagged and tagged antigens will compete for binding to the antibodies on surface. An enzyme-substrate causes colour change, which can be used to quantify the antigen concentration. As the antigens of interest are untagged, high absorbance in a well indicates low concentration of the antigen of interest.

1.7 Aim of thesis

Around half of all characterized microalgal species are estimated to be cobalamin auxotrophs, requiring cobalamin primarily for the synthesis of methionine (Croft et al., 2005). There is a gap in our understanding regarding the required amount of cobalamin needed to support growth of cobalamin-dependent organisms, as well as the potential environmental factors that could inactivate cobalamin. From medical studies it has been shown that N_2O is a potent cobalamin inactivator (Deacon et al., 1980; Lassen et al., 1956). It is however not known whether the concentrations of N_2O normally found in marine environments have the potential to inhibit growth of cobalamin-dependent microalgae.

The aim of this thesis was to investigate the effect of cobalamin depletion and N_2O exposure on the growth of cobalamin-dependent microalgae. This included the following subgoals:

- Establish an *Escherichia coli* model system to investigate the effect of N_2O, in different concentrations, on cobalamin
- Determine the potential for N_2O production from the microbiota of enriched sediment
- Establish the growth of microalgae during cobalamin depletion
- Investigate if the growth of cobalamin-dependent microalgae is affected by the inactivation of cobalamin by N_2O.

2. Materials and methods

Figure 2.1 shows a schematic overview of the experiments conducted in the present thesis, grouped after three main sections.
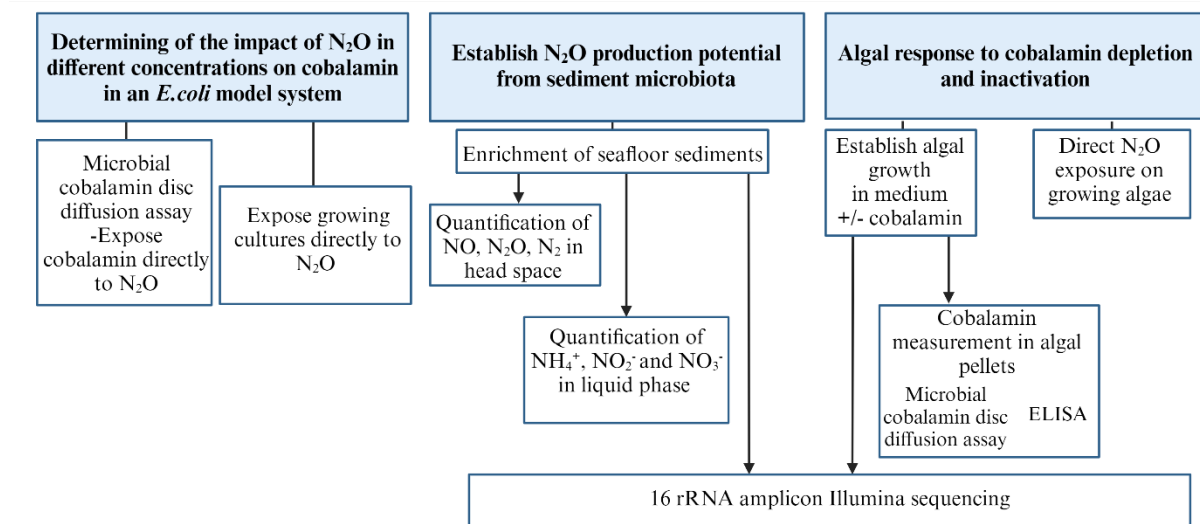
Figure 2.1 Flowchart over experiments conducted in the present thesis.

2.1 Media for *E.coli* cultivation and assay

2.1.1 Cultivation media

Tryptic soy agar was prepared by combining 15g Tryptic soy broth, 7,5g agar powder, and 500ml MilliRo water in a 500ml Duran glass bottle. The mixture was brought to a boil to dissolve all components, followed by autoclaving at 121°C for 15 minutes. To avoid solidification, the agar was kept at 55-60°C in a water bath until plate preparation. Tryptic soy broth (TSB) was accordingly, but without addition of agar.

2.1.2 Microbial cobalamin disc diffusion assay media

The medium was prepared according to the description in Diding (1951). The following components was added in a 1000ml Duran bottle: 3g KH_2PO_4, 7g K_2HPO_4, 0.1g $MgSO_4*7H_2O$, 0.5g $C_6H_5Na_3O_7*2H_2O$, 1g $(NH_4)_2SO_4$, 15g agar powder and ~990g MilliRo water. After mixing thoroughly, the medium was autoclaved at 121°C for 15 min. It was added 10ml sterile filtered glucose with concentration 1g/ml to the medium. Soft agar was made accordingly, but with half the amount of agar. The media with agar was stored at 55-60°C in water bath until

preparation of assay plates. In addition, liquid medium was made in the same manner as described above, except no agar was added. To make liquid medium with cobalamin, sterile filtered cobalamin was added together with the glucose stock to the autoclaved medium, to a final cobalamin concentration of 0.4mg/L. The liquid medium was stored at 4°C until use.

2.2 Cultivation of *E.coli*

2.2.1 Cultivation on agar

Two strains of *E. coli* was cultivated; the wild-type *E.coli* ATCC 11775 and the cobalamin-dependent *E.coli* ATCC 14169. The WT strain was provided by lab engineer Else Marie Aasen, whilst the cobalamin-dependent strain was collected from MediMark© KWIK-STIK^{TM} (Microbiologics, France). Single colonies were collected through streak plate procedure on TSA plates. O/N cultures were made through transferring single colonies from TSA plates to glass tubes containing TSB, followed by incubation at 37°C with shaking for 24 hours.

The *E.coli* strains were also tested for the ability to grow anaerobically on agar. A volume of 100µl O/N culture were spread evenly onto a TSA plate. The plates were placed in a sealed chamber, made anaerobic using a 3.5L AnaeroGen^{TM} bag (Thermo Fisher Scientific, USA). To verify anaerobic conditions, an anaerobic indicator (Thermo Fisher Scientific, USA) was used. The plates were incubated at 37°C for 48 hours.

2.2.2 Cultivation under defined atmosphere

Glass vials of 120 ml, containing 30 ml liquid cobalamin disc diffusion assay medium and triangle magnet (14 mm), were autoclaved at 121°C for 15min. The vials were subsequently capped with sterile septa and helium washed, which involved removing the air and replacing it with helium using a vacuum pump. Helium wash setup was as follows: 7 cycles comprising 180 seconds of vacuum and 30 seconds of helium fill, before a final 20 seconds of helium filling at endpoint. Magnetic stirring was used during the wash procedure, to facilitate gas exchange from liquid to headspace. The pressure in the vials was reduced to 1atm, before 100µl O/N cultures were injected into the vials through septa using a syringe. The cultures added had OD$_{565}$ at approximately 1.0. N$_2$O was subsequently added to the vials with bacterial suspensions resulting in different conditions of 100, 10, 1 and 0 % N$_2$O in the vials. This corresponded to a

liquid concentration of 28, 2.8, 0.28 and 0 µM, respectively. To create vials with 100% N_2O, the air of the helium-washed vials was evacuated using a vacuum pump. N_2O was then injected into the vials with a sterile needle for 15 seconds, followed by reduction of the pressure to 1atm. Vials with 10% N_2O were created by injecting 10ml of N_2O into helium-washed vials, using a gas syringe, from a vial containing only N_2O gas. The pressure in the vials was not evened out after addition of gas to ensure the correct concentration. Vials with 1% N_2O was prepared accordingly, but with the addition of 1ml gas. The vials were incubated in water bath at 20°C with stirring at 500 rpm.

2.3 Microbial cobalamin disc diffusion assay

O/N cultures were diluted to OD_{565} of 0.5, before 1 ml was transferred to Eppendorf tubes and centrifuged at 13000 rpm for 5 min at 4°C. The supernatant was discarded, and the cell pellet was resuspended in 1ml 0.9% NaCl to remove excess cobalamin. Centrifugation of the tubes was performed under the same conditions before the supernatant was removed. This wash-step was repeated once, followed by resuspension of the cell pellet in 1ml microbial cobalamin disc assay liquid medium. The entire contents of the tubes were transferred to new tubes, into which 9ml microbial cobalamin disc assay soft agar was added. After mixing the content thoroughly, the solution was immediately poured over prepared plates containing solidified microbial cobalamin disc diffusion assay agar.

A schematic overview of the microbial cobalamin disc diffusion assay is shown in Figure 2.2. Firstly, sterile paper discs were soaked in either standards of cobalamin with concentrations at 0, 1, 10 and 100 ng/ml, N_2O-exposed cobalamin standards, or samples of which possible cobalamin presence should be detected. The cobalamin standards directly exposed to N_2O had been incubated in sealed glass vials containing 100% N_2O for 6 days at 4°C. Secondly, the paper discs were placed onto prepared plates with disc assay agar and *E.coli* in soft agar overlay. The assay plates were incubated at 37°C for 24 hours before the colony diameter was measured.
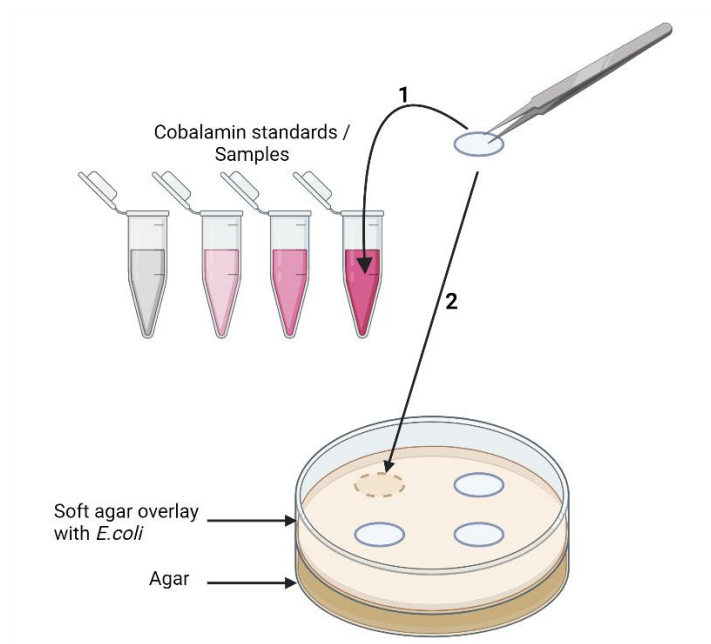
Figure 2.2. Schematic overview of the workflow of microbial cobalamin disc diffusion assay. (1) Discs were soaked in cobalamin standards or the samples of interest. (2) Soaked discs were placed onto the surface of assay plates. The assay plates comprised of a solid agar layer and soft agar overlay containing cobalamin-free *E.coli*. Illustration is created using Biorender.com.

2.4 Sediment enrichment cultures

2.4.1 Establishment of enrichment cultures

Figure 2.3 provides a schematic overview of the workflow process for sediment enrichments. Seawater was autoclaved at 121°C for 15 min, and 50ml was added to sterile 120ml glass vials containing magnet (14mm). Additional compounds were added to the vials, with the combinations as follows: methanol and nitrate, thiosulfate and nitrate and nitrate only. Control vials did not receive any additional compounds. Sediment of high particulate matter from Søndre Møkkalasset in Arendal municipality was then added into each vial. Start controls for DNA analysis were taken from the same sediment batch. This was done by adding one scoop of sediment into 3ml STAR buffer in faeces tubes, which were stored at -20°C until use in analysis. The vials were capped with rubber septa, followed by He-wash as described in 2.2.2 Cultivation under defined atmosphere Incubation of vials occurred at magnet in water bath holding 20°C, with stirring at 400 rpm. At end of incubation, sediment samples for DNA analysis were collected from all vials and stored in the same manner as for the start-controls.
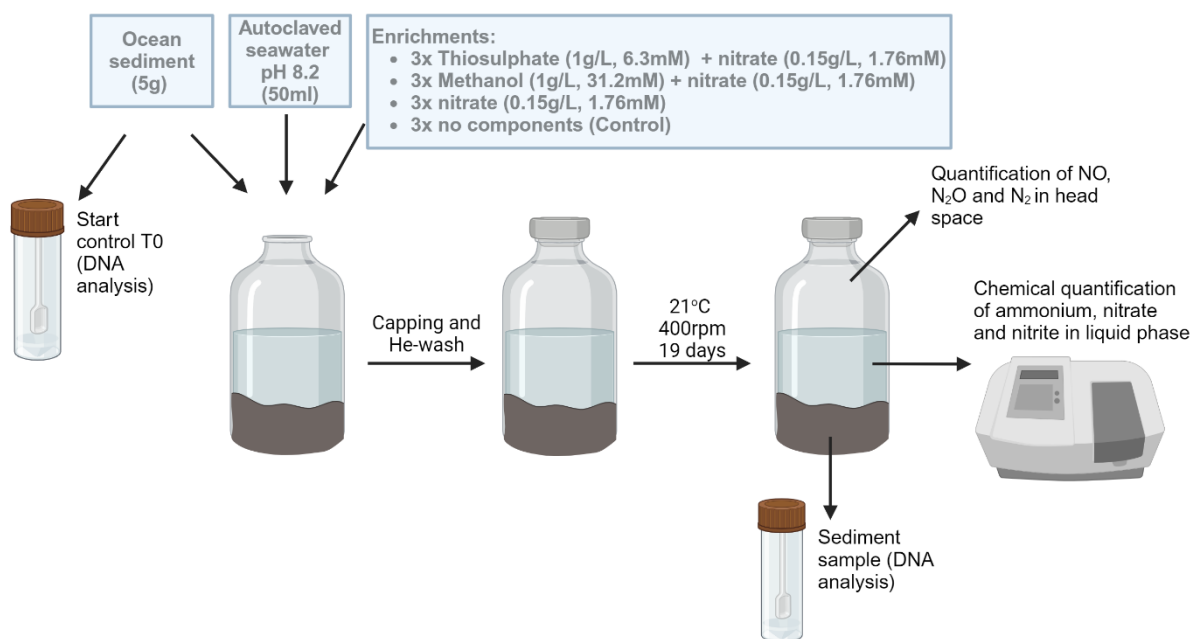
Figure 2.3 Schematic overview of workflow for enriching sediment samples in glass vials. Sediment was added, autoclaved seawater and additional compounds was added to vials. Start controls of sediments used for DNA analysis were taken from the same sediment batch. The vials were capped and the air was removed and replaced with helium. After incubation, different nitrogen compounds were quantified and sediment samples were collected for DNA analaysis. Illustration is created using Biorender.com.

2.4.2 Analysis of gases in headspace

Concentration of NO, N_2O and N_2 in headspace of sediment enrichment cultures were measured using robotized incubation system (Molstad et al., 2007). The gas measurements were calibrated based off known gas standards and the solubility of the different gases at the given temperature.

2.4.3 Analysis of compounds in liquid phase

The vials were removed from magnet and allowed for sedimentation of particles, to ensure clear liquid phase prior to chemical quantification of ammonium, nitrite and nitrate.

The applied method for ammonium quantification was based on the reaction between Ortho-pthaldialdehyde and ammonium in the presence of the reducing agent β-mercaptoethanol, resulting in formation of a detectable fluorescent compound (Roth, 1971). The OPA reagent comprised of 5.4g/L Ortho-pthaldialdehyde ($C_8H_6O_2$) in 10% Ethanol, 360 mM

phosphatebuffer and 0.5‰ β-mercaptoethanol. Standards with known ammonium concentrations at 0, 0.5, 1 and 2 mM were made from a NH_4Cl stock. It was added 65µl sample or standard into Eppendorf tubes containing 975µl OPA reagent. The tubes were vortexed for 15 seconds, followed by incubation in the dark at room temperature for 20 minutes. The absorbance at 420nm were subsequently measured. The standard curve shown in Figure A.1 was made based on the standards, and was used for quantification of ammonium concentrations in the samples.

The quantification of nitrite was based on the reaction between nitrite and sulphanilamide under acidic conditions, resulting in the formation of a diazonium ion (Bratton & Marshall, 1939; Dimitrios, 2007). This reacts with N(1-napthyl)ethylenediamine, forming a detectable water-soluble, red-violet compound. Firstly, standards were made from a KNO_2 stock, with known nitrite concentrations at 0, 0.025, 0.05 and 0.1 mM. Two reagent mixes were prepared. The first comprised of 0.2g/L N(1-naphtyl)ethylenediaminedihydrochloride in 1.5M HCl, while the second comprised of 10g/L sulfanilic acid in 1.5M HCl. The two mixes were combined in a 1:1 manner, of which 850µl was added to Eppendorf tubes containing 170µl of sample or standard. The tubes were vortexed for 15 seconds, followed by incubation in the dark at room temperature for 10 minutes. The absorbance at 543nm was subsequently measured, and a standard curve was used to determine the concentration of nitrite in samples. The standard curve is shown in Figure A.2.

The method applied for quantification of nitrate was based on the reaction between nitrate and salicylic acid under highly acidic conditions, forming nitrosalicylic acid (Zhao & Wang, 2017). The complex turn yellow at pH > 12, and can thus be measured spectrophotometrically. Standards with known nitrate concentrations at 0, 0.5, 2.5 and 5 mM was made from a KNO_3 stock. Nitrite can also react with salicylic acid and was thus removed from the samples prior to addition of the acid. This was done by adding 4.5µl of saturated H_3NSO_3 in H_2O to Eppendorf tubes, followed by the addition of 18µl of sample or standard. The contents were mixed thoroughly by pipetting, allowing N_2 to evaporate. It was added 90µl of a second reagent to the tubes, comprising of 5% (W/v) salicylacid in concentrated H_2SO_4. The tubes were vortexed for 15 seconds, followed by incubation in the dark at room temperature for 10 minutes. Into each tube it was added 900µl of 4M NaOH followed by further incubation in the dark at room temperature for 20 minutes. Lastly, the absorbance at 420nm was measured and a standard curve was made and used for determination of nitrate concentration in the samples. Figure A.3 shows the standard curve.

2.5 Maintenance and cultivation of microalgae

2.5.1 Cultivation media

4L1 medium

Stock solutions of $NaNO_3$, $NaH_2PO_4*H_2O$, $NaSiO_3*9H_2O$, trace elements solution and artificial seawater were made with the components and concentrations given in Table A2, **Table A4** and Table **A5**. A volume of 4ml from each stock solution and trace elements solution was added to artificial seawater, and the total volume was subsequently brought to 1L using artificial seawater. The pH was adjusted to below 4 to avoid precipitation of compounds, followed by autoclaving at 121°C for 15 minutes. Vitamin solution was made of primary vitamin stocks as described in Table A3. It was made two kinds of vitamin solutions, one with cobalamin and one without cobalamin. These were sterile filtered before 0.5 ml was added to separate bottles of autoclaved medium, thus creating both medium with and without cobalamin. The pH of medium was adjusted to ~8.0 before addition of algae culture.

M8a medium

Phosphate-buffer, macronutrients, iron-EDTA and micronutrients stock solutions of 100x were made with the listed components and concentrations as given in

Table **A1**. To make 1L medium, 950ml of ddH2O was first added to a 1L glass bottle. A volume of 10ml of each stock solution was added in the following specific order: phosphate-buffer, macronutrients, iron-EDTA and lastly the micronutrients solution. The medium was supplemented with 3g/L KNO_3 as nitrogen source and additional ddH2O was added to a total medium volume of 1L. The pH was adjusted to ~5.0, followed by autoclaving at 121°C for 15 minutes. Vitamin solution was made and added to autoclaved medium as described for 4L1 medium. Lastly, the pH was adjusted to ~7.0 before addition of algae culture.

2.5.2 Sterile techniques in microalgal cultivation

To avoid contamination of cultures, sterile techniques were emphasized when working with microalgal cultures throughout the entire thesis period. All cultures were cultivated in autoclaved bottles, sealed with cotton stoppers and double layers of aluminium foil. Bottles with gas exchange additionally featured a glass straw, attached to a 0.2μm pore filter, to allow for air flow. Procedures involving the removal of the bottle top were performed in a sterile bench near a gas flame, using both aseptic techniques and sterile equipment.

2.5.3 Cultivating Stem and Inoculum cultures of microalgal strains

Microalgal strain cultures were retrieved from the Culture Collection of Algae and Protozoa (CCAP, Scotland). This was one cobalamin-independent freshwater strain *C. vulgaris* CCAP 211/11B, and two cobalamin-dependent marine strains *I. galbana* CCAP 927/1 and *T. lutea* (Tahitian) CCAP 927/14. All algal cultures were stated as "axenic" upon purchase, meaning that no other organisms should be present in culture. The status of *I.galbana* was however changed during the thesis, stating minimal or no observed bacteria when grown under normal conditions.

Stem cultures were the base for all inoculum cultures and were maintained throughout the experiment period. Inoculum cultures of each algal strain were made to upscale prior to experiments. The medium used for stem cultures and inoculum was 4L1 with all vitamins included for *I.galbana* and *T.lutea* and M8a medium without vitamins for *C.vulgaris* (Guillard, 1975; Kliphuis et al., 2011). Stem cultures were maintained by monthly transferring 2ml culture to 50 ml new medium followed by incubation at 20°C at 130rpm. Light was fixed from the sides, with the average intensity of 79 μmol/s for *C.vulgaris* and 28 μmol/s for the two latter strains. Inoculum cultures were made by adding 20ml stem culture to an autoclaved 1L bottle with gas exchange containing 580 ml prepared medium. The inoculum cultures were incubated at 20°C and 120 rpm in Multitron incubation shaker (Infors HT, Switzerland) for 14 days unless otherwise stated. The light source in the cabinet was fixed from above and ranged from 71 to 85 μmol/s. The inoculum bottles were placed in a manner that ensured approximately similar light intensity.

2.6 Testing algal growth during cobalamin depletion

Figure 2.4 schematically shows the workflow for setting up experiment cultures with and without cobalamin in medium. After incubating the inoculum cultures, OD$_{750}$ was measured. Cultures were collected from each inoculum, taking a volume that ensured similar start OD for all experiment cultures. The collected algal cultures were centrifuged at 4000 rpm at 20°C for 10 minutes in a Multifuge X3R (Thermo Scientific, Germany) to collect algal pellet. The supernatant was discarded from all cultures, and the algal pellets were washed to remove

cobalamin. This was done by resuspending the algal pellets in 5ml of cobalamin-free medium. The suspensions were centrifuged under same conditions as previously in section, followed by the removal of supernatant and resuspension of the washed algae pellets in medium. For each strain, half of the collected pellets were resuspended in medium with cobalamin and the other half were resuspended in cobalamin-free medium. The resuspended algal pellets were poured into separate 500ml Erlenmeyer bottles, which contained medium and had no gas exchange tops. The total volume for each experiment culture was 200ml. The cultures were set in a Multitron incubation shaker (Infors HT, Switzerland) at $20^{\circ}C$ with 120rpm. The light source came from above and ranged from 82.2 to 93.9 µmol/s. The bottles were rotated systematically every other day during the incubation period to ensure approximately equal light exposure. OD_{750} was measured on average every 2-3 day throughout the incubation period. The cultures were regularly checked in microscopy, to validate healthy and growing cells.
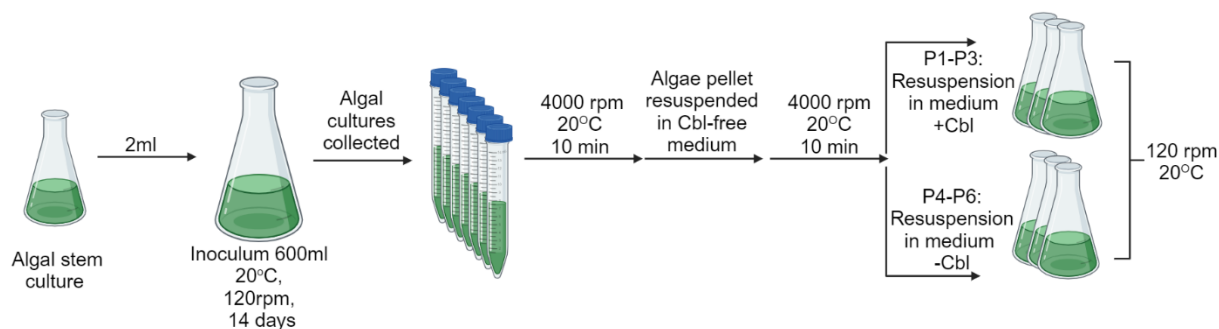
Figure 2.4 Schematic overview of the setup of algal cultures with cobalamin (+Cbl) and without (-Cbl), shown for one strain. Some of the inoculum culture is collected and centrifugated to obtain pellet, which is washed and further resuspended in medium with or without cobalamin. Illustration is created using Biorender.com.

In the middle of the incubation period, the experiment cultures were transferred to new medium. OD_{750} were then measured, and a volume ensuring a similar starting OD for the new cultures was collected from each culture. The collected cultures were centrifuged at 4000rpm at $20^{\circ}C$ for 5 minutes, and the supernatant removed. The algal pellets were resuspended in its respective media and poured into new bottles containing medium. The total volume of the new cultures was 200ml. These cultures were incubated in shaking incubator under the same conditions as described previously in section.

2.7 End point sampling and analysis of algal cultures

At end of incubation, 1ml from each algal culture in 2.6 Testing algal growth during cobalamin depletion was collected and centrifuged at 13000rpm at 4°C for 5 min. Samples were also collected from each of the three stem cultures and centrifuged under equal conditions. The supernatant was discarded, and the pellet kept at -80°C until further use in microbial cobalamin disc diffusion assay, ELISA and 16S rRNA amplicon sequencing.

Algal pellets to be used in microbial cobalamin disc diffusion assay and ELISA were mechanically lysed in FastPrep tubes containing glass beads of sizes 106μm, 425-600μm, and 2mm (Sigma-Aldrich, USA). The pellets were resuspended in 500μl STAR buffer prior to addition into the FastPrep tubes. Mechanical lysis of the cell pellets was conducted at MagNaLyser (Roche Diagnostics, Germany) with speed 6200rpm for 2*20 seconds. The samples were cooled down in between runs. After lysis, the tubes were centrifuged at 13000rpm for 3 minutes at 4°C, before 200μl supernatant was kept for analysis.

ELISA

The SENSISpec ELISA Vitamin B_{12} - Enzyme Immunoassay for quantitative determination of vitamin B_{12} in Food kit was used to perform ELISA on the algae pellets and medium. The analysis was performed following manufacturers protocol. Into separate wells coated with anti-vitamin B_{12}, 50μl of standards, supernatant of mechanically lysed algae pellets and medium was transferred. The standards were provided by manufacturer, holding a cobalamin concentration of 0, 0.4, 1, 4, 10 and 40 ng/ml. It was then immediately added 50μl of vitamin B_{12}-peroxidase into the same wells of the microtiter plate. The microtiter plate was covered and incubated at room temperature with shaking at 120rpm for 60 minutes. Washing of the wells was performed three times as follows: the contents of wells were discarded, 300μl of diluted washing solution was added into each well followed by removal of well contents. A volume of 100μl substrate solution was added into each well, followed by incubation of the plate in the dark at room temperature for 20min. The enzymatic reaction was stopped through adding 100μl stop solution (0.5M H_2SO_4) into each well. A_{450} was subsequently measured with reference wavelength at A_{620} on a Varioscan Lux plate reader (Thermo Fisher Scientific, Finland). The standard curve shown in Figure A.4 was made and used to calculate the cobalamin concentration in the samples.

2.8 Direct N2O exposure of algae

Figure 2.5 presents a schematic overview of the workflow for directly exposing microalgae to N_2O. After incubating the inoculum cultures of all strains for 23 days, the OD_{750} was measured. To ensure active growth of the algae upon experiment, all inoculum cultures were diluted in fresh medium. Before adding the culture to medium, $NaHCO_3$ was added to medium to a final concentration of 2.0 mM to ensure sufficient carbon in medium. The pH was adjusted to ~7.0 for M8a and ~8.0 for 4L1 after addition of carbonate. It was collected a volume of all inoculum cultures, ensuring a similar start OD for the experiment cultures of all strains. The collected volumes were added to new 1L bottles containing new prepared medium, resulting in a final total volume of 600 ml. The experiment cultures were incubated at 20°C at 120rpm in incubation chamber. Light came from above and ranged from 76.2 – 88.5 mmol/s. OD_{750} of cultures were measured every day for the last 3 days of incubation period to ensure that the algae were growing. After incubating for 6 days, the cultures were diluted 1:1 in its respective medium with added carbonate. The air of autoclaved and capped empty glass vials with volume 120ml was evacuated and replaced with either N_2O or Helium as described in 2.2.2 Cultivation under defined atmosphere. Through using a 50ml syringe and needle (1.2x40mm), 30ml algal culture was added to the gas-filled vials. An additional needle was used during the injection to reduce the pressure within vials. As control, 30ml medium was transferred to separate vials with N_2O and Helium. All glass vials were incubated for 24 hours in incubation chamber under the same conditions as described earlier in section. The concentration of O_2 in headspace of all cultures were subsequently measured using robotized incubation system as described in 2.4.2 Analysis of gases in headspace.
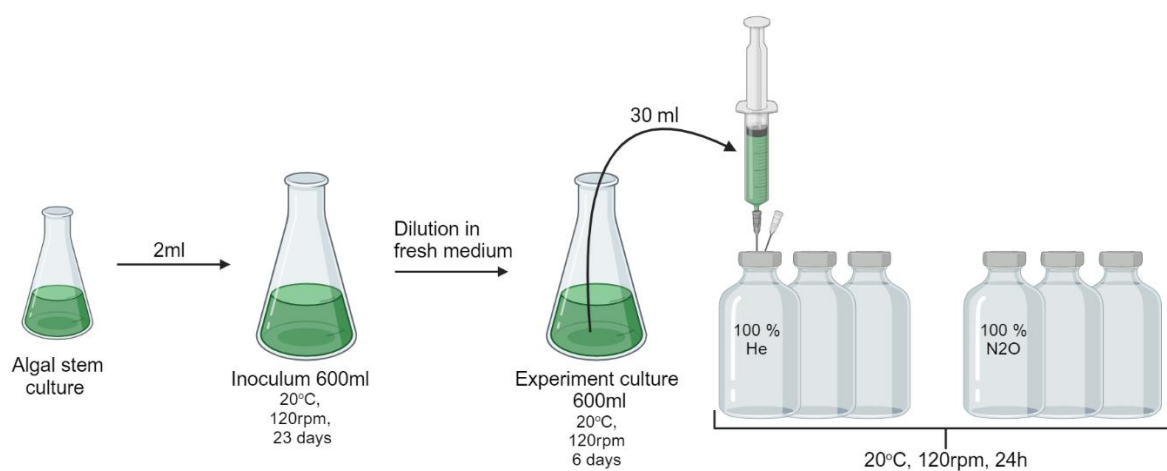
Figure 2.5 Schematic overview of the workflow for directly exposing one algal strain to N$_2$O and Helium in sealed glass vials. Illustration is created using Biorender.com.

2.9 DNA analysis

2.9.1 DNA extraction for 16S rRNA amplicon sequencing

Sample lysis and DNA extraction of algae and sediment samples were performed using the Quick DNA^{TM} Fecal/Soil Microbe 96 MagBead kit (Zymo research, USA).

The initial treatment of the sediment samples and algae pellets was different. The sediment samples were thawed at ice and homogenized before 200µl was transferred to the ZR BashingBead Lysis Tubes provided by manufacturer. A volume of 750µl Lysis Solution (Bashing Bead buffer) was transferred to the tubes. The algae pellet samples were thawed at ice and resuspended directly in 750µl Lysis solution before addition to the Lysis tubes. For the following steps, the samples were treated in the same manner. The samples were mechanically lysed at 6200 rpm for 2*20 seconds in the MagNaLyser, with cooling on ice in between runs. This was followed by centrifugation at 13000rpm at 4°C for 1 min before 200µl of the supernatant was transferred to new tubes and kept at 4°C until DNA extraction.

DNA extraction was performed automatically at KingFisher Flex robot (Thermo Fisher Scientific, USA). The KFFlex plates were prepared and placed into their respective positions in robot. All plates, except for the elution plate, were 96 DeepWell plates. The tip plate contained a 96 DW Tip comb, while the sample plate contained 600µl Quick DNA Mag Binding Buffer, 25µl Mag Binding Beads and 200µl sample lysate in each well. The PreWash and two

additional Wash plates had wells containing 900µl Pre-Wash buffer and 900µl gDNA Wash buffer, respectively. Lastly, the elution plate was a 96 standard plate with each well containing 60µl elution buffer. The program "Zymo_QuickDNAFecalSoil" was run. The concentration of extracted DNA in ng/ml was quantified for all samples using Quibit fluoremeter (Invitrogen, USA).

2.9.2 Library preparation of 16SrRNA amplicons for Illumina sequencing

First stage PCR of 16S rRNA (Amplicon PCR)
PCR mix was made with the following components and volumes: 5µl 5X HOT FIREPol® Blend Master Mix Ready to load, 0.5µl of both 10µM forward (341F) and 10 µM reverse (806R) primer, and nuclease-free water. Variable region 3-4 of the 16SrRNA gene was the target of the primers and the full primer sequences are given in Table A6. The reaction mix was added to wells in a 96 PCR plate together with 2µl extracted DNA to a total volume of 25µl per well. The PCR reaction program on Thermal cycler (Applied Biosystems, Singapore) was as follows: 95°C for 15 min, followed by 25 cycles of 95°C for 30 sec, 55°C for 30 sec and 72°C for 45 sec before 72°C for 7 min and finally 10°C.

Gel electrophoresis was performed to verify the PCR product. A 1% Agarose (Thermo Fisher Scientific, USA) gel, containing PeqGreen DNA/RNA dye (VWR, Germany) was prepared and placed in gel chamber containing 1% Tris/Acetate/EDTA (TAE) buffer. The samples were loaded onto the gel, and a 100bp DNA ladder (Solis BioDyne, Estonia) was used as reference. Gel electrophoresis was performed for 30 minutes at 80V and 400mA.

Clean-up of PCR product
Clean-up was performed at the Biomek4000 robot (Beckman Coulter, USA) using 0.1% Sera-Mag Speed beads solution. In wells of a new PCR plate, 10µl PCR product was combined with 10µl room temperate vortexed magnetic beads (1X). The robot did first incubate the samples for 5 minutes, before placement on magnet for 2 minutes. The supernatant was removed, 100µl 80% ethanol was added into each well, followed by incubation for 30 seconds before removal of ethanol. This wash step was repeated once and removal of all ethanol in the wells was ensured by air-drying for 30 minutes. Lastly, eluation occurred by removing the samples from magnet

and adding of 20µl PCR water into each well. After 2 minutes, the plate was moved to the magnet and incubated for 5 minutes. A volume of 16µl eluate was transferred to a new plate.

Index PCR

A master mix of PCR components, without template DNA and primers was made and 13µl was added into each well of the PCR plate. The mix comprised of 5x FIREPOL® Master Mix Ready to Load (Solis BioDyne, Estonia) with final concentration at 1x and PCR water. epMotion 5070 robot (Eppendorf AG, Germany) was used to dispense index primers into each well. It was made sure that the forward and reverse primer combination in each sample was unique. The final concentration in each well was 0.2µM for both reverse and forward primer. Table A7 gives the full sequence of the Illumina PRK primers used in this thesis. Lastly, DNA template was added with a volume of 2µl into each well. The PCR program was as follows: 5 min at 95°C, 10 cycles with 30 seconds at 95°C, 1 minute at 55°C and 45 seconds at 72°C before 7 minutes at 72°C and lastly 10°C. The PCR product was checked at gel as for amplicon PCR.

Quantification and normalization

The DNA amount in each sample was determined empirically by studying the intensity of each bond on the index PCR gel. The samples were subsequently pooled manually with respect to the DNA amount, ensuring similar amounts of DNA from each sample in the resulting pool.

Clean-up of pooled library

Clean up of the library was performed manually using 0.1% Sera Mag Speed Beads solution. The beads were brought to room temperature and homogenized before 0.8X µl was transferred to the tube with the pooled library. After mixing the content well, the tube was incubated at room temperature for 5 minutes. The tube was set on magnetic stand for 2 minutes, allowing for the supernatant to clear, which then was removed and discarded. With the tube still on magnet, the beads were washed by adding 200µl freshly prepared 80% ethanol. The pellet was not resuspended, and it was made sure that the entire pellet was covered in ethanol. After 30 seconds, the supernatant was removed and discarded. This wash step was repeated once, and it was made sure that all the excess ethanol was removed. The beads were air-dried for 15 minutes with open lid. The tube was removed from the magnetic stand and 50µl PCR water was added. After mixing the content well, the tube was incubated for 2 minutes, and 40µl of the supernatant

was subsequently transferred to a new tube. The DNA concentration in ng/ml was determined using Quibit. The purified product was checked at gel as for amplicon PCR.

The sequencing of the 16S rRNA amplicon library was performed on Miseq instrument by Norwegian Sequencing Centre (NSC) in Oslo.

2.10 Data handling and statistical analysis

2.10.1 Two-sample t-test

Two-sample t-test was performed to validate statistical significance in difference of mean in growth of cobalamin-dependent *E. coli* with respect to N_2O concentration. The analysis was performed in R v4.2.2 (R Core Team, 2024) and the confidence level was set to 0.05.

2.10.2 Processing of 16S rRNA Amplicon Illumina sequencing data

The data from 16S rRNA amplicon sequencing was processed using R and Appendix D: 16S rRNA data processing shows most of the R-code used in the current thesis. Firstly, demultiplexing was performed and involved separating the reads based on information provided by the barcodes added to each sample during index PCR.

Next, the reads for each sample were processed using the open source VSEARCH tool (Rognes et al., 2016). Firstly, the reads were trimmed at the 3' end based on quality scores given as output during demultiplexing. The quality score of a base, or q, measures the probability of that base-call being incorrect (Ewing & Green, 1998). High quality values correspond to low error probabilities. Trimming involves removal of the low-quality ends from the reads, which often results in a higher tendency for the reads to merge. In the present thesis, the R1 reads were trimmed with 20 bases and the R2 reads were trimmed with 60 bases. The minimum read length, i.e. the minimum length of R1 and R2 reads after trimming, was set to 200. The maximum error probability allowed was set to 0.01 and all reads with higher average error probability was discarded. An error probability of 0.01 corresponds to a quality score of 20 and indicates that every 100bp sequenced may contain one error (Ewing & Green, 1998).

The next step of the VSEARCH pipeline involved finding operational taxonomic units (OTUs), i.e. unique variants of 16S sequences in the data (He et al., 2015), through identity clustering. An identity threshold on 0.97 was used, meaning that sequences with ≥ 97% similarity were clustered together to OTUs. The minimum number of copies for an OTU was set to 2, thus excluding reads that only occurred once (singletons). Lastly, the number of reads corresponding to each OTU in each sample was computed, thus creating a read count table. This gives the number of reads assigned to the different OTUs for each sample.

Taxonomic classification was performed to assign the different OTUs to taxa. The SINTAX algorithm, which is implemented in VSEARCH, was used for such purpose. Sintax-cutoff was set to 0.0, meaning that all possible taxonomic classifications were included in the first place, independently of the confidence score given by the algorithm. The confidence score cutoff was later set to 0.6 in R, thus categorizing all classifications on genus level with score below 0.6 as "unclassified".

The data was normalized using total sum scaling (TSS), which involved dividing all the read counts in a sample by the total amount for the same sample. This resulted in relative abundances of each taxa, which altogether summed to 1 for each sample. Normalization was performed in R with package "phyloseq" (McMurdie & Holmes, 2013). Further data wrangling and plotting were performed in R using "phyloseq" and "ggplot2" (Wickham, 2016).

Alpha- and beta diversity

α-diversity refers to the diversity of taxa within a sample (Calle, 2019). The Shannon index is a commonly used diversity index and takes both the number of unique species and their relative abundances within a sample into account. The calculated values reflect both the species richness, i.e. number of different species, and evenness, i.e. the variability of species abundance. The diversity is calculated with the following formula:

$$H' = -\sum \rho_i log(\rho_i)$$

where ρ_i is the relative abundance of the ith taxon in the sample. The Simpsons index is another commonly used metric, which takes the relative abundance of all species within a sample into account (Simpson, 1949). It measures the probability of two individuals drawn from a sample belongs to the same species and is given by:

$$D = \frac{\sum n(n-1)}{N(N-1)}$$

where n is the number of organisms of a certain species and N is the sum of all organisms for all species. The Simpson index is often presented as 1-D, resulting in large numbers representing samples with high richness and low dominance. The α-diversity of samples were calculated using Shannon and Simpson metrices and visualized using the packages phyloseq and ggplot2 in R.

The dissimilarity in taxa composition between samples is referred to as β-diversity and a commonly used dissimilarity measure is the Bray-Curtis metric (Calle, 2019). This is based on quantifying the number of shared species relative to the number of species in each sample (Bray & Curtis, 1957). The dissimilarity is calculated by:

$$BC_{ij} = 1 - \frac{2C_{ij}}{S_i + S_j}$$

where S_i is the total sum of microbes found in sample i, and S_j is the total sum of microbes found in sample j. C_{ij} is the sum of the minimal value for those species found in both samples. The phyloseq package was used to determine β-diversity using Bray-Curtis dissimilarity metric. A matrix with dissimilarity measures in genus composition between samples was decomposed, and the dimensionality of data reduced, through Principal coordinate analysis (PCoA). The results were visualized using phyloseq-package.

Functional annotation

Functional annotation was performed using the FAPROTAX database (Louca et al., 2016). This database uses available literature on cultured representatives to map prokaryotic taxa to metabolic or other ecological functions. The functions represented in the database is mainly related to biogeochemistry in aquatic environments, with special focus on cycling of sulfur, nitrogen, hydrogen, and carbon.

As the database are compatible with python, a FAPROTAX table compatible with R and with names substituted with NCBI taxonomy was made. Functional annotation assumes that each functional group occurs once in the genome. The amplicon sequencing data contained 16S sequence copy numbers, and was thus converted into genome abundances using rrnDB database (Stoddard et al., 2015). The 16S rRNA gene copy numbers were first total sums scaled before

the relative genome abundance was calculated by dividing relative 16S gene copy number on the gene copy number found for that taxon in rrnDB. Of in total 7965 16S rRNA copy numbers, 6045 entries had no match in the database. The genome abundance of such taxa was found by using the mean 16S rRNA gene copy number found in rrnDB database.

Matches between taxa names in the FAPROTAX database and the data with genome relative abundances was used to predict the function of the microbial community. Because the taxonomic resolution of the data was at genus rank, all species names from FAPROTAX were removed. For each entry in the FAPROTAX database, the matching genera was extracted from the genome relative abundance data table and stored in an additional table. Functional information from the FAPROTAX database was added to the matching rows. It was 115 initial OTUs (genera) of in total 531 (22%), that had a match on genus level in the FAPROTAX database. The genera with no match in the FAPROTAX database was tested on family level, and 43 OTUs (8%) had match. Similarly, function was annotated at order level, with resulting 56 OTUs (11%) having a match. In total, 41% of the initial OTUs had match at either genus, family or order level. At last, the relative abundance of all functional groups was divided on the number of occurrences of taxa in FAPROTAX to ensure that the relative abundances would sum to one for each sample.

Artificial intelligence (AI)

AI was used as a tool for in data analysis, for providing some code, but mainly for troubleshooting upon errors. In cases where code was provided, it was manually verified prior to use in data analysis. Additionally, AI was used during the writing process as a synonym dictionary and in some cases to verify grammatic correctness.

3. Results

3.1 The influence of N₂O on cobalamin in an *E.coli* model system

The effect of N_2O on cobalamin was tested in microbial cobalamin disc diffusion assay and by directly exposing growing cobalamin-dependent *E.coli* to N_2O.

3.1.1 Optimalization of microbial cobalamin disc diffusion assay

Microbial cobalamin disc diffusion assay was first performed to evaluate the effect of cobalamin on growth of the cobalamin-dependent *E.coli* ATCC 14169. The assay plate with disc containing standards of 0, 1, 10 and 100 ng/ml cobalamin after 24 hours of incubation is shown at the bottom of Figure 3.1.A. Clear growth zones surrounding the discs with cobalamin was observable, whilst no growth was observed around the disc with 0 ng/ml cobalamin. The measured colony diameter of the cobalamin-dependent *E.coli* for all concentrations of cobalamin tested is shown in Figure 3.1.B. The average colony dm around discs with 1, 10 and 100 ng/ml was 5.5, 12 and 19.5mm, respectively. This corresponded to a strong linear trend between average concentration and average growth diameter, as shown with R^2 of 0.99. In contrast, the cobalamin-independent WT displayed growth over the entire plate, independently of the cobalamin discs, as shown at the top of Figure 3.1.A.
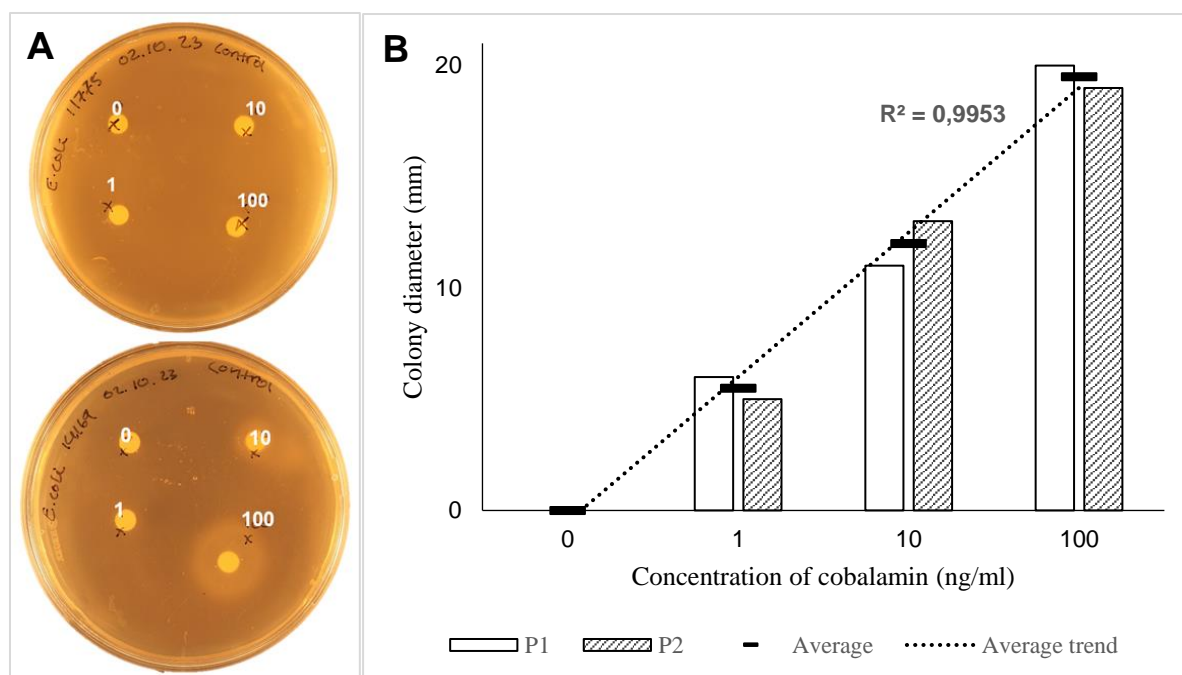
Figure 3.1 A: Microbial cobalamin disc assay plates with discs holding 0, 1, 10 and 100 ng/ml cobalamin marked with white. Top and bottom plate are with cobalamin-independent *E.coli* ATCC 11775 (WT) and cobalamin-dependent *E.coli* ATCC 14169, respectively. **B:** Growth zone diameter of cobalamin-dependent *E.coli* ATCC 14169 around discs containing 0, 1, 10 and 100 ng/ml cobalamin. The y-axis gives the colony diameter in mm, while the x-axis gives the cobalamin concentration of discs in ng/ml. The two bars represent parallel 1 and 2 with the average marked with a black line. The dotted line corresponds to the trend line based on average dm for all concentrations and has $R^2 = 0.99$.

3.1.2 Evaluation of direct exposure of cobalamin to N_2O

When performing microbial cobalamin disc diffusion assay with N_2O-exposed cobalamin standards of 0, 1, 10 and 100 ng/ml, the appearance of the assay plate with cobalamin-dependent *E.coli* after 24 hours was as shown in Figure 3.2.A. There were visible growth zones around all discs containing N_2O-exposed cobalamin, whilst no growth around the disc with 0 ng/ml cobalamin was observed. Figure 3.2.B shows the measured colony diameter of the cobalamin-dependent *E.coli* around discs with N_2O-exposed cobalamin standards and control cobalamin standards. There were no major differences between the growth zones around discs with N_2O-exposed cobalamin compared to the growth zones around control discs. At 1 ng/ml cobalamin, the growth zones around both N_2O-exposed and control discs showed 6 mm. Around discs with 10 ng/ml cobalamin, the average diameter showed 11.5 around N_2O-exposed cobalamin discs and 14 mm around control discs. At 100 ng/ml cobalamin, the average colony diameter showed 21 and 21.5 mm around N_2O-exposed cobalamin and control discs, respectively.
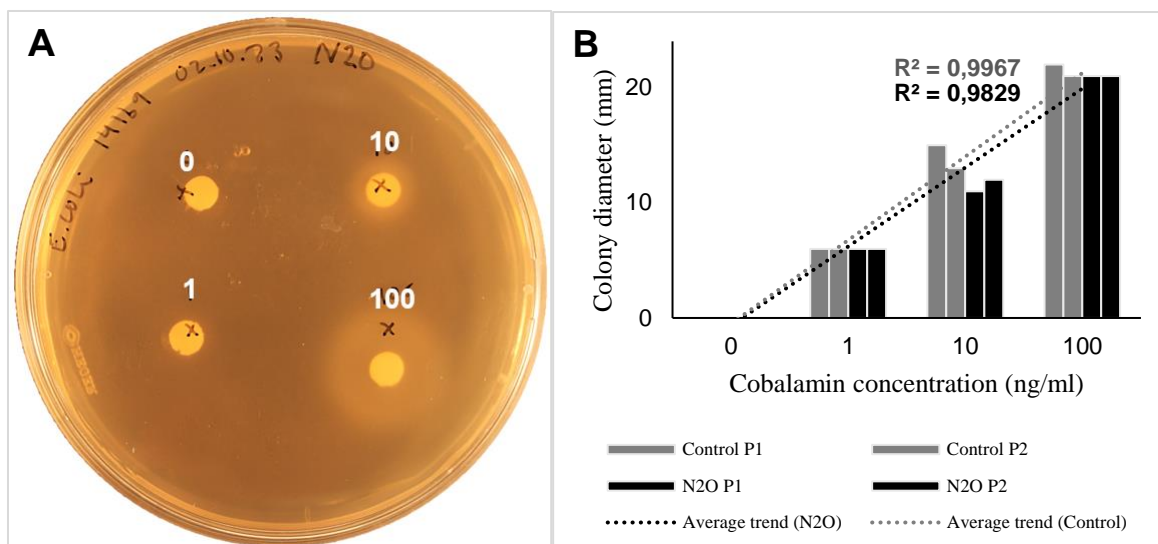
Figure 3.2 A: Microbial cobalamin disc diffusion assay plate with cobalamin-dependent *E.coli* ATCC 14169, incubated for 24h with discs holding 0, 1, 10 and 100 ng/ml N_2O-exposed cobalamin. The concentration in ng/ml is given with white text. **B:** Measured colony diameter of cobalamin-dependent *E.coli* ATCC 14169 at different concentrations of cobalamin. The y-axis gives the growth diameter in mm, while the x-axis gives the cobalamin concentration of discs in ng/ml. Black bars represent the growth zones around discs with N_2O-exposed cobalamin, while the grey bars represent growth zones around control discs. The black dotted line represents the average trend line for N_2O treatment and had $R^2 = 0.98$, while the grey dotted line represents the average trend line for control treatment with $R^2 = 0.99$.

3.1.3 Evaluation of the effect of N_2O on growing *E.coli*

Cultivation of *E.coli* in medium either with or without cobalamin, and either 0% or 100% N_2O in vial, resulted in OD_{600} as shown in Figure 3.3. After 24 hours of incubation, the suspensions of cobalamin-dependent *E.coli*, which were cultivated in the presence of 0% N_2O and cobalamin, displayed an average OD_{600} on 1.1. This was substantially higher relative to the OD of the other suspensions of the same strain. The suspensions of *E.coli,* cultivated in presence of 100% N2O and cobalamin, exhibited the second highest average OD, measured at 0.13. A two-sample t-test revealed significant difference in mean between these two treatments, with a p-value of 0.0072. The suspensions from the two remaining treatments, which lacked cobalamin and had either 100% or 0% N2O in vials, displayed an average OD of 0.088 and 0.060, respectively. After 48 hours, all suspensions for this strain had reached stationary phase, displaying approximately the same OD.

In contrast, the suspensions with cobalamin-independent *E.coli* did not share the same tendency, and displayed similar OD_{600} for suspensions of all treatments, ranging from 0.90 to 1.0. The

suspensions with 0% N_2O in atmosphere showed the highest average OD at 1.0 and 0.99 for the suspensions with and without cobalamin in medium, respectively. The suspensions with 100% N_2O in atmosphere showed average OD at 0.96 and 0.90 for suspensions with and without cobalamin added, respectively.
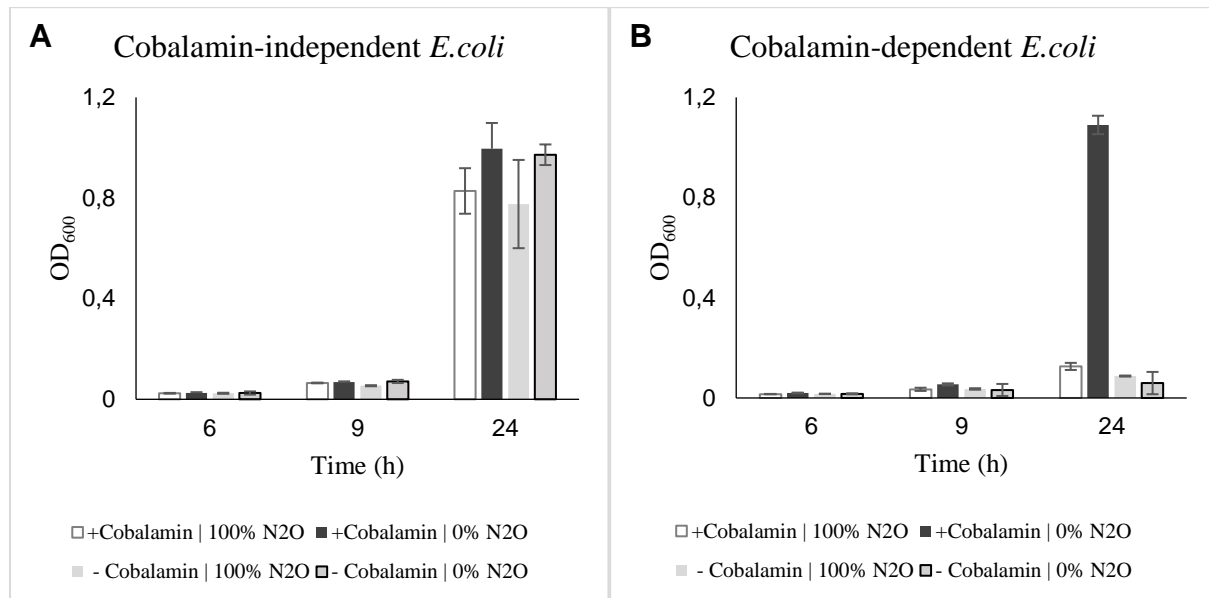
Figure 3.3 OD_{600} of suspensions with cobalamin-independent *E.coli* ATCC 11775 (**A**) and cobalamin-dependent *E.coli* ATCC 14169 (**B**), in presence and absence of cobalamin (+/-) and N_2O (0% / 100%). The y- and x-axis refers to the OD_{600} of suspensions and incubated time in hours, respectively.

By cultivating cobalamin-dependent *E.coli* in medium with cobalamin, and in presence of either 0, 1, 10 or 100 % N_2O in vial, the resulting average OD_{600} after 24 hours was as shown in Figure 3.4. The suspensions with 100% N_2O showed significantly lower OD_{600} after 24 hours relative to the suspensions with 10, 1 and 0 % N_2O, with p-values from two-sample t-tests of <0.05. The average OD showed 0.17 for suspensions in 100% N_2O vials, and 1.0, 0.99 and 0.92 for suspensions in 10, 1 and 0 % N_2O vials, respectively. After 48 hours, the OD of *E.coli* in 100% N_2O vials had reached stationary phase, displaying similar OD as the other suspensions.
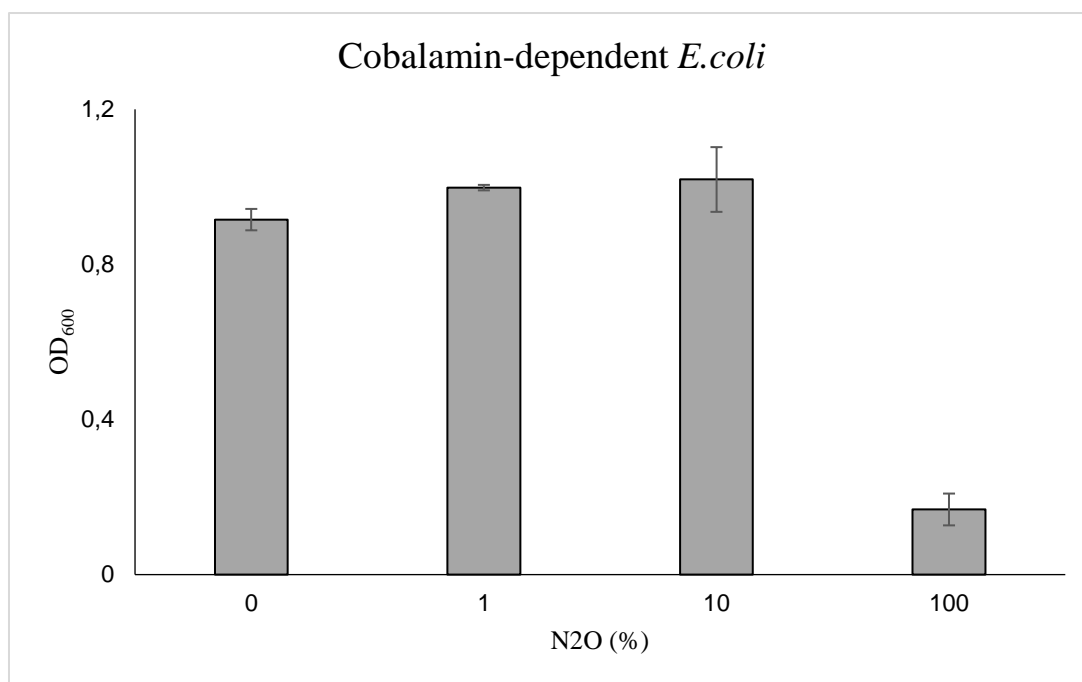
Figure 3.4 Average OD_{600} of suspensions of cobalamin-dependent *E.coli* ATCC 14169 after growing 24h in vials with 100, 10, 1 and 0 % N_2O, corresponding to liquid concentrations at 28, 2.8, 0.28 and 0 mM, respectively. The y-axis refers to to OD_{600}, and the x-axis refers the % N_2O in vials.

3.2 Establishment of N2O production potential from sediment microbiota

After enrichment of sediment with combinations of methanol (31.2 mM), thiosulphate (6.3 mM) and nitrate (1.76 mM), the concentrations of nitrogen compounds in liquid and headspace were measured. In addition, the microbial composition and diversity in the sediments was determined.

3.2.1 Chemical quantification of ammonium, nitrite and nitrate

Concentrations of ammonium, nitrite and nitrate measured in enriched sediment samples after 19 days of incubation, were as shown in Figure 3.5. Overall, the differences in concentration of ammonium were small across the parallels of all enrichment groups and control group. The parallels with methanol and nitrate added showed the highest average concentration of ammonium at 0.13 mM. Sediments with thiosulphate and nitrate added showed the lowest average value with 0.11 mM.

The nitrite measurements showed the highest concentration at 0.75 and 0.95 mM in parallel 2 and 3 with methanol and nitrate added. Parallel 1 of same enrichment group, showed a value of 0.0010 mM. The remaining enrichment groups and control group showed nitrate concentrations on less than 0.1 for all parallels and there was no major divergence in concentration within the groups. The lowest average nitrite concentration was 0.0010 mM, measured in the parallels enriched with thiosulfate and nitrate.

The highest and lowest measured nitrate concentration was 0.21 and 0 mM, found in control parallel 2 and 1, respectively. The third control parallel showed a nitrate concentration of 0.16 mM. The samples enriched with nitrate only showed similar nitrate measures with an average of 0.038 mM. Similarly, the nitrate levels were even in samples enriched with thiosulphate and nitrate and showed an average of 0.055 mM. Lastly, parallel 1, 2 and 3 enriched with methanol and nitrate showed nitrate levels of 0.13, 0.033 and 0.19, respectively.
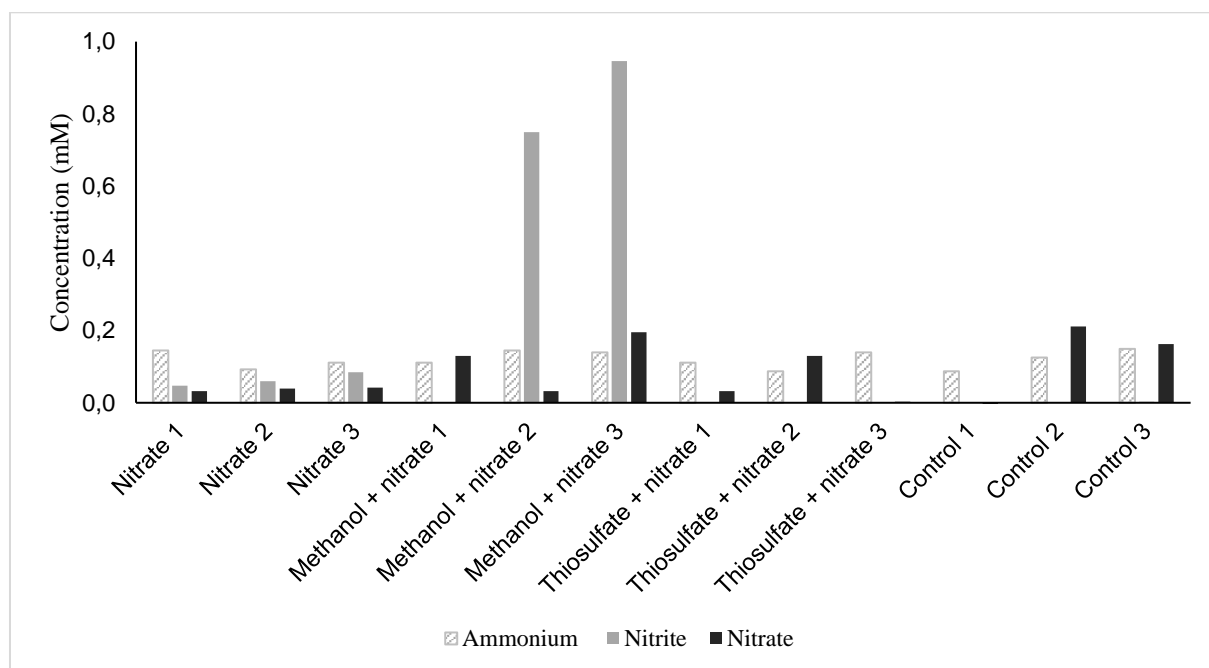
Figure 3.5 The concentration in mM of ammonium, nitrite and nitrate in all enriched sediment samples and controls. The y-axis refers to the concentration of the compounds in mM, whilst the x-axis refers to the sample.

3.2.2 Headspace concentration of nitrogen compounds

End point analysis of N_2, N_2O and NO in enriched sediment samples after 19 days of incubation showed overall highest abundance of N_2, as shown in Figure 3.6. The highest measured N_2 amounts were 147, 119, 137 and 124 μmol in parallel 1-3 enriched with thiosulphate and nitrate and parallel 1 enriched with methanol and nitrate, respectively. Parallel 2 and 3 enriched with

38

methanol and nitrate showed values at 63 and 54 µmol. The parallels enriched with nitrate showed similar values for N_2, with average at 28 µmol. Similarly, the control enrichment group showed similar levels of N_2 for all parallels, with average at 9.7 µmol.

Measurements of NO showed the highest values in parallel 2 and 3 enriched with methanol and nitrate, with 21 and 14 nmol, respectively. The first parallel of the same enrichment group had 0.96 nmol NO. In the samples enriched with thiosulphate and nitrate, NO was not detected in parallels 1 and 3, while parallel 2 showed a presence of 2.8 nmol. Parallel 2 and 3 enriched with nitrate only showed no presence of NO, while parallel 1 showed 2.7 nmol. Lastly, the control group showed no presence of NO in parallel 3, while parallel 1 and 2 showed values on 0.78 and 1.2 nmol, respectively.

The highest measured value of N_2O was 31 and 24 nmol, detected in parallel 2 and 3 enriched with methanol and nitrate. This corresponds to concentrations of 260 and 200 nM. In contrast, the first parallel of the enrichment group showed 1.4 nmol N_2O. The nitrate enrichment group showed similar values of N_2O across the parallels, with an average of 3.8 nmol. This did also apply for the control enrichment group, displaying an average on 0.85 nmol. Lastly, parallel 1 enriched with thiosulphate and nitrate showed the lowest measured N_2O value at 0.64 nmol. The latter two parallels showed 0.75 and 0.71 nmol N_2O.
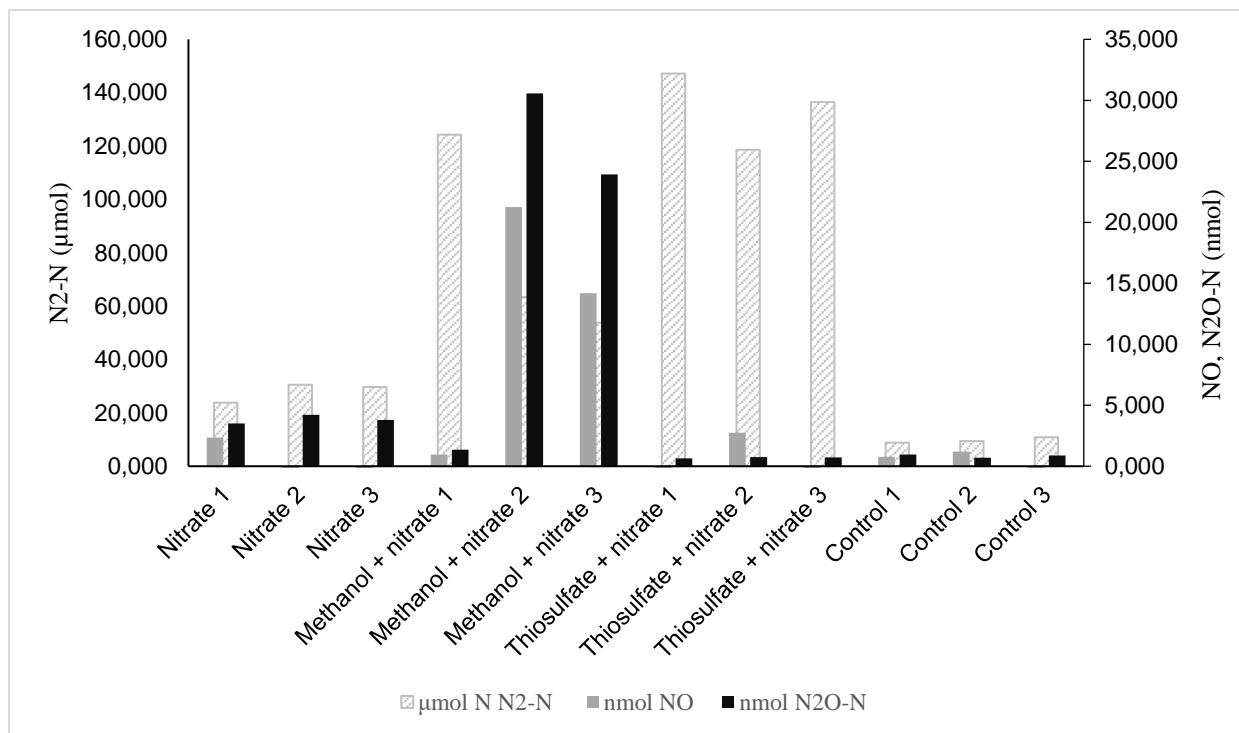
Figure 3.6 End-point measurements of N₂, NO and N₂O in the sediment enrichment cultures. The primary y-axis shows measured values of N_2-N in µmol, whilst the secondary y-axis shows the measured values of NO and N_2O-N in nmol. The x-axis refers to the sample. In samples with nitrate added, the expected amount of N_2 is 121µmol if all nitrate is reduced completely.

3.2.3 Taxonomic composition of sediment enrichments

Taxonomic composition of the sediment samples was determined through analysis of the 16S rRNA amplicon sequencing data. Figure 3.7 shows the relative abundance of the 9 overall most abundant families in each sample. The start control, control and nitrate only parallels had highest amounts of *Desulfobacteraceae, Sandaracinaceae* and *Thioprofundaceae.* In addition, *Oceanispirillaceae* and *Desulfuromonadaceae* was abundant in nitrate only treatment and control treatment, respectively. The methanol and nitrate enrichment group showed highest abundance of the family *Piscirickettsiaceae*, which was represented by the genus *Methylophaga.* The relative abundance of this taxa was 0.0084, 0.32 and 0.55 in parallel 1, 2 and 3, respectively. Parallel 1 of the methanol and nitrate enrichment group did show substantial amounts of *Methylophilaceae*. This family had a relative abundance of 0.49 in parallel 1 and was represented by the genus *Methylophilus.* Parallels enriched with thiosulphate and nitrate showed highest abundances of *Sulfurovaceae* at 0.24, 0.44 and 0.47. This family was represented by the genus *Sulfurovum.*

40
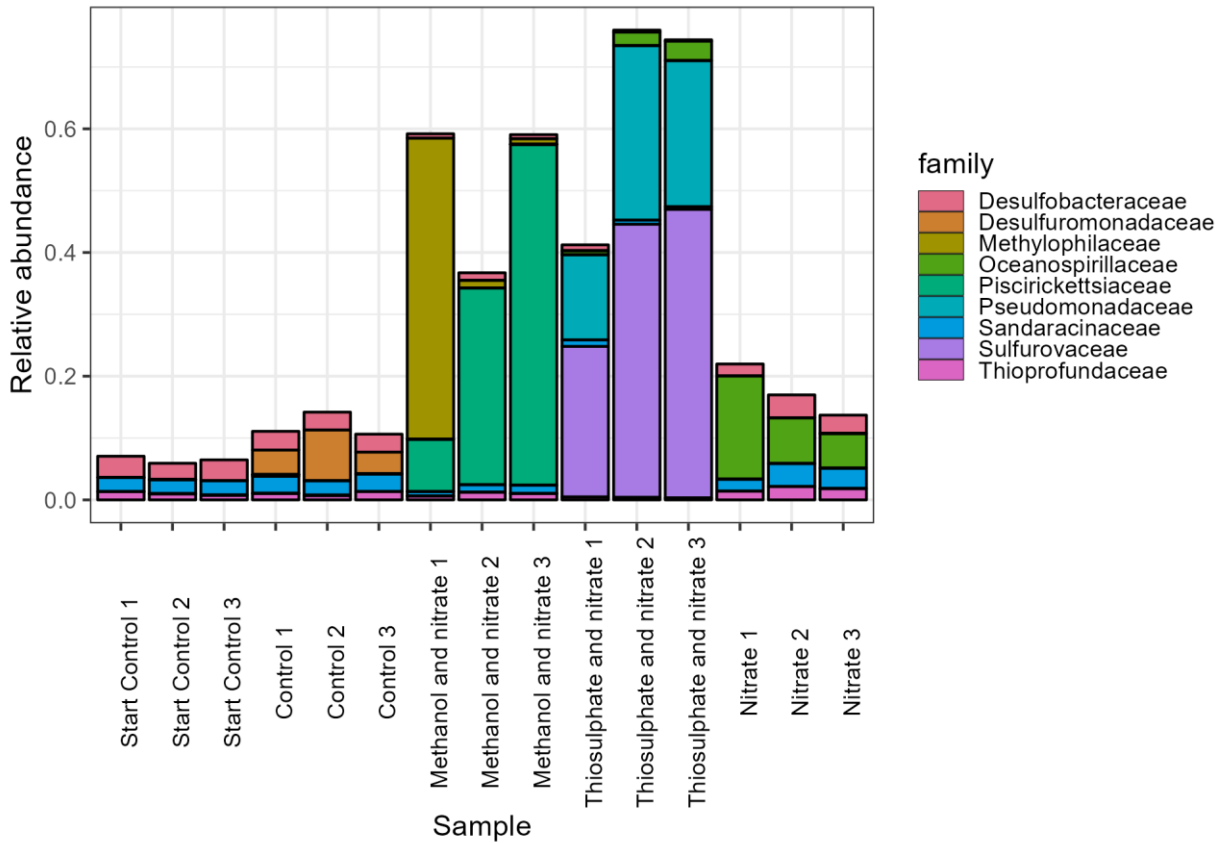
Figure 3.7 The distribution of the overall top 9 most abundant families across in each sample. The y-axis refers to the relative abundance of the different families in each sample, whilst the x-axis refers to the sample.

3.2.4 Microbial diversity of sediment enrichments

α-diversity

The alpha diversity in each sample, calculated using Shannon and Simpson measures, is visualized in Figure 3.8. Both metrics showed the same tendencies in data, with the sediment samples collected at start (start controls) having the highest diversity measures. This group had Shannon measures ranging from 6.3 to 6.5 and Simpson measure at 0.99 for all parallels. Further, the control parallels and the parallels enriched with nitrate only showed second most diversity. The control parallels showed Shannon measure ranging from 5.1 to 5.4 and Simpson measure between 0.98 and 0.99. Nitrate only parallels had diversity measures ranging between 4.8 and 5.4 with Shannon index, and between 0.96 and 0.98 with Simpson index. Parallels enriched with methanol and nitrate, and thiosulphate and nitrate showed overall the lowest diversity. In addition, these enrichment groups showed higher within enrichment group dispersal than the other enrichment groups. Methanol and nitrate enriched parallels showed

41

Shannon and Simpson measures ranging from 3.1 to 4.0 and 0.66 to 0.87, respectively. Parallels enriched with thiosulphate and nitrate showed Shannon measures between 2.4 and 3.9, and Simpson measures between 0.71 and 0.9.
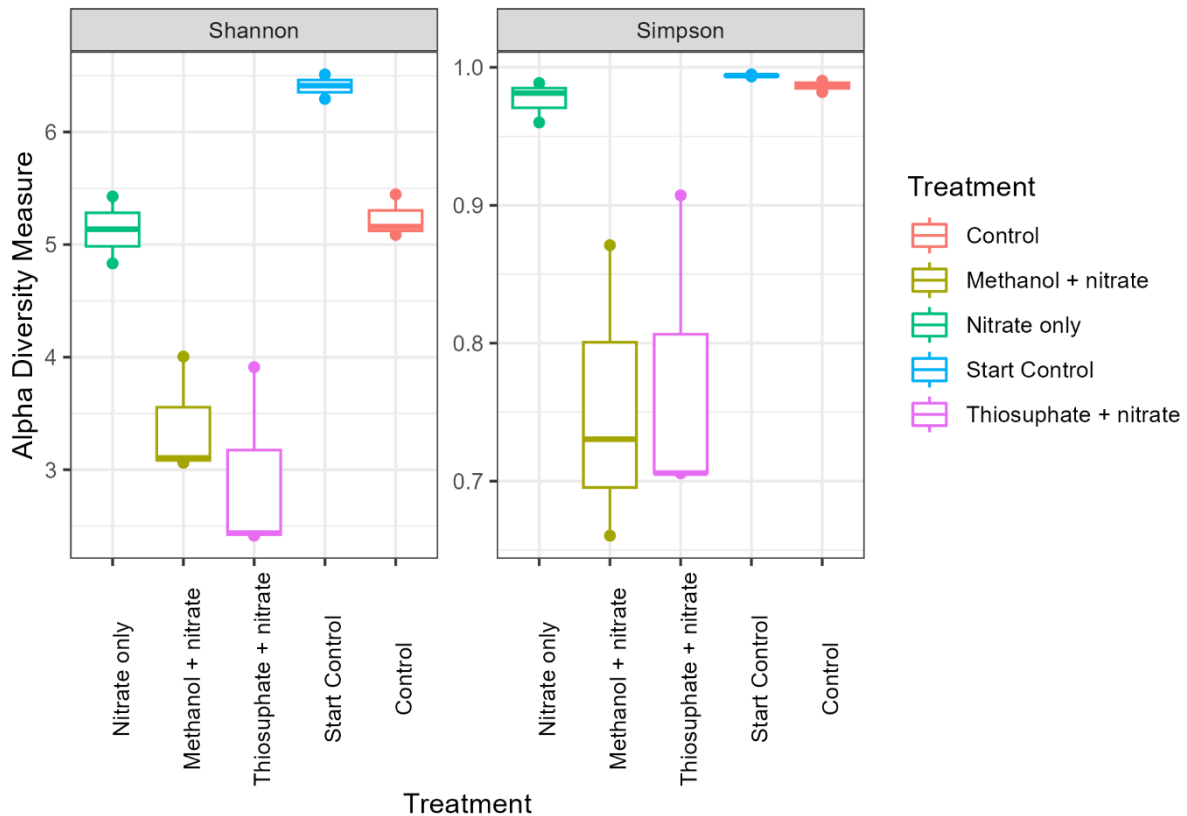
Figure 3.8 Boxplot of alpha diversity of sediment enrichments. The alpha-diversity measure is given at the y-axis with Shannon at left panel and Simpson index (1-D) at right panel. For both panels, the x-axis gives the enrichment treatment. Each treatment has 3 observations each.

β-diversity

By performing a PCoA, using Bray-Curtis dissimilarity index on the sequencing data, the resulting sample distribution on principal coordinate 1 and 2 was as visualized in Figure 3.9. In total, PCo1 and PCo2 explained 52% of the data. The parallels enriched with thiosulphate and nitrate was ordinated furthest away from the other enrichment groups. They showed entire separation from the parallels of other enrichment groups along PCo2. Further, the nitrate only parallels and control parallels were ordinated closely. Visually, the start control parallels displayed the smallest within-group dispersal, and both PCo1 and PCo2 managed to separate this group from the other groups. The highest visual dispersal within a group was seen for the parallels enriched with methanol and nitrate.

42
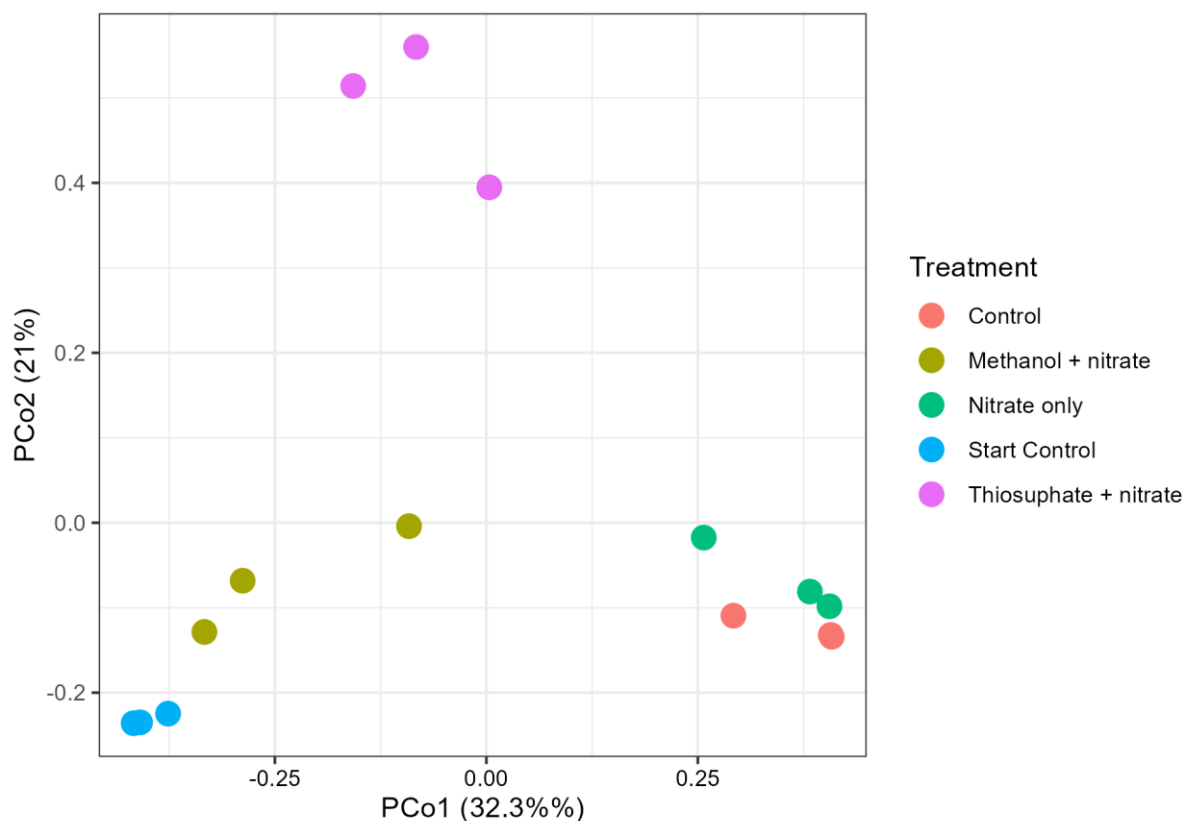
Figure 3.9 PCoA plot, with the x-axis and y-axis showing the first and second principal coordinate, respectively. The PCoA was based on Bray-Curtis dissimilarity index. In total both coordinates explain 52% of the variation in data, with PCo1 explaining 32% and PCo2 explaining 21%. The observations in plot is coloured after enrichment group as explained in legend (given as treatment). Each enrichment group has 3 observations each.

3.2.5 Functional groups

Microbial community functions in sediment samples were predicted, and the 15 groups showing relative abundance above 0.015 is shown in Figure 3.10. Methanol oxidation showed the highest relative abundance with 0.506 in parallel 1 enriched with methanol and nitrate. The functional group was not shown to have abundance above 0.015 in any other sample. Aerobic chemoheterotrophy and sulfate respiration were overall abundant and was observed with abundance above 0.015 in one parallel within all enrichment groups. The highest relative abundances of aerobic chemoheterotrophy were 0.26 in parallel 1 enriched with nitrate and 0.15 in parallel 1 enriched with thiosulphate and nitrate. The highest abundances of sulfate respiration were 0.25, 0.22 and 0.10, found in parallel 3 of start control, parallel 2 of control and parallel 2 enriched with nitrate only, respectively. Parallel 3 with thiosulphate and nitrate added was the only sample that displayed relative abundance of the functional groups nitrate

43

respiration, dark thiosulphate oxidation, thiosulfate respiration, dark sulphur oxidation and sulfur respiration. The abundance was highest for nitrate respiration with a value of 0.22.
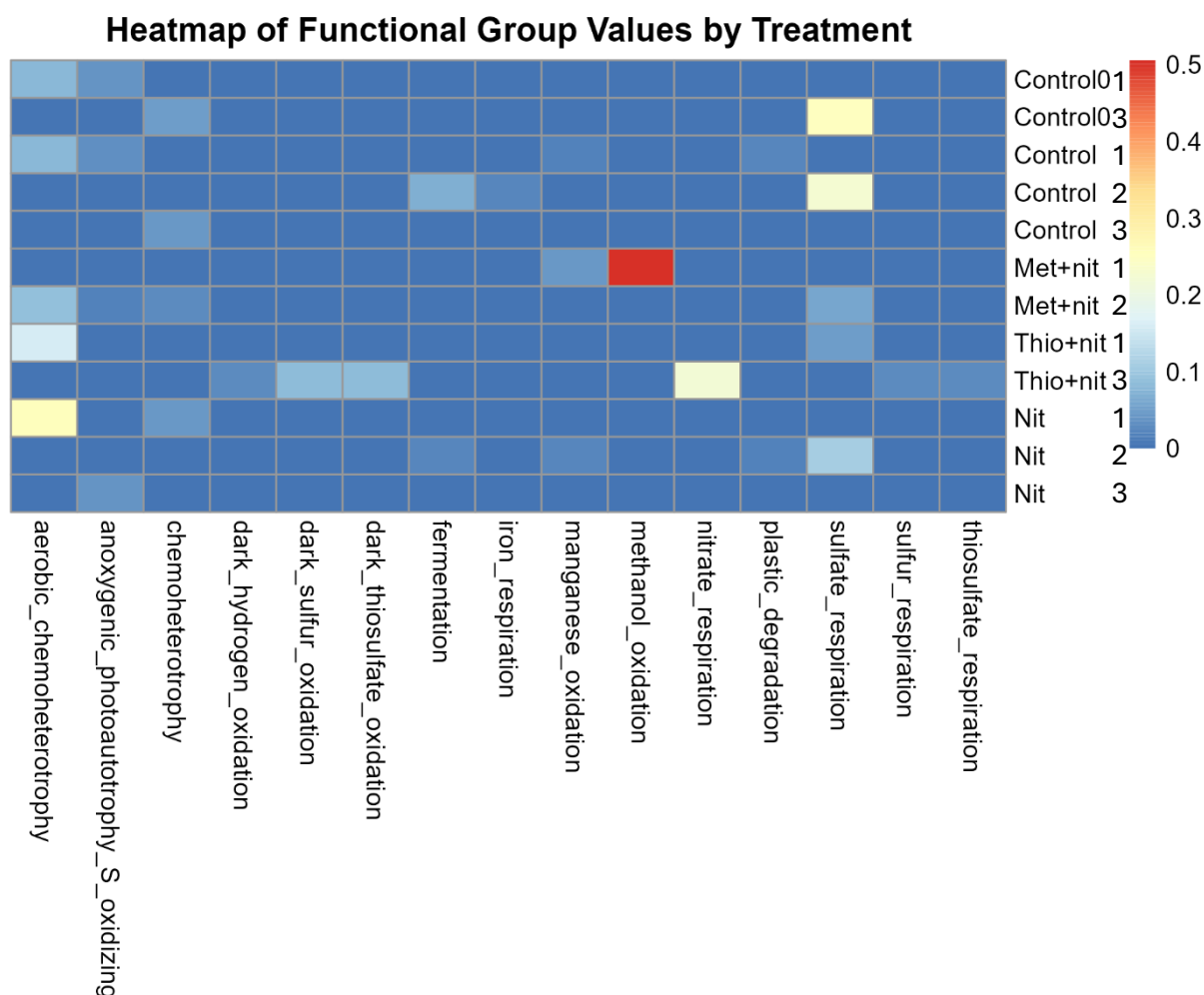
Figure 3.10 Predicted community functions of sediment samples. The heatmap gives the 15 functional groups displaying relative abundance above 0.05 for at least one of the sediment samples. The functional groups are given on x-axis and sample is given on y-axis. The colour of a box indicates the relative abundance of that functional group for the given sample. Label on right shows the colour spectre with corresponding relative abundance. Three samples are excluded from the figure, due to no relative abundance above 0.015 for the functional groups given above. This is "start control 1", "methanol and nitrate 3" and "thiosulphate and nitrate 2".

3.3 Algal response to cobalamin depletion and inactivation

The depletion of cobalamin and the effect of N_2O on growing algae was investigated through 2 main experiments. It was also investigated for the presence of cobalamin and bacteria in algal cultures.

3.3.1 Evaluation of the effect of cobalamin depletion on algal strains

To evaluate the effect of cobalamin on growth of algal strains, the strains was grown in medium with and without cobalamin. Neither *C.vulgaris* CCAP 211/11b, *T.lutea* CCAP 927/14 nor *I.galbana* CCAP 927/1 showed any detectable effect of presence or absence of cobalamin in medium, as shown in Figure 3.11, Figure 3.12 and Figure 3.13, respectively. For each strain, the average OD_{750} showed the same tendencies independently of medium over the entire incubation period. This tendency did also apply after the cultures were transferred to fresh media.

C. vulgaris had start OD at 0.45 for all parallels. The highest OD_{750} was reached at day 29, with an average value of 1.73 for the cultures with cobalamin in medium and 1.58 for the cultures without cobalamin in medium. After transferring the cultures to new medium, the start OD_{750} was 0.4 for all parallels. Average OD reached 0.84 for both cultures with and without cobalamin added at endpoint.
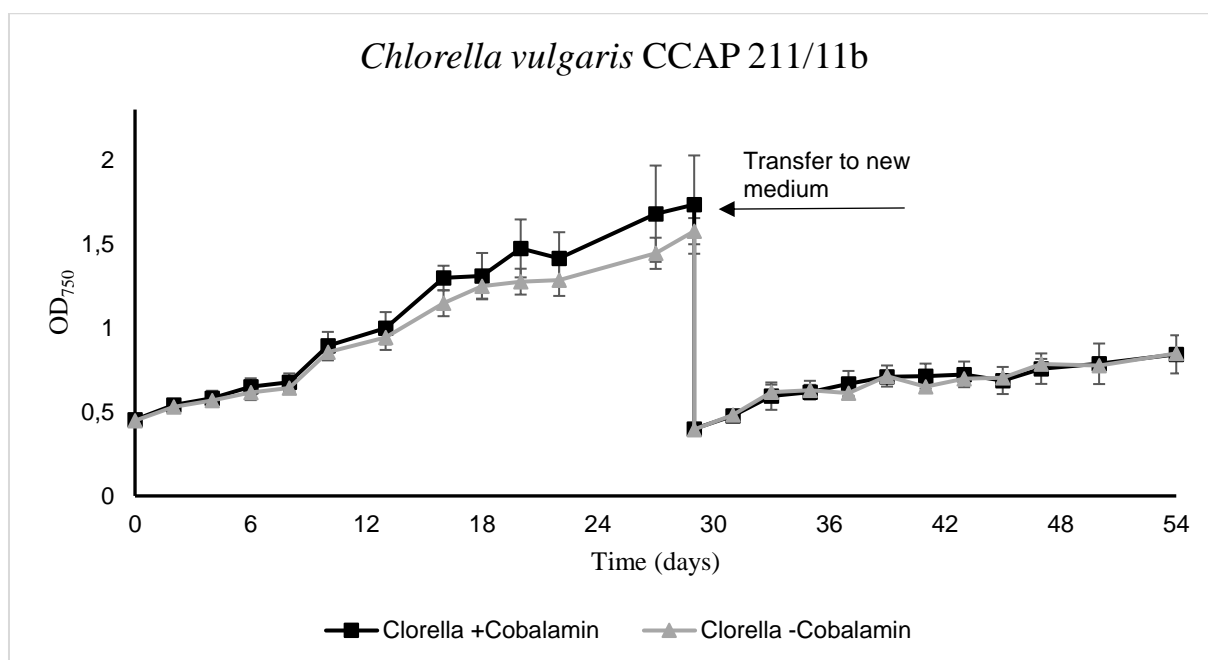
Figure 3.11 Displaying growth of *C. vulgaris* CCAP 211/11b for 54 days. The y- and x-axis refers to the OD_{750} and incubation time (days), respectively. Black line represents the average OD of triplicates grown in medium with cobalamin and grey represents the average OD of triplicates grown in cobalamin-free medium. The SD is given for for each triplicate. The reduction in OD at day 29 is due to transfer of the culture in fresh medium.

T.lutea had start OD_{750} at 0.41 for all parallels. The largest average OD was at day 29, with 0.92 for cultures with cobalamin in medium and 0.84 for cultures without cobalamin. After transfer to new medium, the start OD was in average 0.35 for cultures with cobalamin in medium and 0.32 for cultures without cobalamin. The maximum average OD of the second period was reached at day 50 with values of 0.47 and 0.49 for cultures with and without cobalamin added, respectively.
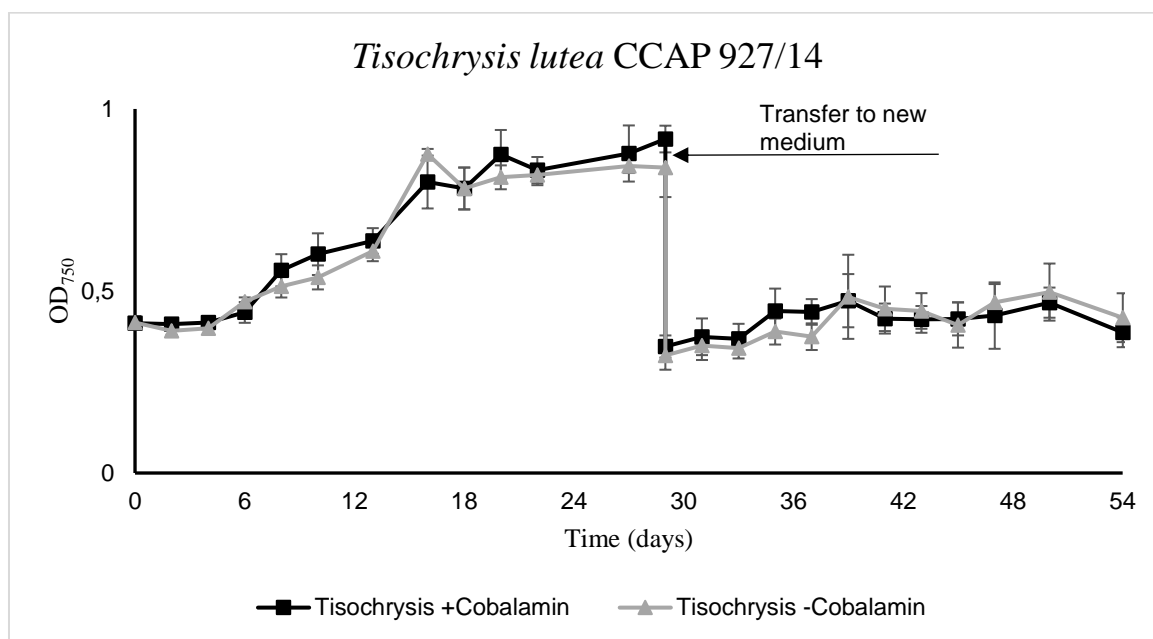
Figure 3.12 Displaying growth of *T. lutea* CCAP 927/14 for 54. The y- and x-axis refers to the OD at A_{750} and incubation time (days), respectively. Black line represents the average OD of triplicates grown in medium with cobalamin and grey represents the average OD of triplicates grown in cobalamin-free medium. SD is given for each triplicate. The reduction in OD at day 29 is due to dilution of the culture in fresh medium.

I.galbana started with average OD_{750} at 0.045 for cultures with cobalamin in medium and 0.047 for cultures without cobalamin. The growth was similar, and the highest average OD was measured at day 33, showing 0.91 and 1.0 for cultures with and without cobalamin added, respectively. After transferring to new medium, the highest average OD reached was at day 47, with values of 0.74 and 0.75 for cultures with and without cobalamin.
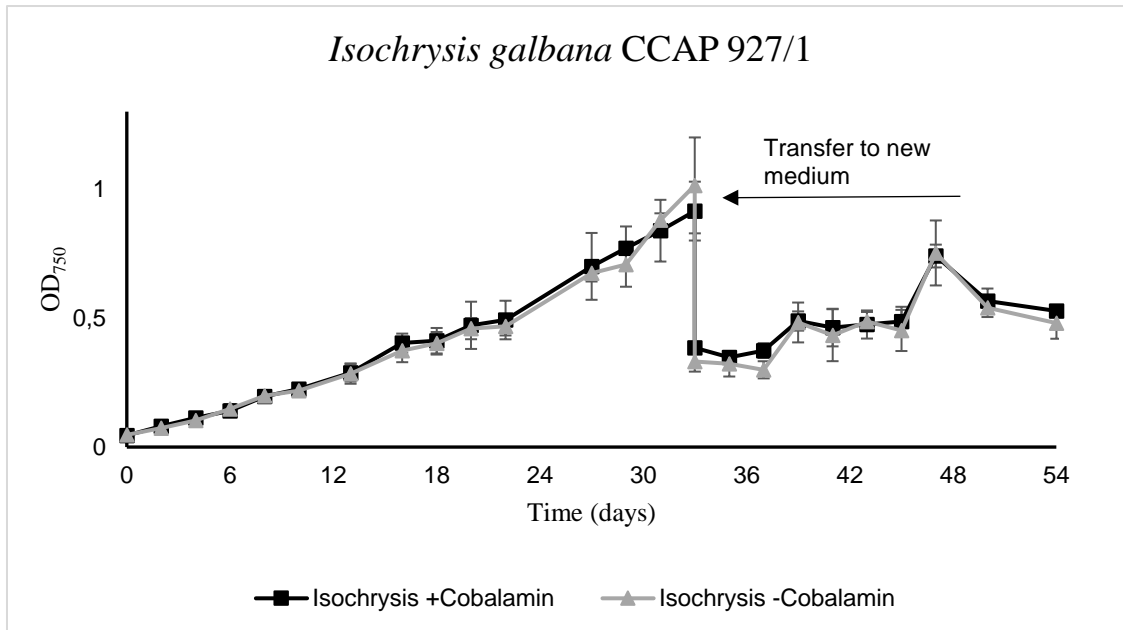
Figure 3.13 Displaying growth of *I. galbana* CCAP 927/14 for 54 days. The y- and x-axis refers to the OD at A_{750} and incubation time (days), respectively. Black line represents the average OD of triplicates grown in medium with cobalamin and grey represents the average OD of triplicates grown in cobalamin-free medium. SD is given for each triplicate. The reduction in OD at day 33 is due to dilution of the culture in fresh medium.

3.3.2 Evaluation of algal response to direct exposure of N_2O with O_2 as proxy

By exposing growing algal suspensions to N_2O and Helium, the end-point oxygen level in vials for each strain was as shown in Figure 3.14. Vials with *I.galbana* showed levels of oxygen ranging from 67 to 116 µmol in vials with N_2O and from 81 to 166 µmol in helium vials. *T.lutea* had oxygen ranging from 96 to 149 µmol in N_2O vials and from 89 to 192 µmol in vials with helium. *C.vulgaris* vials with N_2O showed oxygen levels between 76 and 126 µmol, whilst the vials with helium had levels between 75 and 119 µmol. Control vials with had oxygen levels ranging from 14 to 129 µmol for N_2O vials, and from 92 to 131 µmol for helium vials.
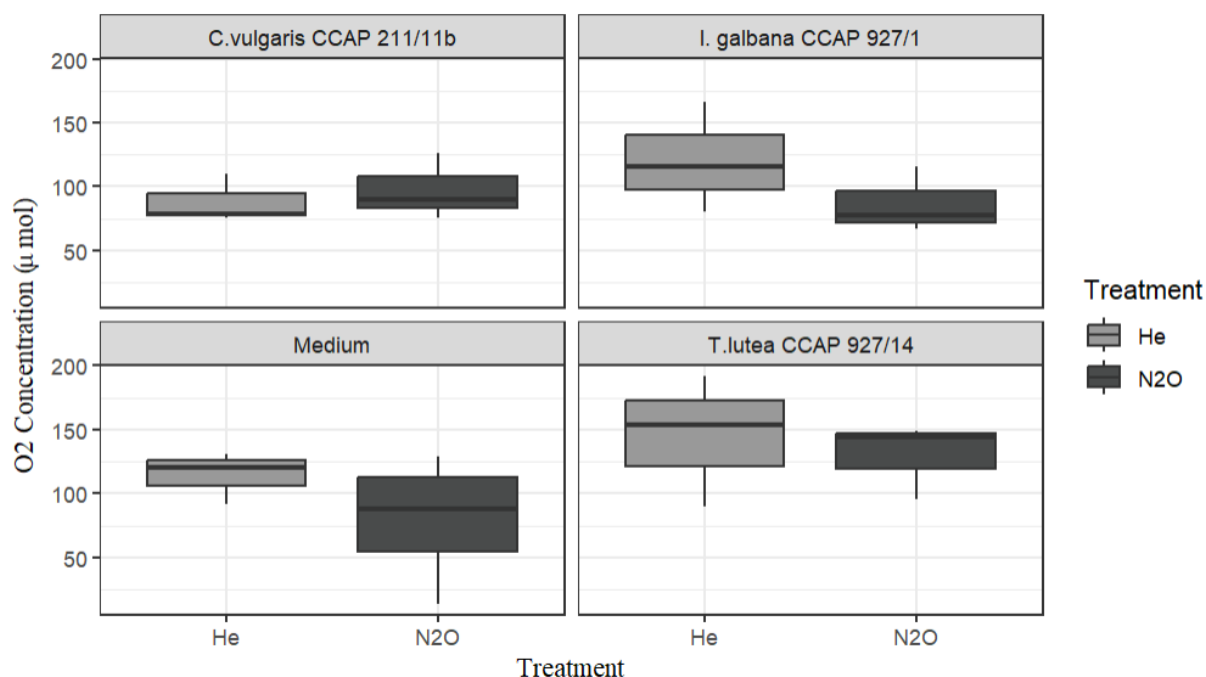
Figure 3.14 Boxplot over measured oxygen in vials with algal culture and N_2O or helium. The figure is faceted after strain and medium. The y-axis refers to the measured oxygen in µmol, whilst the x-axis refers to the treatment, i.e. N_2O or Helium in vials. The treatment is also given with color, with light grey representing vials with Helium and dark grey representing vials with N_2O. The median value is given with a thick black line representing the middle value of oxygen for each strain within each treatment.

3.3.3 Evaluation of potential cobalamin contamination of algal cultures

To investigate if cobalamin contamination was the cause of the observed algal growth pattern in 3.3.1 Evaluation of the effect of cobalamin depletion on algal strains, ELISA and microbial cobalamin disc assay were performed.

ELISA

ELISA was performed to quantify cobalamin concentration in algal suspension pellets collected at incubation end, and the results were as shown in Figure 3.15. Only the suspensions of *I. galbana* without cobalamin in medium and 4L1 medium with cobalamin showed average cobalamin concentration above the given sensitivity of assay (0.3 ng/ml). *I.galbana* showed an average cobalamin concentration on 0.32 ng/ml for the suspensions without cobalamin added to medium and 0.21 ng/ml for the suspensions with cobalamin added to medium. 4L1 medium with cobalamin showed a concentration of 0.33 ng/ml, whilst the medium without cobalamin showed a concentration of 0.21 ng/ml. It was detected 0.26 ng/ml cobalamin in both types of

M8a medium. *T.lutea* showed in average 0.11 and 0.19 ng/ml cobalamin in suspensions with and without cobalamin added to medium, respectively. C.*vulgaris* showed no major difference in cobalamin concentration for suspensions with and without cobalamin added, with values of 0.068 and 0.064 ng/ml.
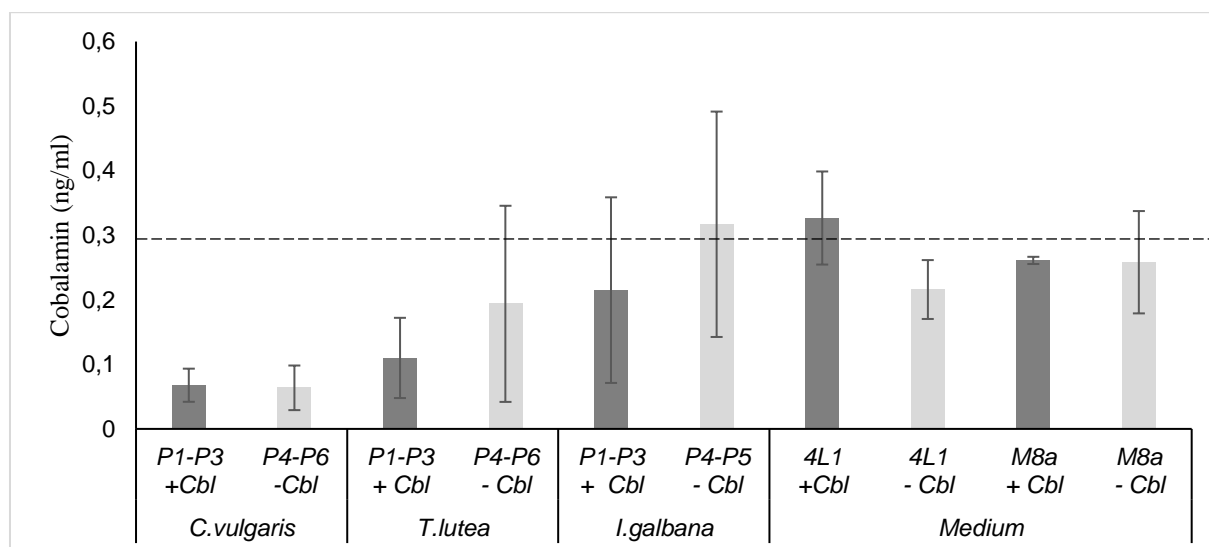
Figure 3.15 The measured concentration in ng/ml of cobalamin in algal suspensions and medium, quantified with ELISA. The x-axis refers to the sample: including cultures of each species grown in medium with or without cobalamin (+Cbl / -Cbl) or the different media used for algal cultivation with or without cobalamin (+Cbl / -Cbl). The y-axis gives the concentration of cobalamin in ng/ml. The line marked at y = 0.3 ng/ml marks the sensitivity of assay.

Microbial cobalamin disc assay

Microbial cobalamin disc assay performed on the mechanically lysed algae pellets collected at end of incubation and medium gave the resulting plates after 24 hours of incubation as shown in Figure 3.16. It was not observed any growth of the cobalamin-dependent *E.coli* around any discs after 24 hours. After 48 hours there was observed a slight growth around the discs with media containing cobalamin, i.e. 4L1+ and M8a+.
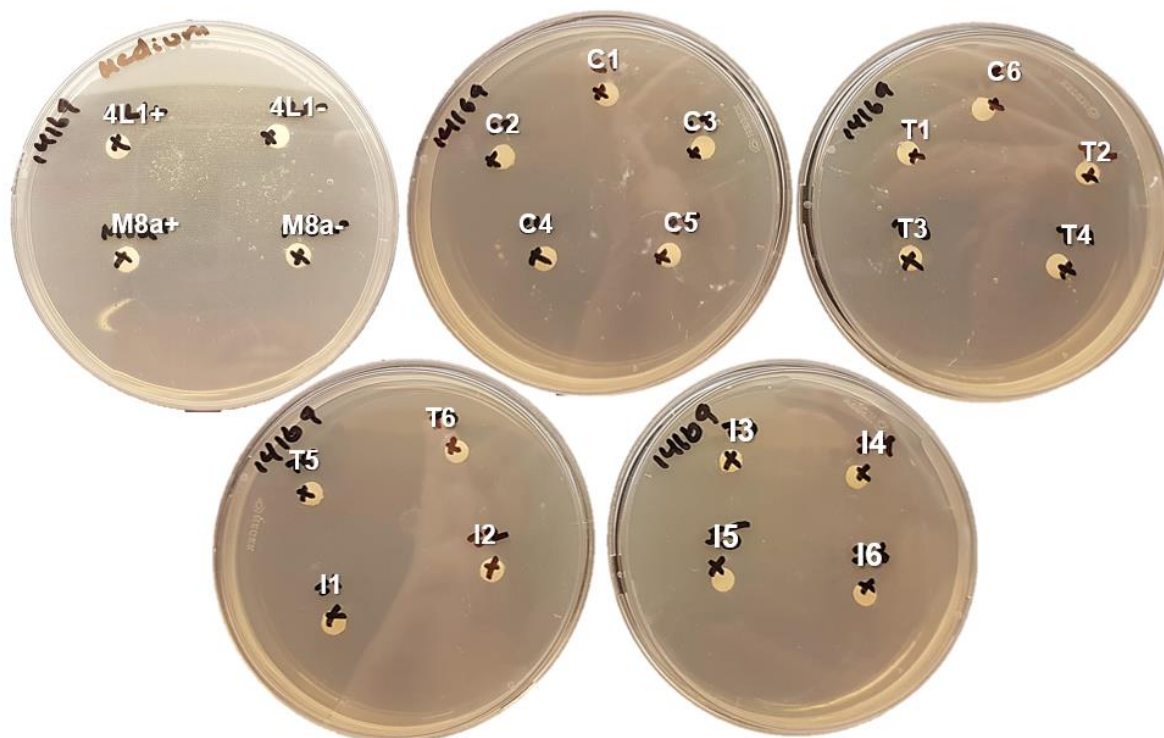
Figure 3.16 Appearance of microbial cobalamin disc diffusion assay plates with cobalamin-dependent *E.coli* 14169 after 24h. Top left is the media plate, with discs coated with 4L1 medium with (+) and without (-) cobalamin, in addition to M8a with (+) and without (-) cobalamin. The other assay plates have discs holding the cell lysate of each experiment culture for each strain. Cell lysate of sample 1-3 and 4-6 comes from suspensions with and without cobalamin, respectively. The top middle plate have discs holding *C.vulgaris* suspensions 1-5. Top right plate holds discs with *C.vulgaris* suspension 6 and *T.lutea* suspensions 1-4. Bottom left shows the plate with disc coated in *T.lutea* suspension 5-6 and *I.galbana* suspensions 1-2. The last plate holds the discs coated in *I.galbana* suspension 3-6.

3.3.4 Evaluation of potential bacterial contamination of algal cultures

Through analysis of 16S rRNA sequencing data, the relative abundance of bacteria in the algal samples from 3.3.1 Evaluation of the effect of cobalamin depletion on algal strains and stem cultures was determined. The relative read count of bacteria relative to algae was calculated, and revealed the proportions shown in Table A8. In total, 3 samples showed substantially higher relative abundance of bacteria relative to algae. This was the last parallel of the *T.lutea* cultures without cobalamin in medium (sample 6) and the stem cultures of both *T.lutea* and *I.galbana,* displaying porportions on 0.95, 0.66 and 8.2, respectively. The abundance of bacteria relative to algae in Chlorella samples was similar for all samples, showing an average on 0,0018 (SD = 0,0003). The first five *T.lutea* samples analysed had low relative abundance of bacteria relative to algae, with proportion values ranging from 0.0025 to 0.0060. The other six samples of

I.galbana showed proportions ranging from 0.022 to 0.0044. The top 10 most abundant genera across all samples was as shown in Figure 3.17. This shows that the same three samples with highest abundance of bacteria relative to algae given above, shows highest abundance of the genera. *I.galbana* stem culture shows highest relative abundance of *Delftia*, *Acinetobacter, Tepidiphilus, Enterococcus, Neobacillus* and *Anoxybacillus*. The relative abundance of the top 10 genera was less for *T.lutea*, and showed highest abundance of *Methylophaga*. *Ralstonia, Tepidiphilus, Acinetobacter* and *Delftia*. The last parallel without cobalamin in medium of *T.lutea* showed high abundance of the genus *Alkalihalobacillus*, and there were little presence of other bacterial genera in this sample.
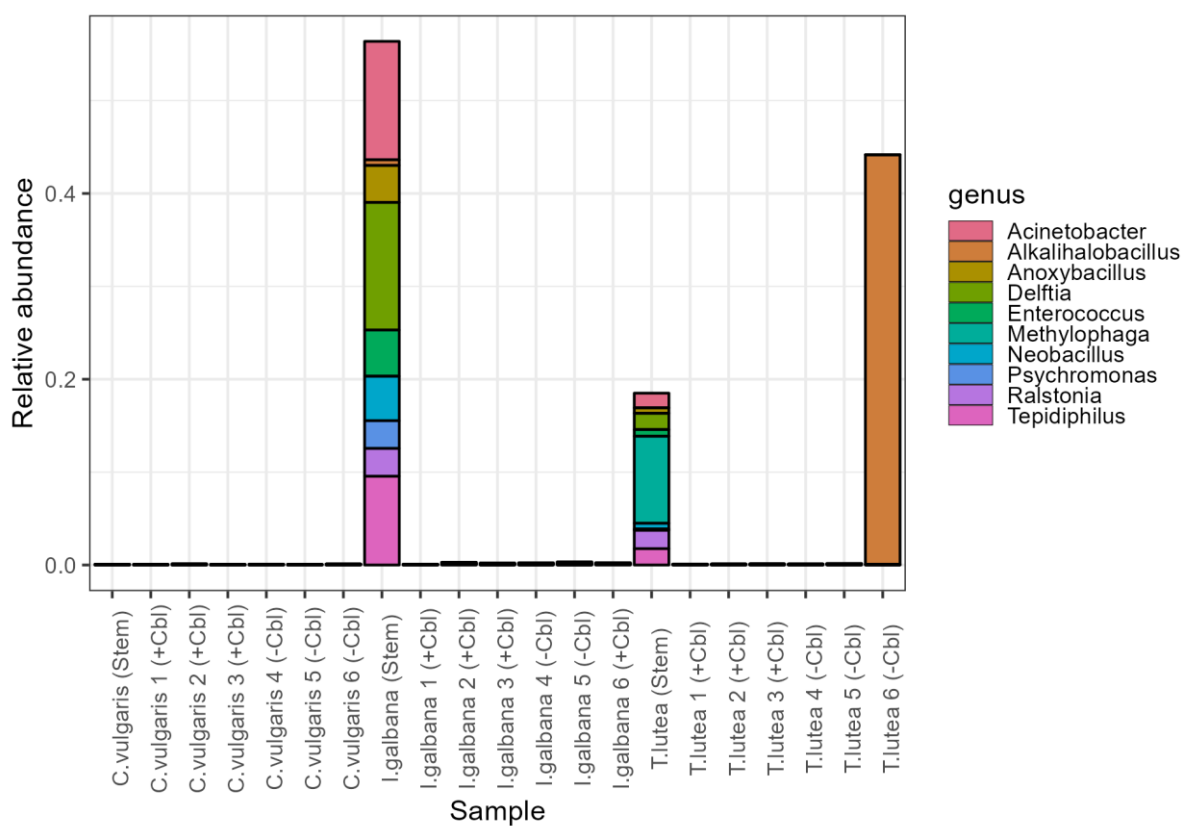
Figure 3.17 Relative abundance of the 10 most abundant genera across all algal samples. The y-axis refers to the relative abundance of the genus, whilst the x-axis refers to the sample.

4. Discussion

4.1 Inactivation mechanism of cobalamin by N_2O

A significant reduction in the growth of cobalamin-dependent *E.coli* was found when grown in presence of 100% N_2O, corresponding to a liquid concentration of 28µM (Figure 3.3). When cobalamin is biologically active in growing organisms as cofactor for METH, it is cycled between the reduced cob(I)alamin and oxidized cob(III)alamin forms (Matthews et al., 2008). In the presence of N_2O, cob(I)alamin can be oxidized to the catalytically inactive form cob(II)alamin (Alston, 1991). This form cannot be utilized by the enzyme, resulting in inactivation of METH and prevented growth of cobalamin-dependent *E.coli*. As the oxidation of cob(I)alamin by N_2O leads to the formation of N_2, the N_2O in the closed vials will eventually deplete, allowing enzyme activity to recover. This could be an explanation to why suspensions initially containing 100% N_2O also had reached stationary phase after 48 hours. Deacon and coworkers have reported that the recovery of METH activity after exposure to N_2O is possible (1980). On the other hand, irreversible inactivation of methionine synthase has also been reported (Frasca et al., 1986). These observations were however conducted on purified enzyme *in vitro* and not *in vivo*. As the enzyme activity was not measured in this thesis, it cannot be stated whether the observed delayed growth is a result of a reversible state of the enzyme or another factor.

When *E.coli* was grown with 1% and 10% N_2O present in vials, it was not observed any difference in OD after 24 hours compared to control (Figure 3.4). This indicates that the inactivation occurs between 10% and 100% N_2O, corresponding to liquid concentrations between 2.8 and 28 µM N_2O. Moreover, clinical studies have shown toxicity upon exposure with 50% N_2O (Deacon et al., 1980; Lassen et al., 1956), indicating that inactivation occurs around this concentration. Growth measurements in the present thesis were only collected at endpoint, and it is therefore a possibility that there has been a small, overlooked effect during the incubation period. Hence, continuous measurements of OD during the entire incubation period could reveal any minor effects during growth.

The cobalamin that had been directly exposed to N_2O prior to use in microbial cobalamin disc assay was in the most oxidized state, i.e. cob(III)alamin, and oxidation by N_2O will most likely not occur. It was therefore not observed any difference in growth of cobalamin-dependent *E.coli* in the disc assay (Figure 3.2).

4.2 N_2O production potential in marine sediments

The highest measured N_2O accumulation from microbiota of enriched sediment was 0.25 and 0.20 µM, observed for the latter two parallels enriched with methanol and nitrate (Figure 3.6). This is in the higher range of what is generally observed in marine environments, which ranges from ~0.006 – 0.035 µM (Heo et al., 2022; Zhan & Chen, 2009; Zhan et al., 2017). Furthermore, the highest accumulation of nitrite and NO was also measured in these parallels (Figure 3.5; Figure 3.6). In contrast, the first parallel of similar enrichment group did not show these tendencies but showed a N_2 accumulation indicating that the added nitrate had been reduced. These findings therefore indicate that denitrification in the latter two parallels occur, but it is delayed relative to the other parallel. A potential explanation for the difference in accumulation of denitrification intermediates between the samples enriched with methanol and nitrate, is the bacterial diversity and taxonomy. Firstly, the enrichment group showed the highest visual dispersal on the PCoA plot, indicating relatively high dissimilarity in taxa composition between the samples of the group (Figure 3.9). The diversity within each sample also varied but was overall low relative to the diversity observed in controls and samples enriched with nitrate only (Figure 3.8). These findings are in line with the taxonomic composition of the three parallels, showing that the taxonomic profile of the latter two parallels was quite different from the first parallel (Figure 3.7). Not surprisingly, the most enriched bacterial genera could utilize methanol as energy and carbon source. *Methylophaga* was present in all parallels, and is common marine methylotrophs, long regarded as strictly aerobic until representatives with nitrate reducing potential was found in anoxic conditions (Auclair et al., 2010; Labbe et al., 2007). In addition to methanol oxidation, members of this genus could therefore potentially contribute to denitrification in the sediments. Additionally, the first parallel showed enrichment of *Methylophilus*. This genus belongs to family *Methylophilaceae*, which is common in marine environments, utilizing primarily methanol as carbon and energy source (Chistoserdova et al., 2007). The predicted community functioning showed abundance of methanol oxidation

potential in the first parallel, while no abundance above 0.015 was detected in the latter two parallels (Figure 3.10). This indicates that the abundance is primarily caused by the presence of the *Methylophilus* genus.

The samples enriched with thiosulphate and nitrate showed accumulation of N_2, indicating that complete denitrification has occurred (Figure 3.6). The amount of N_2 was above the expected 121µmol in two of the parallels, which can be explained by uncertainty of method or by the presence of nitrogen in the sediments prior to enrichment. These samples were ordinated furthest away from the samples of the other enrichment groups on the PCoA plot, which indicates that the bacterial composition of this group is least similar to the diversity of the other enrichment groups (Figure 3.9). The alpha diversity estimates showed an overall low diversity within the samples compared to the controls and samples enriched with nitrate only, which is explained by the enrichment of certain bacterial taxa (Figure 3.8). The low diversity in these samples was probably due to the enrichment of *Sulfurovum*, belonging to the family *Sulfurovaceae* (Figure 3.7). This genus was first isolated from hydrothermal sediments and belongs to the class ε-Proteobacteria (Inagaki et al., 2004). The enrichment of *Sulfurovum* upon addition of thiosulphate is in accordance with the literature (Mori et al., 2018). Species of *Sulfurovum* are chemolitoautotrophs, using elemental sulfur or thiosulfate as sole electron donor, and oxygen or nitrogen as electron acceptor (Inagaki et al., 2004). These characteristics are reflected by the predicted microbial community functions, which showed abundance of sulphate and thiosulphate respiration potential (Figure 3.10). The genus has been associated with denitrification when nitrate is present in medium, due to observed formation of gas bubbles indicative of nitrate reduction (Mori et al., 2018). Another study also associated the genus with the potential of performing denitrification, due to the presence of the *norB* gene, encoding nitric oxide reductase (Pettersen et al., 2022). As nitric oxide reductase leads to the formation of N_2O, it is therefore a potential for N_2O production from sediments with high abundance of *Sulfurovum*.

4.3 Potential for cobalamin inhibition by N2O in marine environments

The observed inactivation concentration of this thesis was 28µM (100% N_2O vials), which is far above the accumulated levels measured in the enrichment experiment (0.25 µM), and the concentrations typically found in seawater of marine environments (~0.006 – 0.035 µM) (Heo et al., 2022; Zhan & Chen, 2009; Zhan et al., 2017). Meanwhile, the investigations of the permanently ice-covered lakes in Antarctica shows that supersaturation of N_2O in some environments can occur (Murray et al., 2012; Priscu, 1997). The ice-covered lakes were characterized by poorly ventilation in addition to low average temperature and pH. Lake Vida contained high levels of sulfur, and sulfur-oxidizing ε-proteobacteria, including *Sulfurovum,* was abundant (Murray et al., 2012). Metabolic processes are affected by temperature, which can affect the production and reduction of intermediates. For instance, has laboratory studies performed on intact soil found increasing N_2O/N_2 ratio upon decreasing temperature during denitrification (Bailey & Beuchamp, 1973; Holtan-Hartwig et al., 2002). pH has also revealed effect on the N_2O/N_2 product ratio. Investigations of denitrification by the model organism *Paracoccus denitrificans* showed drastic increase in N_2O/N_2 product ratio when pH was lowered to below 6.25 (Bergaust et al., 2010). These findings therefore suggest that despite the overall concentration of N_2O in marine environments being below inhibitory level, given the suitable environmental conditions, there could potentially be some places where the concentrations exceed the inhibitory level.

4.4 Lack of effect of cobalamin depletion on microalgae

Surprisingly, there was no effect of cobalamin depletion on growth of *I.galbana* and *T.lutea* under cobalamin depletion (Figure 3.12, Figure 3.13). This contradicts the existing literature, stating that these species require cobalamin for growth (Croft et al., 2005; Nef et al., 2019). In fact, the same strain of *T.lutea* have previously shown significant reduction of growth upon cobalamin depletion (Nef et al., 2019). Hence, a clear difference in growth patterns between parallels with cobalamin and cobalamin-depleted parallels would be expected for these strains. The findings therefore indicate that there is a source of cobalamin in the cultures.

As all cultures were initially grown in medium with cobalamin, the wash step performed once during preparation of cultures might not be sufficient to remove all cobalamin. The requirement of cobalamin is in trace amounts, and the slightest presence could support growth. The wash step could have been repeated once or twice, to ensure that all the initial cobalamin was removed. However, a limitation to this approach is that increased centrifugation introduces more mechanical stress, which can affect algal growth negatively. Upon centrifugation, both high gravitational forces and shear stress can cause the damage of cells (Knuckey et al., 2006). The robustness of microalgae towards such stresses varies with species. For instance was the tolerance of *I.galbana* towards shear stress tested by Michels and coworkers, which found reduction of viability of cultures from ~100% to 74.9% when exposed to shear stress at 5.4 Pa, equivalent to 100 rpm (2016). Furthermore, the reported ability of certain surveyed microalgal species to take up and store cobalamin (Maruyama et al., 1989), further emphasizes that complete removal of cobalamin could be difficult.

There might also be presence of cobalamin-producing microbes in the cultures, despite that all cultures were stated as axenic at start. The algal provider CCAP uses plate-streaking method on high-nutrient agar and microscopy of algal cultures to validate axenity status (CCAP admin, personal communication, January 10, 2024). A study comparing plate growing test against culture-independent approaches for testing axenity status of microalgae, showed that only the plate tests supported axenity status (Pokorny et al., 2022) "The common plate anomaly" is referring to the commonly observed inconsistency between total and cultivable microbial counts of natural microbial communities (Jannasch & Jones, 1959; Pokorny et al., 2022; Ward et al., 1990). The nature behind the inconsistency is complex and could be due to various reasons. For instance, can high nutrient agars inhibit the growth of a large portion of microorganisms, as many microbes are oligotrophic (Pokorny et al., 2022). This also includes many marine microbes, as many marine habitats are nutrient depleted (Lauro et al., 2009). Furthermore, metabolic requirements of bacteria are often complex and diverse, and standard media might exclude the growth of syntrophic bacteria (Pokorny et al., 2022). The lack of signalling molecules or other metabolites normally provided as by-products from other microbes can result in nongrowing cells (Nichols et al., 2008). In further correspondence with the culture provider CCAP, it was informed that very low levels of bacteria (1-2 per subsample) are commonly observed in microscopy for some algal strains, particularly marine strains. This is despite that the test plate of the same cultures shows no growth. Furthermore, the status of

I.galbana changed from "axenic" to "minimal observed bacteria during normal growth conditions" during the thesis. Taken together, this information therefore indicate the presence of bacteria and possibly cobalamin-producers, and that the abundance of bacteria is possibly higher in the marine algae and especially in *I.galbana.* This is consistent with the findings of this thesis, showing presence of bacteria in all cultures, with the highest presence in the stem cultures of *I.galbana* and *T.lutea*. The cultures of *C.vulgaris* did show very low counts of bacteria in all cultures, including the stem culture, which indicates that these cultures are nearly axenic. Experiment culture 6 of *T.lutea* did show very high presence of bacteria, dominated by the genus *Alkalihalobacillus.* As this genus was not observed in high quantities in any other culture, this is likely contamination. Of the most abundant bacterial taxa found in the stem cultures of *I.galbana* and *T.lutea*, all belonged to either Proteobacteria or Firmicutes phylum. *Acinetobacter, Delftia, Methylophaga* and *Ralstonia* belongs to proteobacteria, and are commonly found in natural environments such as soil and aquatic environments (Auclair et al., 2010; Jung & Park, 2015; Ryan & Adley, 2014; Wen et al., 1999). *Anoxybacillus, Enterococcus* and *Neobacillus* belongs to Firmicutes and have previously been isolated from environments such as soil, marine waters, marine sediments, plants and high temperature habitats (Byappanahalli et al., 2012; Goh et al., 2013; Routhu et al., 2021). As Proteobacteria and Firmicutes both have representatives with potential for cobalamin production (Doxey et al., 2015; Lu et al., 2020), these findings therefore suggest the potential presence of cobalamin-producers in the cobalamin-dependent algae cultures from start. The low abundance of bacteria in the experiment cultures relative to the stem cultures, could be due to the dilution of stem culture when setting up the experiment.

4.5 Lack of effect of N_2O on oxygen production by microalgae

Based on the experimental setup used in the current thesis, it cannot be concluded with any effect of N_2O on algal growth. Direct exposure of growing microalgal cultures to N_2O, showed lower median for oxygen concentrations, for both *I.galbana* and *T.lutea* in N_2O vials (Figure 3.14). It was however still overlap in the measured oxygen concentrations with controls and the tendency in lower median for N_2O vials was also shown for the vials with only medium. The observed tendency might therefore be caused by analytical variation and not an actual effect. Photosynthetic activity has been measured with oxygen as proxy previously, however often

with recorded DO buildup as indication of activity (Ramírez-Rueda et al., 2020; Scarsella et al., 2012; Takeuchi et al., 1993). In these studies, the start concentration of DO was controlled and the DO accumulation of algal cultures was monitored continuously using probes throughout the incubation period.

4.6 Technical considerations and future aspects

4.6.1 Sediment enrichments to measure N_2O potential

The temperature of marine environments depends on factors like depth and latitude. As the enrichments in the present thesis were incubated at 20°C, the temperature was relatively high and not representative of all marine waters. Since low temperature waters often have been associated with high levels of N_2O (Murray et al., 2012; Prisu et al., 1996; Zhan & Chen, 2009; Zhan et al., 2017), the enrichment cultures could have be incubated at multiple temperatures to ensure a more representative view. In addition, the pH in seawater of enrichments were around 8, corresponding to the average pH of seawater (Doney et al., 2020). An increase in concentration of CO_2 in seawater caused by anthropogenic activity can though lower the seawater pH in the long term. Consequently, testing the enrichment of sediments under different acidic conditions would be of interest to potentially see if the accumulation of N_2O differed. Lastly, the enrichment experiment was only conducted with an end-point analysis of the nitrogen gas concentrations in headspace. Continuous measurements, revealing the full gas kinetic profile of the enrichments would be favourable, revealing more information of the intermediate accumulation profiles.

4.6.2 Cobalamin depleted algal growth

To avoid potential cobalamin-producing bacterial contaminants, the algal cultures should preferably have been treated with antibiotics before grown in absence of cobalamin. The study conducted by Nef and coworkers on the same *T.lutea* strain emphasizes this, as the cultures used received antibiotics prior to experiment (2019).

4.6.3 Cobalamin measuring methods

To check for the presence of cobalamin in the algal cultures and in fresh medium, both microbial cobalamin disc assay and ELISA was conducted (Figure 3.15, Figure 3.16). In both cases, there were no clear results, as the concentration in the cultures were below the detection area of both assays. These assays have therefore difficulty with detecting the cobalamin concentration in marine environments. The results therefore underline the scarcity of affordable, rapid and sensitive analytical methods for accurate cobalamin measurement in environmental samples (Sañudo-Wilhelmy et al., 2014).

4.6.4 Algal exposure to N2O

Various limitations are associated with the conducted method for algal exposure to N_2O. Firstly, the injection of algal cultures through thin needles is exposing the algal cells to stress. This was taken into consideration and the needle used was of maximum thickness supported by the rubber septa of glass vials. Further, lack of control over the oxygen parameter is a major limitation. In addition to dissolved oxygen in the injected cultures, the injection itself is adding an unknown amount of oxygen to the vials together with the algal cultures. Preferably, the concentration of oxygen should have been measured continuously over a longer incubation period. The O_2 concentration in the vials at start would then be known and if there were a difference in production over time, this would be easier detectable. Alternatively, the build-up of dissolved oxygen could be measured instead similarly as previous studies.

5. Conclusion

A main finding was that 100% N_2O inactivated growth of cobalamin-dependent *E.coli*, while no effect was detected for 1 and 10%, but this could be due to experimental setup. While these results indicate that the inactivation may occur between 10% and 100%, the current thesis was not able to determine the exact inactivation concentration, which should be investigated further. The observed inactivation concentration was still substantially above the levels of N_2O observed in sediment enrichments and the levels normally associated with marine environments. Hence, the results indicates that the levels of N_2O usually found in marine environments are too low to affect the growth of resident cobalamin-dependent organisms. Nevertheless, certain environments have been documented to have N_2O concentrations exceeding the level of cobalamin inactivation.

The present thesis showed surprisingly no effect of cobalamin depletion on growth of cobalamin-dependent *I.galbana* and *T.lutea*. This could potentially be due to the presence of cobalamin-producing microorganisms from start or another factor, like a microalgal storage of cobalamin. As the cause remains unknown, this opens for further investigation. Furthermore, it was not succeeded to evaluate the effect of N_2O on oxygen production from microalgae, and further experiments should investigate this.

6. References

Ahmad, M. T., Shariff, M., Md Yusoff, F., Goh, Y. M., & Banerjee, S. (2020). Applications of microalga *Chlorella vulgaris* in aquaculture. *Reviews in Aquaculture*, *12*(1), 328-346. https://doi.org/10.1111/raq.12320

Alston, T. A. (1991). Inhibition of vitamin B_{12}-dependent methionine biosynthesis by chloroform and carbon tetrachloride. *Biochemical Pharmacology*, *42*(12), R25-28. https://doi.org/10.1016/0006-2952(91)90226-u

Auclair, J., Lépine, F., Parent, S., & Villemur, R. (2010). Dissimilatory reduction of nitrate in seawater by a *Methylophaga* strain containing two highly divergent *narG* sequences. *The ISME Journal*, *4*(10), 1302-1313. https://doi.org/10.1038/ismej.2010.47

Aydin, S. (2015). A short history, principles, and types of ELISA, and our laboratory experience with peptide/protein analyses using ELISA. *Peptides*, *72*, 4-15. https://doi.org/10.1016/j.peptides.2015.04.012

Azam, F., & Malfatti, F. (2007). Microbial structuring of marine ecosystems. *Nature Reviews Microbiology*, *5*(10), 782-791. https://doi.org/10.1038/nrmicro1747

Bailey, L. D., & Beuchamp, E. G. (1973). Effects of temperature on NO_3^- and NO_2^- reduction, nitrogenous gas production, and redox potential in a saturated soil *Canadian Journal of Soil Science*, *53*(2), 213-218. https://doi.org/10.4141/cjss73-032

Baker, G. C., Smith, J. J., & Cowan, D. A. (2003). Review and re-analysis of domain-specific 16S primers. *Journal of Microbiological Methods*, *55*(3), 541-555. https://doi.org/10.1016/j.mimet.2003.08.009

Baker, H., & Sobotka, H. (1962). Microbiological Assay Methods for Vitamins. *Advances in Clinical Chemistry*, *5*, 173-285. https://doi.org/10.1016/S0065-2423(08)60075-X

Balabanova, L., Averianova, L., Marchenok, M., Son, O., & Tekutyeva, L. (2021). Microbial and Genetic Resources for Cobalamin (Vitamin B_{12}) Biosynthesis: From Ecosystems to Industrial Biotechnology. *International Journal of Molecular Sciences*, *22*(9), 4522. https://doi.org/10.3390/ijms22094522

Balouiri, M., Sadiki, M., & Ibnsouda, S. K. (2016). Methods for *in vitro* evaluating antimicrobial activity: A review. *Journal of Pharmaceutical Analysis*, *6*(2), 71-79. https://doi.org/10.1016/j.jpha.2015.11.005

Banerjee, R. (1997). The Yin-Yang of cobalamin biochemistry. *Chemistry & Biology*, *4*(3), 175-186. https://doi.org/10.1016/s1074-5521(97)90286-6

Bange, H. W., & Andreae, M. O. (1999). Nitrous oxide in the deep waters of the world's oceans. *Global Biogeochemical Cycles*, *13*(4), 1127-1135. https://doi.org/10.1029/1999GB900082

Barbier, E. B. (2017). Marine ecosystem services. *Current Biology*, *27*(11), R507-R510. https://doi.org/10.1016/j.cub.2017.03.020

Beauvais, M., Schatt, P., Montiel, L., Logares, R., Galand, P. E., & Bouget, F. Y. (2023). Functional redundancy of seasonal vitamin B_{12} biosynthesis pathways in coastal marine microbial communities. *Environmental Microbiology*, *25*(12), 3753-3770. https://doi.org/10.1111/1462-2920.16545

Bendif, E. M., Probert, I., Schroeder, D. C., & de Vargas, C. (2013). On the description of *Tisochrysis lutea* gen. nov. sp. nov. and *Isochrysis nuda* sp. nov. in the Isochrysidales, and the transfer of *Dicrateria* to the Prymnesiales (Haptophyta). *Journal of Applied Phycology*, *25*(6), 1763-1776. https://doi.org/10.1007/s10811-013-0037-0

Bharti, R., & Grimm, D. G. (2021). Current challenges and best-practice protocols for microbiome analysis. *Briefings in Bioinformatics*, *22*(1), 178-193. https://doi.org/10.1093/bib/bbz155

Bratton, A. C., & Marshall, E. K. (1939). A new coupling component for sulfanilamide determination. *Journal of Biological Chemistry*, *128*(2), 537-550. https://doi.org/10.1016/S0021-9258(18)73708-3

Bray, J. R., & Curtis, J. T. (1957). An Ordination of the Upland Forest Communities of Southern Wisconsin. *Ecological Monographs*, *27*(4), 326-349. https://doi.org/10.2307/1942268

Breider, F., Yoshikawa, C., Makabe, A., Toyoda, S., Wakita, M., Matsui, Y., Kawagucci, S., Fujiki, T., Harada, N., & Yoshida, N. (2019). Response of N_2O production rate to ocean acidification in the western North Pacific. *Nature Climate Change*, *9*(12), 954-958. https://doi.org/10.1038/s41558-019-0605-7

Byappanahalli, M. N., Nevers, M. B., Korajkic, A., Staley, Z. R., & Harwood, V. J. (2012). Enterococci in the environment. *Microbiology and molecular biology reviews : MMBR*, *76*(4), 685-706. https://doi.org/10.1128/MMBR.00023-12

Calle, M. L. (2019). Statistical Analysis of Metagenomics Data. *Genomics Inform*, *17*(1), e6. https://doi.org/10.5808/GI.2019.17.1.e6

Chanarin, I. (1980). Cobalamins and Nitrous Oxide - A review. *Journal of Clinical Pathology*, *33*(10), 909-916. https://doi.org/10.1136/jcp.33.10.909

Chistoserdova, L., Lapidus, A., Han, C., Goodwin, L., Saunders, L., Brettin, T., Tapia, R., Gilna, P., Lucas, S., Richardson, P. M., & Lidstrom, M. E. (2007). Genome of *Methylobacillus* flagellatus, molecular basis for obligate methylotrophy, and polyphyletic origin of methylotrophy. *Journal of Bacteriology*, *189*(11), 4020-4027. https://doi.org/10.1128/jb.00045-07

Croft, M. T., Lawrence, A. D., Raux-Deery, E., Warren, M. J., & Smith, A. G. (2005). Algae acquire vitamin B12 through a symbiotic relationship with bacteria. *Nature*, *438*(7064), 90-93. https://doi.org/10.1038/nature04056

Deacon, R., Lumb, M., Perry, J., Chanarin, I., Minty, B., Halsey, M., & Nunn, J. (1980). Inactivation of Methionine Synthase by Nitrous Oxide. *European Journal of Biochemistry*, *104*(2), 419-422. https://doi.org/10.1111/j.1432-1033.1980.tb04443.x

Dereven'kov, I. A., Salnikov, D. S., Silaghi-Dumitrescu, R., Makarov, S. V., & Koifman, O. I. (2016). Redox chemistry of cobalamin and its derivatives. *Coordination Chemistry Reviews*, *309*, 68-83. https://doi.org/10.1016/j.ccr.2015.11.001

Diding, N. (1951). A simple cup assay of Vitamin-B12 with a stable B12-requiring mutant of *Eschericia-Coli*. *Scandinavian Journal of Clinical & Laboratory Investigation*, *3*(3), 215-216. https://doi.org/10.3109/00365515109060602

Dimitrios, T. (2007). Analysis of nitrite and nitrate in biological fluids by assays based on the Griess reaction: Appraisal of the Griess reaction in the l-arginine/nitric oxide area of research. *Journal of Chromatography B*, *851*(1), 51-70. https://doi.org/10.1016/j.jchromb.2006.07.054

Doney, S. C. (2010). The Growing Human Footprint on Coastal and Open-Ocean Biogeochemistry. *Science*, *328*(5985), 1512-1516. https://doi.org/10.1126/science.1185198

Doney, S. C., Busch, D. S., Cooley, S. R., & Kroeker, K. J. (2020). The Impacts of Ocean Acidification on Marine Ecosystems and Reliant Human Communities. *Annual Review of Environment and Resources, Vol 45*, *45*, 83-112. https://doi.org/10.1146/annurev-environ-012320-083019

Doxey, A. C., Kurtz, D. A., Lynch, M. D. J., Sauder, L. A., & Neufeld, J. D. (2015). Aquatic metagenomes implicate *Thaumarchaeota* in global cobalamin production. *The ISME Journal*, *9*(2), 461-471. https://doi.org/10.1038/ismej.2014.142

Drummond, J. T., & Matthews, R. G. (1994). Nitrous oxide inactivation of cobalamin-dependent methionine synthase from *Escherichia coli*: characterization of the damage to the enzyme and prosthetic group. *Biochemistry*, *33*(12), 3742-3750. https://doi.org/10.1021/bi00178a034

Ellis, K. A., Cohen, N. R., Moreno, C., & Marchetti, A. (2017). Cobalamin-independent Methionine Synthase Distribution and Influence on Vitamin B_{12} Growth Requirements in Marine Diatoms. *Protist*, *168*(1), 32-47. https://doi.org/10.1016/j.protis.2016.10.007

Ewing, B., & Green, P. (1998). Base-calling of automated sequencer traces using phred. II. Error probabilities. *Genome Research*, *8*(3), 186-194. https://doi.org/10.1101/gr.8.3.186

Frasca, V., Riazzi, B. S., & Matthews, R. G. (1986). *In vitro* inactivation of methionine synthase by nitrous oxide. *Journal of Biological Chemistry*, *261*(34), 15823-15826. https://www.ncbi.nlm.nih.gov/pubmed/3536916

Freing, A., Wallace, D. W., & Bange, H. W. (2012). Global oceanic production of nitrous oxide. *Philos Trans R Soc Lond B Biol Sci*, *367*(1593), 1245-1255. https://doi.org/10.1098/rstb.2011.0360

Gao, F., Teles, I., Wijffels, R. H., & Barbosa, M. J. (2020). Process optimization of fucoxanthin production with *Tisochrysis lutea*. *Bioresource Technology*, *315*, 123894. https://doi.org/10.1016/j.biortech.2020.123894

Gao, H., Mao, Y. P., Zhao, X. T., Liu, W. T., Zhang, T., & Wells, G. (2019). Genome-centric metagenomics resolves microbial diversity and prevalent truncated denitrification pathways in a denitrifying PAO-enriched bioprocess. *Water Research*, *155*, 275-287. https://doi.org/10.1016/j.watres.2019.02.020

Gleick, P. H., Pacific Institute for Studies in Development, E. a. S., & Stockholm Environment, I. (1993). *Water in crisis : a guide to the world's fresh water resources*. Oxford University Press.

Glibert, P. M., & Mitra, A. (2022). From webs, loops, shunts, and pumps to microbial multitasking: Evolving concepts of marine microbial ecology, the mixoplankton paradigm, and implications for a future ocean. *Limnology and Oceanography*, *67*(3), 585-597. https://doi.org/10.1002/lno.12018

Goh, K. M., Kahar, U. M., Chai, Y. Y., Chong, C. S., Chai, K. P., Ranjani, V., Illias, R. M., & Chan, K. G. (2013). Recent discoveries and applications of *Anoxybacillus*. *Applied Microbiology and Biotechnology*, *97*(4), 1475-1488. https://doi.org/10.1007/s00253-012-4663-2

Gómez-Consarnau, L., Sachdeva, R., Gifford, S. M., Cutter, L. S., Fuhrman, J. A., Sañudo-Wilhelmy, S. A., & Moran, M. A. (2018). Mosaic patterns of B-vitamin synthesis and utilization in a natural marine microbial community. *Environmental Microbiology*, *20*(8), 2809-2823. https://doi.org/10.1111/1462-2920.14133

Gonzalez, J. C., Banerjee, R. V., Huang, S., Sumner, J. S., & Matthews, R. G. (1992). Comparison of cobalamin-independent and cobalamin-dependent methionine synthases from *Escherichia coli*: two solutions to the same chemical problem. *Biochemistry*, *31*(26), 6045-6056. https://doi.org/10.1021/bi00141a013

Goulding, C. W., Postigo, D., & Matthews, R. G. (1997). Cobalamin-Dependent Methionine Synthase Is a Modular Protein with Distinct Regions for Binding Homocysteine, Methyltetrahydrofolate, Cobalamin, and Adenosylmethionine. *Biochemistry*, *36*(26), 8082-8091. https://doi.org/10.1021/bi9705164

Griffiths, J. R., Kadin, M., Nascimento, F. J. A., Tamelander, T., Törnroos, A., Bonaglia, S., Bonsdorff, E., Brüchert, V., Gårdmark, A., Järnström, M., Kotta, J., Lindegren, M., Nordström, M. C., Norkko, A., Olsson, J., Weigel, B., Zydelis, R., Blenckner, T., Niiranen, S., & Winder, M. (2017). The importance of benthic-pelagic coupling for marine ecosystem functioning in a changing world. *Global Change Biology*, *23*(6), 2179-2196. https://doi.org/10.1111/gcb.13642

Guillard, R. R. L. (1975). Culture of Phytoplankton for Feeding Marine Invertebrates. In W. L. Smith & M. H. Chanley (Eds.), *Culture of Marine Invertebrate Animals: Proceedings — 1st Conference on Culture of Marine Invertebrate Animals Greenport* (pp. 29-60). Springer US. https://doi.org/10.1007/978-1-4615-8714-9_3

He, Y., Caporaso, J. G., Jiang, X.-T., Sheng, H.-F., Huse, S. M., Rideout, J. R., Edgar, R. C., Kopylova, E., Walters, W. A., Knight, R., & Zhou, H.-W. (2015). Stability of operational taxonomic units: an important but neglected property for analyzing microbial diversity. *Microbiome*, *3*(1), 20. https://doi.org/10.1186/s40168-015-0081-x

Heal, K. R., Carlson, L. T., Devol, A. H., Armbrust, E. V., Moffett, J. W., Stahl, D. A., & Ingalls, A. E. (2014). Determination of four forms of vitamin B_{12} and other B vitamins in seawater by liquid chromatography/tandem mass spectrometry. *Rapid Commun Mass Spectrom*, *28*(22), 2398-2404. https://doi.org/10.1002/rcm.7040

Helliwell, K. E., Collins, S., Kazamia, E., Purton, S., Wheeler, G. L., & Smith, A. G. (2014). Fundamental shift in vitamin B_{12} eco-physiology of a model alga demonstrated by experimental evolution. *The ISME Journal*, *9*(6), 1446-1455. https://doi.org/10.1038/ismej.2014.230

Helliwell, K. E., Wheeler, G. L., Leptos, K. C., Goldstein, R. E., & Smith, A. G. (2011). Insights into the Evolution of Vitamin B_{12} Auxotrophy from Sequenced Algal Genomes. *Molecular Biology and Evolution*, *28*(10), 2921-2933. https://doi.org/10.1093/molbev/msr124

Heo, J.-M., Kim, H.-R., Eom, S.-M., Yoon, J.-E., Shim, J., Lim, J.-H., Kim, J.-H., Thangaraj, S., Park, K.-T., Joo, H., & Kim, I.-N. (2022). Distribution and Production of N2O in the Subtropical Western North Pacific Ocean During the Spring of 2020 [Original Research]. *Frontiers in Marine Science*, *9*. https://doi.org/10.3389/fmars.2022.854651

Hirota, A., Ijiri, A., Komatsu, D. D., Ohkubo, S. B., Nakagawa, F., & Tsunogai, U. (2009). Enrichment of nitrous oxide in the water columns in the area of the Bering and Chukchi Seas. *Marine Chemistry*, *116*(1), 47-53. https://doi.org/10.1016/j.marchem.2009.09.001

Holtan-Hartwig, L., Dörsch, P., & Bakken, L. R. (2002). Low temperature control of soil denitrifying communities:: kinetics of N_2O production and reduction. *Soil Biology & Biochemistry*, *34*(11), 1797-1806, Article Pii s0038-0717(02)00169-4. https://doi.org/10.1016/s0038-0717(02)00169-4

Hu, Q., Sommerfeld, M., Jarvis, E., Ghirardi, M., Posewitz, M., Seibert, M., & Darzins, A. (2008). Microalgal triacylglycerols as feedstocks for biofuel production: perspectives and advances. *Plant J*, *54*(4), 621-639. https://doi.org/10.1111/j.1365-313X.2008.03492.x

Inagaki, F., Takai, K., Nealson, K. H., & Horikoshi, K. (2004). *Sulfurovum lithotrophicum* gen. nov., sp nov., a novel sulfur-oxidizing chemolithoautotroph within the *ε-Proteobacteria* isolated from Okinawa Trough hydrothermal sediments. *International Journal of Systematic and Evolutionary Microbiology*, *54*, 1477-1482. https://doi.org/10.1099/ijs.0.03042-0

Jannasch, H. W., & Jones, G. E. (1959). Bacterial populations in sea water as determined by different methods of enumeration. *Limnology and Oceanography*, *4*(2), 128-139. https://doi.org/10.4319/lo.1959.4.2.0128

Jung, J., & Park, W. (2015). *Acinetobacter* species as model microorganisms in environmental microbiology: current state and perspectives. *Applied Microbiology and Biotechnology*, *99*(6), 2533-2548. https://doi.org/10.1007/s00253-015-6439-y

Kazamia, E., Czesnick, H., Thi, T. V. N., Croft, M. T., Sherwood, E., Sasso, S., Hodson, S. J., Warren, M. J., & Smith, A. G. (2012). Mutualistic interactions between vitamin B$_{12}$-dependent algae and heterotrophic bacteria exhibit regulation. *Environmental Microbiology*, *14*(6), 1466-1476. https://doi.org/10.1111/j.1462-2920.2012.02733.x

Khozin-Goldberg, I., Iskandarov, U., & Cohen, Z. (2011). LC-PUFA from photosynthetic microalgae: occurrence, biosynthesis, and prospects in biotechnology. *Applied Microbiology and Biotechnology*, *91*(4), 905-915. https://doi.org/10.1007/s00253-011-3441-x

Kliphuis, A., Janssen, M., End, E., Martens, D., & Wijffels, R. (2011). Light respiration in *Chlorella sorokiniana*. *Journal of Applied Phycology*, *23*, 935-947. https://doi.org/10.1007/s10811-010-9614-7

Knuckey, R. M., Brown, M. R., Robert, R., & Frampton, D. M. F. (2006). Production of microalgal concentrates by flocculation and their assessment as aquaculture feeds. *Aquacultural Engineering*, *35*(3), 300-313. https://doi.org/10.1016/j.aquaeng.2006.04.001

Kraft, B., Strous, M., & Tegetmeyer, H. E. (2011). Microbial nitrate respiration – Genes, enzymes and environmental distribution. *Journal of Biotechnology*, *155*(1), 104-117. https://doi.org/10.1016/j.jbiotec.2010.12.025

Labbe, N., Laurin, V., Juteau, P., Parent, S., & Villemur, R. (2007). Microbiological community structure of the biofilm of a methanol-fed, marine denitrification system, and identification of the methanol-utilizing microorganisms. *Microb Ecol*, *53*(4), 621-630. https://doi.org/10.1007/s00248-006-9168-z

Lassen, H. C. A., Henriksen, E., Neukirch, F., & Kristensen, H. (1956). Treatment of Tetanus: Severe Bone-Marrow depression after prolonged Nitrous-Oxide Anesthesia. *The Lancet*, *267*(6922), 527-530. https://doi.org/10.1016/S0140-6736(56)90593-1

Lauro, F. M., McDougald, D., Thomas, T., Williams, T. J., Egan, S., Rice, S., DeMaere, M. Z., Ting, L., Ertan, H., Johnson, J., Ferriera, S., Lapidus, A., Anderson, I., Kyrpides, N., Munk, A. C., Detter, C., Han, C. S., Brown, M. V., Robb, F. T., . . . Cavicchioli, R. (2009). The genomic basis of trophic strategy in marine bacteria. *Proceedings of the National Academy of Sciences of the United States of America*, *106*(37), 15527-15533. https://doi.org/10.1073/pnas.0903507106

Louca, S., Parfrey, L. W., & Doebeli, M. (2016). Decoupling function and taxonomy in the global ocean microbiome. *Science*, *353*(6305), 1272-1277. https://doi.org/10.1126/science.aaf4507

Lu, X., Heal, K. R., Ingalls, A. E., Doxey, A. C., & Neufeld, J. D. (2020). Metagenomic and chemical characterization of soil cobalamin production. *The ISME Journal*, *14*(1), 53-66. https://doi.org/10.1038/s41396-019-0502-0

Lycus, P., Lovise Bøthun, K., Bergaust, L., Peele Shapleigh, J., Reier Bakken, L., & Frostegård, Å. (2017). Phenotypic and genotypic richness of denitrifiers revealed by a novel isolation strategy. *The ISME Journal*, *11*(10), 2219-2232. https://doi.org/10.1038/ismej.2017.82

Madsen, E. L. (2016). *Environmental microbiology : from genomes to biogeochemistry* (Second edition. ed.). Wiley Blackwell.

Malin, G., & Steinke, M. (2004). Dimethyl sulfide production: what is the contribution of the coccolithophores? In H. R. Thierstein & J. R. Young (Eds.), *Coccolithophores: From Molecular Processes to Global Impact* (pp. 127-164). Springer Berlin Heidelberg. https://doi.org/10.1007/978-3-662-06278-4_6

Maruyama, I., Ando, Y., Maeda, T., & Hirayama, K. (1989). Uptake of Vitamin B_{12} by Various Strains of Unicellular Algae *Chlorella*. *NIPPON SUISAN GAKKAISHI*, *55*(10), 1785-1790. https://doi.org/10.2331/suisan.55.1785

Matthews, R. G., Koutmos, M., & Datta, S. (2008). Cobalamin-dependent and cobamide-dependent methyltransferases. *Current Opinion in Structural Biology*, *18*(6), 658-666. https://doi.org/10.1016/j.sbi.2008.11.005

McMurdie, P. J., & Holmes, S. (2013). phyloseq: An R Package for Reproducible Interactive Analysis and Graphics of Microbiome Census Data. *Plos One*, *8*(4), Article e61217. https://doi.org/10.1371/journal.pone.0061217

Mendoza, J., Purchal, M., Yamada, K., & Koutmos, M. (2023). Structure of full-length cobalamin-dependent methionine synthase and cofactor loading captured. *Nature Communications*, *14*(1). https://doi.org/10.1038/s41467-023-42037-4

Menon, S., Denman, K. L., Brasseur, G., Chidthaisong, A., Ciais, P., Cox, P. M., Dickinson, R. E., Hauglustaine, D., Heinze, C., & Holland, E. (2007). *Couplings between changes in the climate system and biogeochemistry*.

Michels, M. H. A., van der Goot, A. J., Vermuë, M. H., & Wijffels, R. H. (2016). Cultivation of shear stress sensitive and tolerant microalgal species in a tubular photobioreactor equipped with a centrifugal pump. *Journal of Applied Phycology*, *28*(1), 53-62. https://doi.org/10.1007/s10811-015-0559-8

Mignard, S., & Flandrois, J. P. (2006). 16S rRNA sequencing in routine bacterial identification: A 30-month experiment. *Journal of Microbiological Methods*, *67*(3), 574-581. https://doi.org/10.1016/j.mimet.2006.05.009

Minot, G. R., & Murphy, W. P. (1926). Treatment of pernicious anemia by a special diet. *Journal of the American Medical Association*, *87*(7), 470-476. https://doi.org/10.1001/jama.1926.02680070016005

Molstad, L., Dörsch, P., & Bakken, L. R. (2007). Robotized incubation system for monitoring gases (O_2, NO, N_2O N_2) in denitrifying cultures. *Journal of Microbiological Methods*, *71*(3), 202-211. https://doi.org/10.1016/j.mimet.2007.08.011

Mori, K., Yamaguchi, K., & Hanada, S. (2018). *Sulfurovum denitrificans* sp nov., an obligately chemolithoautotrophic sulfur-oxidizing epsilonproteobacterium isolated from a hydrothermal field. *International Journal of Systematic and Evolutionary Microbiology*, *68*(7), 2183-2187. https://doi.org/10.1099/ijsem.0.002803

Murray, A. E., Kenig, F., Fritsen, C. H., McKay, C. P., Cawley, K. M., Edwards, R., Kuhn, E., McKnight, D. M., Ostrom, N. E., Peng, V., Ponce, A., Priscu, J. C., Samarkin, V., Townsend, A. T., Wagh, P., Young, S. A., Yung, P. T., & Doran, P. T. (2012). Microbial life at -13 °C in the brine of an ice-sealed Antarctic lake. *Proceedings of the National Academy of Sciences of the United States of America*, *109*(50), 20626-20631. https://doi.org/10.1073/pnas.1208607109

Nef, C., Jung, S., Mairet, F., Kaas, R., Grizeau, D., & Garnier, M. (2019). How haptophytes microalgae mitigate vitamin B_{12} limitation. *Scientific Reports*, *9*(1), 8417. https://doi.org/10.1038/s41598-019-44797-w

Nichols, D., Lewis, K., Orjala, J., Mo, S., Ortenberg, R., O'Connor, P., Zhao, C., Vouros, P., Kaeberlein, T., & Epstein, S. S. (2008). Short peptide induces an "uncultivable" microorganism to grow in vitro. *Applied and Environmental Microbiology*, *74*(15), 4889-4897. https://doi.org/10.1128/aem.00393-08

Okbamichael, M., & Sañudo-Wilhelmy, S. A. (2004). A new method for the determination of Vitamin B in seawater. *Analytica Chimica Acta*, *517*(1-2), 33-38. https://doi.org/10.1016/j.aca.2004.05.020

Otte, J. M., Blackwell, N., Ruser, R., Kappler, A., Kleindienst, S., & Schmidt, C. (2019). N$_2$O formation by nitrite-induced (chemo)denitrification in coastal marine sediment. *Scientific Reports*, *9*. https://doi.org/10.1038/s41598-019-47172-x

Pajares, S., & Ramos, R. (2019). Processes and Microorganisms Involved in the Marine Nitrogen Cycle: Knowledge and Gaps. *Frontiers in Marine Science*, *6*. https://doi.org/10.3389/fmars.2019.00739

Pejchal, R., & Ludwig, M. L. (2005). Cobalamin-Independent Methionine Synthase (MetE): A Face-to-Face Double Barrel That Evolved by Gene Duplication. *PLOS Biology*, *3*(2), e31. https://doi.org/10.1371/journal.pbio.0030031

Pepper, I. L., & Gentry, T. J. (2014). *Environmental Microbiology: Third Edition*.

Pettersen, R., Ormaasen, I., Angell, I. L., Keeley, N. B., Lindseth, A., Snipen, L., & Rudi, K. (2022). Bimodal distribution of seafloor microbiota diversity and function are associated with marine aquaculture. *Marine Genomics*, *66*. https://doi.org/10.1016/j.margen.2022.100991

Pokorny, L., Hausmann, B., Pjevac, P., & Schagerl, M. (2022). How to Verify Non-Presence-The Challenge of Axenic Algae Cultivation. *Cells*, *11*(16). https://doi.org/10.3390/cells11162594

Priscu, J. C. (1997). The biogeochemistry of nitrous oxide in permanently ice-covered lakes of the McMurdo Dry Valleys, Antarctica. *Global Change Biology*, *3*(4), 301-315. https://doi.org/10.1046/j.1365-2486.1997.00147.x

Prisu, J. C., Downes, M. T., & McKay, C. P. (1996). Extreme supersaturation of nitrous oxide in a poorly ventilated Antarctic lake. *Limnology and Oceanography*, *41*(7), 1544-1551. https://doi.org/10.4319/lo.1996.41.7.1544

R Core Team. (2024). *R: A Language and Enviroment for Statistical Computing*. In R Foundation for Statistical Computing. https://www.R-project.org/

Ramírez-Rueda, A., Velasco, A., & González-Sánchez, A. (2020). The Effect of Chemical Sulfide Oxidation on the Oxygenic Activity of an Alkaliphilic Microalgae Consortium Deployed for Biogas Upgrading. *Sustainability*, *12*(16), Article 6610. https://doi.org/10.3390/su12166610

Raux, E., Schubert, H. L., & Warren*, M. J. (2000). Biosynthesis of cobalamin (vitamin B$_{12}$): a bacterial conundrum. *Cellular and Molecular Life Sciences CMLS*, *57*(13), 1880-1893. https://doi.org/10.1007/PL00000670

Richter, C. A., Evans, A. N., Heppell, S. A., Zajicek, J. L., & Tillitt, D. E. (2023). Genetic basis of thiaminase I activity in a vertebrate, zebrafish. *Scientific Reports*, *13*(1). https://doi.org/10.1038/s41598-023-27612-5

Rickes, E. L., Brink, N. G., Koniuszy, F. R., Wood, T. R., & Folkers, K. (1948). Crystalline Vitamin B$_{12}$. *Science*, *107*(2781), 396-397. https://doi.org/10.1126/science.107.2781.396

Rognes, T., Flouri, T., Nichols, B., Quince, C., & Mahé, F. (2016). VSEARCH: a versatile open source tool for metagenomics. *PeerJ*, *4*, Article e2584. https://doi.org/10.7717/peerj.2584

Roth, J. R., Lawrence, J. G., Rubenfield, M., Kieffer-Higgins, S., & Church, G. M. (1993). Characterization of the cobalamin (vitamin B$_{12}$) biosynthetic genes of *Salmonella typhimurium*. *Journal of Bacteriology*, *175*(11), 3303-3316. https://doi.org/10.1128/jb.175.11.3303-3316.1993

Roth, M. (1971). Fluorescence reaction for amino acids. *Analytical Chemistry*, *43*(7), 880-882. https://doi.org/10.1021/ac60302a020

Routhu, S. R., Ragi, N. C., Yedla, P., Shaik, A. B., Venkataraman, G., Cheemalamarri, C., Chityala, G. K., Amanchy, R., Sripadi, P., & Kamal, A. (2021). Identification, characterization and evaluation of novel antifungal cyclic peptides from *Neobacillus*

drentensis. *Bioorganic Chemistry*, *115*, 105180.
https://doi.org/10.1016/j.bioorg.2021.105180

Ryan, M. P., & Adley, C. C. (2014). *Ralstonia* spp.: emerging global opportunistic pathogens. *European Journal of Clinical Microbiology & Infectious Diseases*, *33*(3), 291-304. https://doi.org/10.1007/s10096-013-1975-9

Safi, C., Zebib, B., Merah, O., Pontalier, P.-Y., & Vaca-Garcia, C. (2014). Morphology, composition, production, processing and applications of *Chlorella vulgaris*: A review. *Renewable and Sustainable Energy Reviews*, *35*, 265-278. https://doi.org/10.1016/j.rser.2014.04.007

Sannino, D. R., Kraft, C. E., Edwards, K. A., & Angert, E. R. (2018). Thiaminase I Provides a Growth Advantage by Salvaging Precursors from Environmental Thiamine and Its Analogs in *Burkholderia thailandensis*. *Applied and Environmental Microbiology*, *84*(18), e01268-01218. https://doi.org/10.1128/AEM.01268-18

Sañudo-Wilhelmy, S. A., Gómez-Consarnau, L., Suffridge, C., & Webb, E. A. (2014). The Role of B Vitamins in Marine Biogeochemistry. In C. A. Carlson & S. J. Giovannoni (Eds.), *Annual Review of Marine Science, Vol 6* (Vol. 6, pp. 339-367). https://doi.org/10.1146/annurev-marine-120710-100912

Scarsella, M., Torzillo, G., Cicci, A., Belotti, G., De Filippis, P., & Bravi, M. (2012). Mechanical stress tolerance of two microalgae. *Process Biochemistry*, *47*(11), 1603-1611. https://doi.org/10.1016/j.procbio.2011.07.002

Schneider, L. K., Wüst, A., Pomowski, A., Zhang, L., & Einsle, O. (2014). No Laughing Matter: The Unmaking of the Greenhouse Gas Dinitrogen Monoxide by Nitrous Oxide Reductase. In P. M. H. Kroneck & M. E. S. Torres (Eds.), *The Metal-Driven Biogeochemistry of Gaseous Compounds in the Environment* (pp. 177-210). Springer Netherlands. https://doi.org/10.1007/978-94-017-9269-1_8

Selva Kumar, L. S., & Thakur, M. S. (2011). Competitive immunoassay for analysis of vitamin B_{12}. *Anal Biochem*, *418*(2), 238-246. https://doi.org/10.1016/j.ab.2011.07.011

Simpson, E. H. (1949). Measurement of Diversity. *Nature*, *163*(4148), 688-688. https://doi.org/10.1038/163688a0

Smith, E. L. (1948). Purification of Anti-pernicious Anemia Factors from Liver. *Nature*, *161*(4095), 638-639. https://doi.org/10.1038/161638a0

Stoddard, S. F., Smith, B. J., Hein, R., Roller, B. R. K., & Schmidt, T. M. (2015). rrnDB: improved tools for interpreting rRNA gene abundance in bacteria and archaea and a new foundation for future development. *Nucleic Acids Research*, *43*(D1), D593-D598. https://doi.org/10.1093/nar/gku1201

Sørensen, J., Tiedje, J. M., & Firestone, R. B. (1980). Inhibition by sulfide of nitric and nitrous oxide reduction by denitrifying *Pseudomonas fluorescens*. *Appl Environ Microbiol*, *39*(1), 105-108. https://doi.org/10.1128/aem.39.1.105-108.1980

Takeuchi, T., Yokoyama, K., Kobayashi, K., Suzuki, M., Tamiya, E., Karube, I., Utsunomiya, K., Imai, O., & Masuda, Y. (1993). PHOTOSYNTHETIC ACTIVITY SENSOR FOR MICROALGAE BASED ON AN OXYGEN-ELECTRODE INTEGRATED WITH OPTICAL FIBERS. *Analytica Chimica Acta*, *276*(1), 65-68. https://doi.org/10.1016/0003-2670(93)85039-m

Toyoda, S., Yoshida, O., Yamagishi, H., Fujii, A., Yoshida, N., & Watanabe, S. (2019). Identifying the origin of nitrous oxide dissolved in deep ocean by concentration and isotopocule analyses. *Scientific Reports*, *9*(1), 7790. https://doi.org/10.1038/s41598-019-44224-0

Waldrop, G. L., Holden, H. M., & St Maurice, M. (2012). The enzymes of biotin dependent CO_2 metabolism: What structures reveal about their reaction mechanisms. *Protein Science*, *21*(11), 1597-1619. https://doi.org/10.1002/pro.2156

Wang, L., Zhao, H., Bi, R., Chen, X., Lyu, Z., & Liu, W. (2024). Roles and sources of B vitamins in the marine ecosystem. *Reviews in Fish Biology and Fisheries*, *34*(1), 111-130. https://doi.org/10.1007/s11160-023-09818-y

Ward, D. M., Weller, R., & Bateson, M. M. (1990). 16S rRNA sequences reveal numerous uncultured microorganisms in a natural community. *Nature*, *345*(6270), 63-65. https://doi.org/10.1038/345063a0

Wen, A. M., Fegan, M., Hayward, C., Chakraborty, S., & Sly, L. I. (1999). Phylogenetic relationships among members of the *Comamonadaceae*, and description of *Delftia acidovorans* (den Dooren de Jong 1926 and Tamaoka *et al*. 1987) gen. nov., comb. nov. *International Journal of Systematic Bacteriology*, *49*, 567-576. https://doi.org/10.1099/00207713-49-2-567

Wickham, H. (2016). *ggplot2: Elegant Graphics for Data Analysis*. Springer-Verlag New York. https://ggplot2.tidyverse.org

Winand, R., Bogaerts, B., Hoffman, S., Lefevre, L., Delvoye, M., Braekel, J. V., Fu, Q., Roosens, N. H., Keersmaecker, S. C., & Vanneste, K. (2019). Targeting the 16S rRNA gene for bacterial identification in complex mixed samples: Comparative evaluation of second (Illumina) and third (Oxford Nanopore Technologies) generation sequencing technologies. *Int J Mol Sci*, *21*(1). https://doi.org/10.3390/ijms21010298

Wood, J. M., Kennedy, F. S., & Wolfe, R. S. (1968). Reaction of multihalogenated hydrocarbons with free and bound reduced vitamin B_{12}. *Biochemistry*, *7*(5), 1707-1713. https://doi.org/10.1021/bi00845a013

Yu, Y., Lee, C., Kim, J., & Hwang, S. (2005). Group-specific primer and probe sets to detect methanogenic communities using quantitative real-time polymerase chain reaction. *Biotechnol Bioeng*, *89*(6), 670-679. https://doi.org/10.1002/bit.20347

Zhan, L., & Chen, L. (2009). Distributions of N_2O and its air-sea fluxes in seawater along cruise tracks between 30° S–67° S and in Prydz Bay, Antarctica. *Journal of Geophysical Research: Oceans*, *114*(C3). https://doi.org/10.1029/2007JC004406

Zhan, L., Wu, M., Chen, L., Zhang, J., Li, Y., & Liu, J. (2017). The Air-Sea Nitrous Oxide Flux along Cruise Tracks to the Arctic Ocean and Southern Ocean. *Atmosphere*, *8*(11), 216. https://doi.org/10.3390/atmos8110216

Zhao, L., & Wang, Y. (2017). Nitrate Assay for Plant Tissues. *Bio Protoc*, *7*(2), e2029. https://doi.org/10.21769/BioProtoc.2029

7. Appendix

Appendix A: Components of M8a medium

Table A1. Stock solutions of M8a medium

Solution	Compound	Stock concentration	Concentration in final medium (mM)
Phosphate-buffer	KH_2PO_4	74.0 g/l	5.44
	$Na_2HPO_4*2H_2O$	26.0 g/l	1.46
Macronutrients	$MgSO_4*7H_2O$	40.0 g/l	1.62
	$CaCl_2*2H_2O$	1.3 g/l	0.09
Iron-EDTA	Fe*Na*EDTA	11.6 g/l	0.316
	$Na_2EDTA*2H_2O$	3.72 g/l	0.100
Micronutrients	H_3BO_3	6.2 mg/l	0.001
	$MnCl_2*4H_2O$	1.3 g/l	0.066
	$ZnSO_4*7H_2O$	0.32 g/l	0.011
	$CuSO_4*5H_2O$	0.183 g/l	0.007

Appendix B: Components of L1 medium

Table A2. Trace elements stock solution

Component	Primary stock solution (g/L dH$_2$O)	Quantity / L stock solution	Concentration in final medium (M)
Na$_2$EDTA*2H$_2$O	-	4.36 g	$1.17*10^{-5}$
FeCl$_3$*6H$_2$O	-	3.15 g	$1.17*10^{-5}$
MnCl$_2$*4H$_2$O	178.10	1 ml	$9.09*10^{-7}$
ZnSO$_4$*7H$_2$O	23.0	1 ml	$8.0*10^{-8}$
CoCl$_2$*6H$_2$O	11.9	1 ml	$5.0*10^{-8}$
CuSO$_4$*5H$_2$O	2.50	1 ml	$1.0*10^{-8}$
Na$_2$MoO$_4$*2H$_2$O	19.9	1 ml	$8.22*10^{-8}$
H$_2$SeO$_3$	1.29	1 ml	$1.0*10^{-8}$
NiSO$_4$*6H$_2$O	2.63	1 ml	$1.0*10^{-8}$
Na$_3$VO$_4$	1.84	1 ml	$1.9*10^{-8}$
K$_2$CrO$_4$	1.94	1 ml	$1.0*10^{-8}$

Table A3. Vitamin stock solution

Component	Primary stock solution (g/L dH20)	Quantity / L stock solution	Concentration in final medium (M)
Thiamine*HCl (vitamin B1)	-	200 mg	$2.96*10^{-7}$
Biotin (vitamin H)	0.1	10 ml	$2.05*10^{-9}$
Cyanocobalamin (vitamin B12) *	1.0	1 ml	$3.69*10^{-10}$

*In medium without cobalamin, it was made a vitamin stock solution with Thiamin and biotin as shown above, but without cyanocobalamin added.

Table A4. Stock solutions

Component	Stock solution (g/L dH2O)	Quantity /L medium	Concentration in final medium (M)
$NaNO_3$	75.0	1 ml	$8.82*10^{-4}$
$NaH_2PO_4*H_2O$	5.0	1 ml	$3.62*10^{-5}$
$Na_2SiO_3*9H_2O$	30.0	1 ml	$1.06*10^{-4}$

Table A5. Artificial seawater

Component	Concentration (g/L)	Concentration (mM)
NaCl	24.5	419.0
Na_2SO_4	3.2	22.5
$CaCl_2*2H_2O$	0.8	5.42
K_2SO_4	0.85	4.88
$MgCl_2*6H_2O$	9.8	48.2

Appendix C: 16S rRNA sequencing primers

Table A6. 16S rRNA PRK primers targeting V3-V4 used in first-stage PCR

Primer name	Direction	Sequence, 5' → 3'
PRK341F (Yu et al., 2005)	Forward	CCTACGGGRBGCASCAG
PRK806R (Yu et al., 2005)	Reverse	GGACTACYVGGGTATCTAAT

Table A7. Illumina PRK primers used in index PCR. Sequences are from (Yu et al., 2005).

Primer name	Direction	Sequence, 5' → 3'
F9	Forward	aatgatacggcgaccaccgagatctacactctttccctacacgacgctcttccgatctgtttcgCCTACGGGRBGCASCAG
F10	Forward	aatgatacggcgaccaccgagatctacactctttccctacacgacgctcttccgatctcgtacgCCTACGGGRBGCASCAG
F11	Forward	aatgatacggcgaccaccgagatctacactctttccctacacgacgctcttccgatctgagtggCCTACGGGRBGCASCAG
F12	Forward	aatgatacggcgaccaccgagatctacactctttccctacacgacgctcttccgatctggtagcCCTACGGGRBGCASCAG
F13	Forward	aatgatacggcgaccaccgagatctacactctttccctacacgacgctcttccgatctactgatCCTACGGGRBGCASCAG
F14	Forward	aatgatacggcgaccaccgagatctacactctttccctacacgacgctcttccgatctatgagcCCTACGGGRBGCASCAG
F15	Forward	aatgatacggcgaccaccgagatctacactctttccctacacgacgctcttccgatctattcctCCTACGGGRBGCASCAG
F16	Forward	aatgatacggcgaccaccgagatctacactctttccctacacgacgctcttccgatctcaaaagCCTACGGGRBGCASCAG
R12	Reverse	caagcagaagacggcatacgagatTACAAGgtgactggagttcagacgtgtgctcttccgatctGGACTACYVGGGTATCTAAT
R13	Reverse	caagcagaagacggcatacgagatTTGACTgtgactggagttcagacgtgtgctcttccgatctGGACTACYVGGGTATCTAAT
R14	Reverse	caagcagaagacggcatacgagatGGAACTgtgactggagttcagacgtgtgctcttccgatctGGACTACYVGGGTATCTAAT
R15	Reverse	caagcagaagacggcatacgagatTGACATgtgactggagttcagacgtgtgctcttccgatctGGACTACYVGGGTATCTAAT
R16	Reverse	caagcagaagacggcatacgagatGGACGGgtgactggagttcagacgtgtgctcttccgatctGGACTACYVGGGTATCTAAT

Appendix D: 16S rRNA data processing

1 Initial 16S rRNA Illumina data processing

The initial processing of Illumina amplicon data included de-multiplexing, VSEARCH pipeline and taxonomic classification using the SINTAX algoritm as described in https://arken.nmbu.no/~larssn/MiDiv/README_amplicons.html. The VSEARCH pipeline had readcounts_vsearch_OTU.txt as output. The OTU's were classified through taxonomy classification using SINTAX. This resulted the output file: taxonomy_vsearch_OTU.txt. These files and the metadata-file, containing sample information, was taken further in data analysis.

```r
#libraries
library(tidyverse)  #tidying, transformation and visualisation of data

library(readxl)     #importing data from excel
library(phyloseq)   #analysis of taxonomic data
library(ggplot2)    #graphics
library(dplyr)      #filter and formating data
library(tibble)     #needed to convert columns to row names
library(colorspace) #color palette
```

2 Filtering the SINTAX results

The confidence score for each classification was set to 0 in the SINTAX algorithm. The code below sets this to 0.6. The species column was also removed due to the taxonomic resolution being at genus level.

```r
setwd("~/Master_R/Illumina")

taxonomy.tbl.06 <- read_delim("taxonomy_vsearch_OTU_table.txt", delim = "\t
", show_col_types = FALSE) %>%
  mutate(genus = if_else(genus_score < 0.6, "unclassified", genus))

#remove species columns
taxonomy.tbl.06 <- taxonomy.tbl.06[, -c(14,15)]

#(save table):
#write.table(taxonomy.tbl, file = "taxonomy_tbl.txt", sep = "\t",
#             row.names = FALSE)
```

3 Creating a phyloseq object

The phyloseq package is a tool that is used to import, store, analyse, and graphically display complex phylogenetic sequencing data (McMurdie & Holmes, 2013).

3.1 Data wrangling: Getting the data on the right format for phyloseq

Three tables were needed for compatibility with phyloseq:

- OTU: First column with OTUs, next is the readcount of the certain OTU in all samples

- Taxonomy: First column with OTUs, and following columns have the different taxonomic levels: domain, phylum etc.

- Sample: metadata The data was already in R, but not on the correct format and had to be "wrangled" some more.

Taxonomy table

```
#Load tax table:
taxonomy.tbl <- read_delim("taxonomy_tbl_06.txt", delim = "\t", show_col_ty
pes = FALSE) %>%
  select(-contains("score"))

#phyloseq objects need to have row.names, changing the OTU column to be row
names:
tax_mat <- taxonomy.tbl %>%
    tibble::column_to_rownames("OTU")

#phyloseq requires a matrix input of the tax table:
tax_mat <- as.matrix(tax_mat)

#transform to Taxonomy phyloseq object:
TAX = tax_table(tax_mat)
```

OTU table

```
#load table from VSEARCH output
readcount.tbl <- read_delim("readcounts_vsearch_OTU.txt", delim = "\t", sho
w_col_types = FALSE)

#renaming the OTU column and renaming table:
names(readcount.tbl)[names(readcount.tbl) == '#OTU ID'] <- 'OTU'
OTU.tbl <- readcount.tbl

#phyloseq objects need rownames, changing the OTU column to be rownames:
```

```
otu_mat <- OTU.tbl %>%
    tibble::column_to_rownames("OTU")

#phyloseq requires the OTU table to be in matrix format for input:
otu_mat <- as.matrix(otu_mat)

#creating OTU phyloseq object:
OTU = otu_table(otu_mat, taxa_are_rows = TRUE)
```

Sample table

```
#load the metadata excel sheet:
sample.tbl <- read_delim("Sample_table_S.txt", delim = "\t", show_col_types
= FALSE)
#phyloseq objects needs rownames:
samples_df <- sample.tbl %>%
    tibble::column_to_rownames("SampleID")
#Sample can be left as dataframe. Creating the sample phyloseq object:
samples = sample_data(samples_df)
```

3.2 Phyloseq object

The data are now in the proper format for input in the `phyloseq()` command. This will create a phyloseq object, on which further metagenomic analysis can be performed.

```
#creating the phyoseq object with the 3 inputs created above
phyloseq_obj <- phyloseq(OTU, TAX, samples)
```

4 Normalization of the phyloseq_obj

The code below gives the code for TSS normalization of the data in phyloseq object.

```
#Creating a function, important for the transform_sample_counts() below:

TSS <- function(Xj){
  Yj <- Xj / sum(Xj)
  return(Yj)
}


#The function is used by the transform_sample_counts command to normalize t
he data in phyloseq-object
physeq.tss <- transform_sample_counts(phyloseq_obj, TSS)
```

```
# Checking that the data is actually normalized. The relative abundance of
every sample should sum to 1:
colSums(otu_table(physeq.tss))
```

5 Filtering for sediment samples

The phyloseq object created above contains both algae and sediment taxonomic data, in addition to positive and negative control. Want to separate sediment and algae into separate objects, and remove controls, before further analysis is done. In addition, certain taxa are removed, ensuring that only bacteria are kept and Mitochondira and Chloroplast DNA is excluded. In addition, for the sediment samples, both a normalized and a non-normalized phyloseq object will be used in further analysis. Hence, the filtering is performed twice.

5.1 Normalized data

The code below does the following filtering: keeping only sediment samples, removes taxa with a total count of 0 from phyloseq object, removes positive and negative control (named "MethodControl" i Sample-table) and filters out what is not bacteria.

```
phyloseq.obj.sediment.normalized <- physeq.tss %>%
  subset_samples(Sample_type == "Sediment") %>%
  prune_taxa(taxa_sums(.)>0, .) %>%
  subset_samples(Treatment != "MethodControl") %>%
  subset_taxa(
    domain == "Bacteria" &
    family  != "Mitochondria" &
    class   != "Chloroplast"
  )

#save(phyloseq.obj.sediment.unormalized, file = "phyloseq.obj.sediment.unor
malized.RData")
```

5.1 Unnormalized data
```
phyloseq.obj.sediment.unnormalized <- phyloseq_obj %>%
  subset_samples(Sample_type == "Sediment") %>%
  prune_taxa(taxa_sums(.)>0, .) %>%
  subset_samples(Treatment != "MethodControl") %>%
  subset_taxa(
    domain == "Bacteria" &
    family  != "Mitochondria" &
    class   != "Chloroplast"
  )
```

```
#save(phyloseq.obj.sediment.unormalized, file = "phyloseq.obj.sediment.unor
malized.RData")
```

6 Data analysis on sediment samples

6.1 Alpha-diversity

The `plot_richness` function estimates several alpha-diversity metrics using the `estimate_richness` function (McMurdie & Holmes, 2013). The function returns a ggplot object. The required input is untrimmed, non-normalized count data.

```
p.div <- plot_richness(
  phyloseq.obj.sediment.unnormalized,
  x="Treatment",
  color = "Treatment",
  measures = c("Shannon","Simpson")) +
  geom_boxplot() +
  theme_bw() +
  scale_x_discrete(limits = c("Nitrate only", "Methanol + nitrate",
"Thiosulphate + nitrate", "Start Control", "Control")) +
  theme(axis.text.x = element_text(angle = 90))

print(p.div)
```

6.2 Beta-diversity analysis

The `ordinate` function performs a principal coordinate analysis (PCoA) of a distance matrix. The distances are calculated using Bray-Curtis dissimilarity index. The distance matrix is decomposed into eigenvectors and eigenvalues. Vectors gives the position on x-and y-axis while eigenvalues indicate something about the proportion explained by the different axis.

```
ord.obj <- ordinate(phyloseq.obj.sediment.unnormalized, method = "PCoA", di
stance = "bray")
plot_scree(ord.obj) #plotting ordination eigenvalues using ggplot graphic
```

```
plot_ordination(phyloseq.obj.sediment.unnormalized, ord.obj, color = "Treat
ment") +
  geom_point(size = 4) +
 theme_bw() +
```

```
 labs(
    y = "PCo2 (21%)",
    x = "PCo1 (32.3%%)",
    main = "PCoA")
```

6.3 Most abundant OTUs across all sediment samples

The normalized data is used when finding the most abundant taxa across all samples.

```
#sums the counts of each taxa, names and total counts is stored in total.ab
undance:
total.abundance <- taxa_sums(phyloseq.obj.sediment.normalized)


#total.abundance is sorted in decreasing order and the names of the first 1
0 elements are stored in "most.abundant.10"
most.abundant.10 <- names(sort(total.abundance, decreasing = TRUE))[1:10]


#creating a new phyloseq-object which only includes the top 10 OTUs
physeq.obj.top10 <- prune_taxa(most.abundant.10, phyloseq.obj.sediment.norm
alized)


#melts the pruned phyloseq object into a dataframe
ps.table.top10 <- psmelt(physeq.obj.top10)

#rename the samples, so they are more informative
ps.table.top10$Sample <- recode(ps.table.top10$Sample,
                         `Sample22` = "Start Control 1",
                         `Sample23` = "Start Control 2",
                         `Sample24` = "Start Control 3",
                         `Sample25` = "Control 1",
                         `Sample26` = "Control 2",
                         `Sample27` = "Control 3",
                         `Sample28` = "Methanol and nitrate 1",
                         `Sample29` = "Methanol and nitrate 2",
                         `Sample30` = "Methanol and nitrate 3",
                         `Sample31` = "Thiosulphate and nitrate 1",
                         `Sample32` = "Thiosulphate and nitrate 2",
                         `Sample33` = "Thiosulphate and nitrate 3",
                         `Sample34` = "Nitrate 1",
                         `Sample35` = "Nitrate 2",
                         `Sample36` = "Nitrate 3")

#visualizing the relative abundance of the top abunadant families across al
l samples
```

```
family.allsamples <- ggplot(ps.table.top10) +
  geom_col(aes(x = Sample, y = Abundance, fill = family), color = "black")
+
  theme_bw() +
  theme(axis.text.x = element_text(angle = 90)) +
  guides(fill = guide_legend(keyheight = 0.1)) +
  labs(x = "Sample", y = "Relative abundance") +
  scale_fill_discrete_qualitative(palette = "Dark 3") +
  scale_x_discrete(limits = c("Start Control 1", "Start Control 2", "Start
Control 3", "Control 1", "Control 2", "Control 3", "Methanol and nitrate 1"
, "Methanol and nitrate 2", "Methanol and nitrate 3", "Thiosulphate and nit
rate 1", "Thiosulphate and nitrate 2", "Thiosulphate and nitrate 3", "Nitra
te 1", "Nitrate 2", "Nitrate 3"))
print(family.allsamples)
```

7 Filtering for algae samples

Like the sediment samples, the algae samples were filtered out in a separate phyloseq-object.
The code below does the following filtering: keeping only sediment samples, removes taxa
with a total count of 0 from phyloseq object and filters out what is not bacteria. Negative and
positive control was marked as "sediment" in metadata and is thus automatically removed
when only "Algae" is kept.

```
phyloseq.obj.algae.normalized <- physeq.tss %>%
  subset_samples(Sample_type == "Algae") %>%
  prune_taxa(taxa_sums(.)>0, .) %>%
  subset_taxa(
    domain == "Bacteria" &
    family != "Mitochondria" &
    class  != "Chloroplast" &
    phylum != "Cyanobacteria/Chloroplast"
  )

#save(phyloseq.obj.algae.normalized, file = "phyloseq.obj.algae.normalized.
RData")
```

7.7.1 Most abundant OTUs across all algae samples

```
#sums the counts of each taxa, names and total counts is stored in total.ab
undance:
```

```r
total.abundance <- taxa_sums(phyloseq.obj.algae.normalized)


#total.abundance is sorted in decreasing order and the names of the first 1
0 elements are stored in "most.abundant.10":
most.abundant.10 <- names(sort(total.abundance, decreasing = T))[1:10]


#creating a new phyloseq-object which only includes the top 10 OTUs:
physeq.obj.top10 <- prune_taxa(most.abundant.10, phyloseq.obj.algae.normali
zed)


#melts the pruned phyloseq object into a dataframe:
ps.table.top10 <- psmelt(physeq.obj.top10)

#renaming the samples, so they are more informative
ps.table.top10$Sample <- recode(ps.table.top10$Sample,
                                `Sample1` = "C.vulgaris 1 (+Cbl)",
                                `Sample2` = "C.vulgaris 2 (+Cbl)",
                                `Sample3` = "C.vulgaris 3 (+Cbl)",
                                `Sample4` = "C.vulgaris 4 (-Cbl)",
                                `Sample5` = "C.vulgaris 5 (-Cbl)",
                                `Sample6` = "C.vulgaris 6 (-Cbl)",
                                `Sample7` = "C.vulgaris (Stem)",
                                `Sample8` = "T.lutea 1 (+Cbl)",
                                `Sample9` = "T.lutea 2 (+Cbl)",
                                `Sample10` = "T.lutea 3 (+Cbl)",
                                `Sample11` = "T.lutea 4 (-Cbl)",
                                `Sample12` = "T.lutea 5 (-Cbl)",
                                `Sample13` = "T.lutea 6 (-Cbl)",
                                `Sample14` = "T.lutea (Stem)",
                                `Sample15` = "I.galbana 1 (+Cbl)",
                                `Sample16` = "I.galbana 2 (+Cbl)",
                                `Sample17` = "I.galbana 3 (+Cbl)",
                                `Sample18` = "I.galbana 4 (-Cbl)",
                                `Sample19` = "I.galbana 5 (-Cbl)",
                                `Sample20` = "I.galbana 6 (+Cbl)",
                                `Sample21` = "I.galbana (Stem)"
                                )


#visualizing the relative abundance of the top abunadant families across al
l samples
genus.allsamples <- ggplot(ps.table.top10) +
  geom_col(aes(x = Sample, y = Abundance, fill = genus), color = "black") +
  theme_bw() +
  theme(axis.text.x = element_text(angle = 90)) +
```

```
  guides(fill = guide_legend(keyheight = 0.1)) +
  scale_fill_discrete_qualitative(palette = "Dark 3") +
  labs(x = "Sample", y = "Relative abundance")
print(genus.allsamples)
```

Appendix E: Proportion of bacteria relative to algae in algal cultures

Table A8. The proportion of bacteria rel.abundance / Algae rel. abundance

| SampleID	Species	Sample type	Chloroplast rel. abundance	Bacteria rel. abundance	Other/Chloroplast
1	Chlorella	Experiment + Cb	0,998	0,00191	0,00191
2	Chlorella	Experiment + Cb	0,997	0,00234	0,00235
3	Chlorella	Experiment + Cb	0,998	0,00167	0,00167
4	Chlorella	Experiment - Cb	0,998	0,00153	0,00153
5	Chlorella	Experiment - Cb	0,998	0,00162	0,00162
6	Chlorella	Experiment - Cb	0,998	0,00192	0,00193
7	Chlorella	Stem	0,998	0,0018	0,0018
8	Tisochrysis	Experiment + Cb	0,997	0,00256	0,00257
9	Tisochrysis	Experiment + Cb	0,997	0,00245	0,00246
10	Tisochrysis	Experiment + Cb	0,996	0,00405	0,00406
11	Tisochrysis	Experiment - Cb	0,997	0,0031	0,00311
12	Tisochrysis	Experiment - Cb	0,995	0,00599	0,00602
13	Tisochrysis	Experiment - Cb	0,513	0,487	0,949
14	Tisochrysis	Stem	0,603	0,396	0,657
15	Isochrysis	Experiment + Cb	0,993	0,00719	0,00724
16	Isochrysis	Experiment + Cb	0,979	0,0212	0,0217
17	Isochrysis	Experiment + Cb	0,996	0,00439	0,00441
18	Isochrysis	Experiment - Cb	0,995	0,00514	0,00517
19	Isochrysis	Experiment - Cb	0,994	0,0065	0,00654
20	Isochrysis	Experiment - Cb	0,995	0,00447	0,00449
21	Isochrysis	Stem	0,108	0,882	8,2

Appendix F: Standard curves
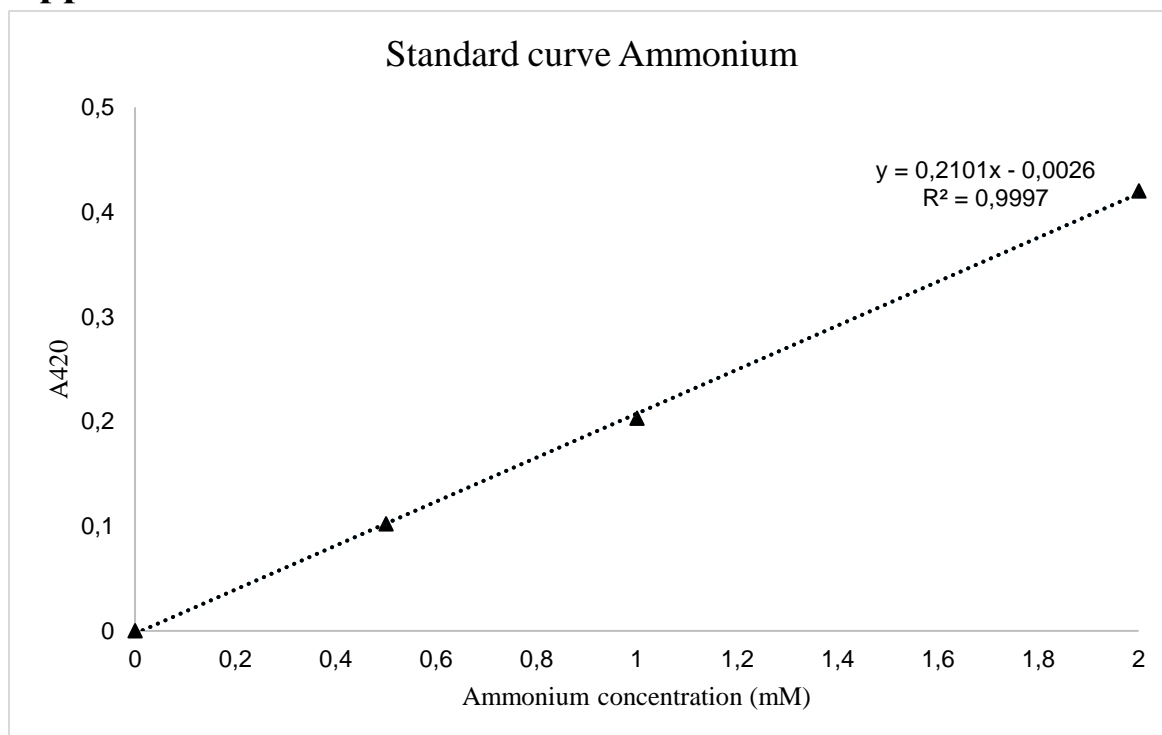
Figure A.1. Standard curve for used for quantification of ammonium. The x-axis refers to the ammonium concentration in mM and the y-axis refers to the absorbance at 420nm. The trend line based on the measured standards have equation y= $0.2101x - 0.0026$ and $R^2 = 0.9997$.
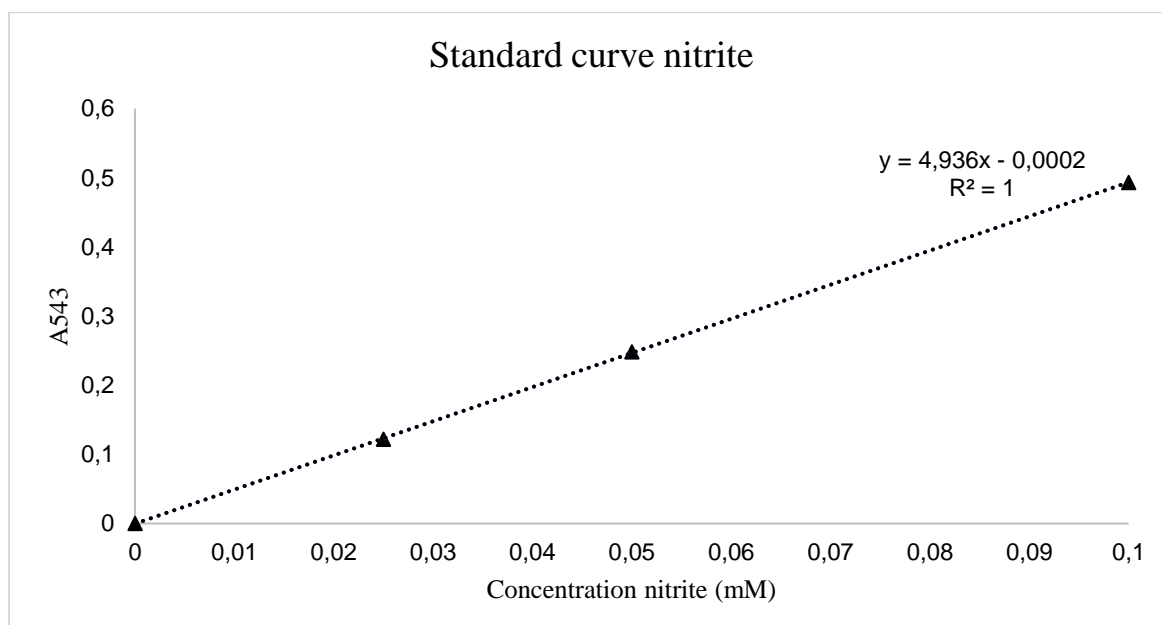

Figure A.2. Standard curve for used for quantification of nitrite. The x-axis refers to the nitrite concentration in mM and the y-axis refers to the absorbance at 543 nm. The trend line based on the measured standards have equation y= $4.94x - 0.0002$ and $R^2 = 1$.
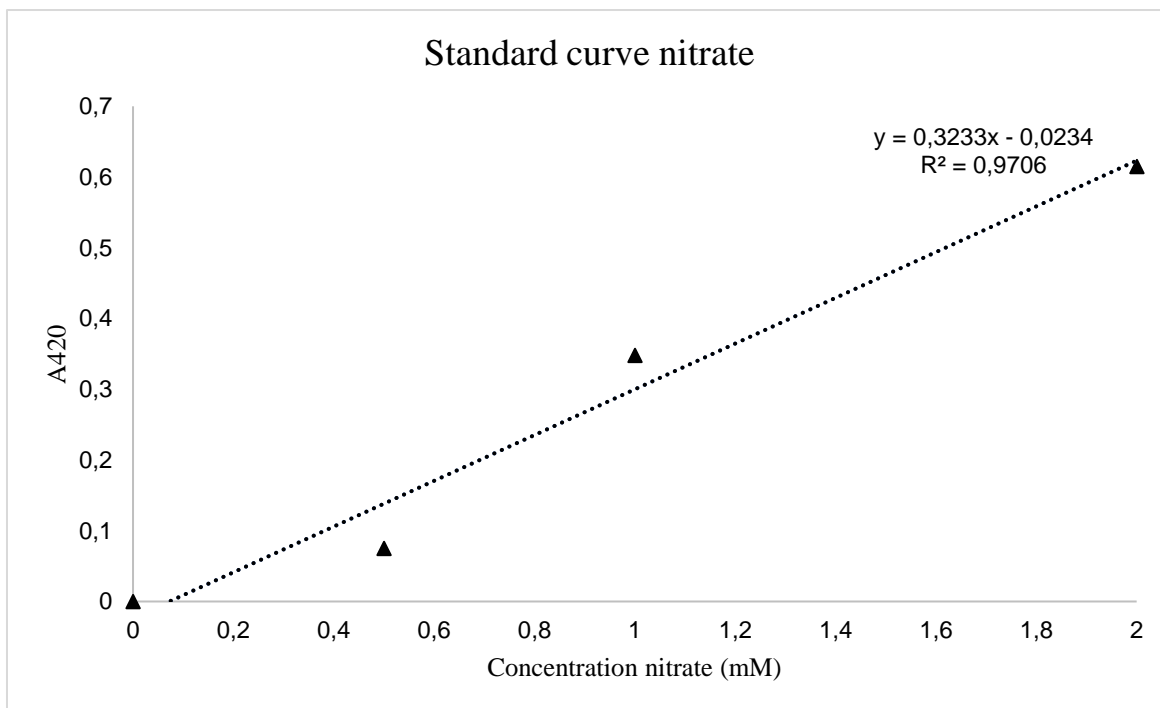
Figure A.3. Standard curve for used for quantification of nitrate. The x-axis refers to the nitrate concentration in mM and the y-axis refers to the absorbance at 420 nm. The trend line based on the measured standards have equation y= $0.3233x - 0.0234$ and $R^2 = 0.971$.
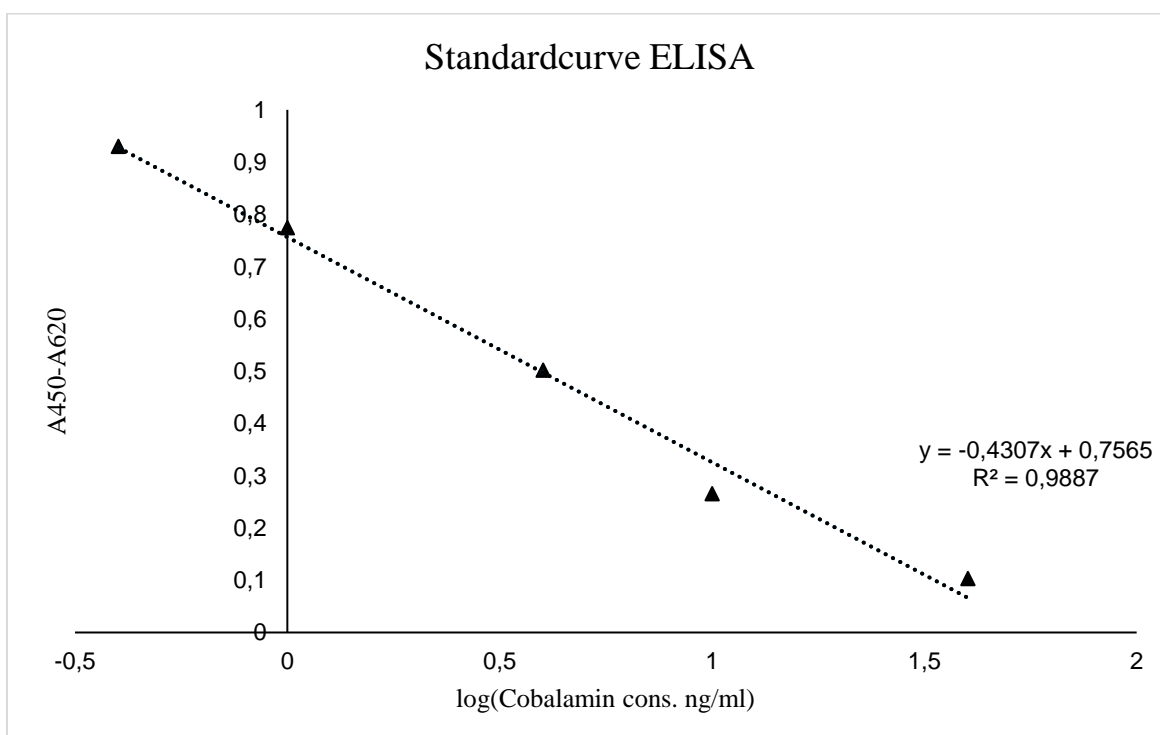

Figure A.4 Standard curve used in ELISA to quantify the concentration of cobalamin in algal cultures. The x-axis refers to the logarithm of cobalamin concentration in ng/ml, whilst the x-axis refers to the A450 minus the reference wavelength A620. The equation of trend line is y=$-0.431x + 0.757$ and $R^2 = 0.989$.